Research and Development Technical Report

ECOM–7023

ATMOSPHERIC OPTICAL ENVIRONMENT

by

Mishri L. Vatsia

September 1972

ECOM

UNITED STATES ARMY ELECTRONICS COMMAND . FORT MONMOUTH, N. J.

123

UNCLASSIFIED
Security Classification

DOCUMENT CONTROL DATA - R & D

(Security classification of title, body of abstract and indexing annotation must be entered when the overall report is classified)

1. ORIGINATING ACTIVITY (Corporate author) U. S. Army Electronics Command Night Vision Laboratory Fort Belvoir, Virginia	2a. REPORT SECURITY CLASSIFICATION Unclassified 2b. GROUP

3. REPORT TITLE

ATMOSPHERIC OPTICAL ENVIRONMENT

4. DESCRIPTIVE NOTES (Type of report and inclusive dates)

Technical Report

5. AUTHOR(S) (First name, middle initial, last name)

Mishri L. Vatsia

6. REPORT DATE	7a. TOTAL NO. OF PAGES	7b. NO. OF REFS
September 1972	118	117

8a. CONTRACT OR GRANT NO.	9a. ORIGINATOR'S REPORT NUMBER(S)
b. PROJECT NO. 1S662709D617	ECOM-7023
c.	9b. OTHER REPORT NO(S) (Any other numbers that may be assigned this report)
d.	

10. DISTRIBUTION STATEMENT

Approved for public release; distribution unlimited.

11. SUPPLEMENTARY NOTES	12. SPONSORING MILITARY ACTIVITY
	U. S. Army Electronics Command Night Vision Laboratory, ATTN: AMSEL-NV-VI Fort Belvoir, Virginia

13. ABSTRACT

A knowledge of the fundamental optical properties of the terrestrial atmospheric environment is essential for solving various problems in the multidisciplinary field of Visionics including the areas of vision, psychology, atmospheric physics, infrared physics, simulation, astrogeophysics, and electro-optical technology. The aim of this report is to generalize the recent work of the author and summarize the data from other worldwide sources published by the first quarter of the year 1972. This report included a treatment of the atmospheric radiation, the atmospheric transmission, and the transfer of contrast by the atmosphere. The fundamental characteristics of the daytime and nighttime radiation including some important recent measurements of the solar, twilight, and nightglow radiation spectra are presented. An extensive chapter on atmospheric transmission includes the fundamental properties of the terrestrial atmosphere and basic principles of atmospheric absorption and scattering. A fairly complete collection of the most important data on atmospheric transmittance in the 0.4 μm to 15 μm spectral region is presented. The effects of atmospheric turbulence on the propagation of imagery are described. A detailed analysis of the transfer of contrast by the atmosphere is presented, and its significance on the performance of electro-optical devices is emphasized.

DD FORM 1 NOV 68 1473 REPLACES DD FORM 1473, 1 JAN 64, WHICH IS OBSOLETE FOR ARMY USE.

UNCLASSIFIED
Security Classification

14. KEY WORDS	LINK A		LINK B		LINK C	
	ROLE	WT	ROLE	WT	ROLE	WT
Solar Radiation						
Airglow						
Moonlight						
Atmospheric Transmission						
Atmospheric Attenuation						
Atmospheric Contrast Transfer						
Night Sky Radiation						
Atmospheric Scattering						
Atmospheric Absorption						
Atmospheric Optics						
Atmospheric Optical Environment						
Environment						

1 4 42.741—Ft Belvoir

Reports Control Symbol OSD-1366

RESEARCH AND DEVELOPMENT TECHNICAL REPORT

ECOM-7023

ATMOSPHERIC OPTICAL ENVIRONMENT

by

Mishri L. Vatsia

VISIONICS TECHNICAL AREA
NIGHT VISION LABORATORY

Project 1S662709D617

September 1972

U. S. ARMY ELECTRONICS COMMAND
FORT MONMOUTH, NEW JERSEY

SUMMARY

A knowledge of the fundamental optical properties of the terrestrial atmospheric environment is essential for solving various problems in the multidisciplinary field of visionics including the areas of vision, psychology, atmospheric physics, infrared physics, simulation, astrogeophysics, and electro-optical technology. The aim of this report is to generalize the recent work of the author and to summarize the data from other world-wide sources published by the first quarter of 1972. This report includes a treatment of the atmospheric radiation, the atmospheric transmission, and the transfer of contrast by the atmosphere. The fundamental characteristics of the daytime and nighttime radiation including some important recent measurements of the solar, twilight, and nightglow radiation spectra are presented. An extensive chapter on atmospheric transmission includes the fundamental properties of the terrestrial atmosphere and basic principles of atmospheric absorption and scattering. A fairly compiete collection of the most important data on atmospheric transmittance in the 0.4 μm to 15 μm spectral region is presented. The effects of atmospheric turbulence on the propagation of imagery are described. A detailed analysis of the transfer of contrast by the atmosphere is presented, and its significance on the performance of electro-optical devices is emphasized.

FOREWORD

It is my pleasant duty to acknowledge the general guidance and moral support provided by Mr. John Johnson, Director, Visionics Technical Area, and Mr. Benjamin Goldberg, Director, Night Vision Laboratory, during the course of this study. I am indebted to many colleagues who provided constructive criticism and comments during this study. I am especially grateful to Dr. Robert W. Fenn and Mr. John E. A. Selby for their critical reviewing of the manuscript and many helpful suggestions. I am grateful to Mr. Harry Bibber who provided excellent artistic guidance on illustrations and to Betty L. Dobson for her patience in typing the original manuscript. The readers are requested to forward their constructive criticism and comments addressed to Director, Night Vision Laboratory, U. S. Army Electronics Command, Attn: AMSEL-NV VI (Dr. M. L. Vatsia), Fort Belvoir, Virginia 22060.

CONTENTS

CONTENTS (cont'd)

ILLUSTRATIONS

ILLUSTRATIONS (cont'd)

ILLUSTRATIONS (cont'd)

ILLUSTRATIONS (cont'd)

TABLES

ATMOSPHERIC OPTICAL ENVIRONMENT

I. ATMOSPHERIC RADIATION

1. Daytime Radiation. During the day, the predominant radiation on the earth is the solar radiation which is propagated to the earth through the intervening space and terrestrial atmosphere. The electromagnetic spectrum of the solar radiation extends in wavelengths from a fraction of an angstrom to hundreds of meters including the gamma and x-rays, and the ultraviolet, visible, infrared, micro, and radio waves. There are a number of publications which present interesting features of the solar radiation.[1-3] The earlier measurements of solar radiation were made mainly with ground-based instrumentation. However, recently, high-altitude aircraft, balloon, rocket, and space-borne instruments have been used for solar energy studies. The solar radiation incident on the earth's surface varies in magnitude and spectral composition due to the fluctuations in solar emissions, the attenuation of the atmosphere, and the variations in solar distance. The solar-distance variation produces a maximum change of ± 3.5 percent during the year in the solar irradiance on the earth's surface. The variations in the solar spectrum due to fluctuations in solar activity are comparatively much smaller in magnitude. The fluctuations in the *incoming solar radiation*, *insolation*, at a fixed location on the globe are mainly caused by the terrestrial atmosphere especially due to variations in the cloud cover, water vapor, and aerosols in the atmosphere.

The solar constant is the amount of total solar energy received per unit time per unit area exposed normally to the solar rays at the average sun-earth distance in the absence of the atmosphere. The spectral distribution of this energy as a function of wavelength is the solar spectral radiant incidance* (irradiance). Thekaekara has reported the latest state-of-the-art on the measurement and computation of the solar constant and the solar spectral radiant incidance.[4,5] Table I and Fig. 1 contain the NASA standard, solar spectral radiant incidance data as proposed by Thekaekara. The new NASA

---

*For radiometric nomenclature, the reader is referred to the proposed MIL Standard for Infrared Terms and Definitions, Part 1, Appendix C, of Final Report QL-TR-71-7, MICOM Contract DAAH01-71-C-0433, Ford-Philco Corporation, Aeronutronic Division, Newport Beach, Calif. 92663 (1971).

[1] K. Ya. Kondratyev, *Radiation in the Atmosphere*, Academic Press, New York (1969).

[2] N. Robinson, editor, *Solar Radiation*, Elsevier Publishing Company, New York (1966).

[3] J. W. T. Walsh, *The Science of Daylight*, Macdonald & Co., London (1961).

[4] M. P. Thekaekara, *J. Environmental Sci.* *13*, (4) 6 (1970).

[5] M. P. Thekaekara and A. J. Drummond, *Nature Physical Science* *229*, 6 (1971).

Table I. NASA Standard Solar Spectral Radiant Incidance (Irradiance)

λ - Wavelength in micrometers

E(λ) - Solar spectral irradiance averaged over small bandwidth centered at λ in $W\,m^{-2}\,\mu m^{-1}$

E(0-λ) - Area under the solar spectral irradiance curve in the wavelength range 0 to λ in $W\,m^{-2}$

D(0-λ) - Percentage of the solar constant associated with wavelengths shorter than λ

Solar Constant = 1353 $W\,m^{-2}$

λ	E(λ)	E(0-λ)	D(0-λ)	λ	E(λ)	E(0-λ)	D(0-λ)	λ	E(λ)	E(0-λ)	D(0-λ)
.120	.100	.0059999	.00044	.525	1852	352.591	26.059	1.70	207	1221.23	90.261
.140	.030	.0072999	.00053	.530	1842	361.826	26.742	1.75	188	1230.78	90.967
.150	.07	.00786	.00057	.535	1816	370.976	27.418	1.80	199	1239.2[illegible]	91.593
.160	.23	.00938	.00068	.540	1783	379.979	28.084	1.85	162	1246.78	92.149
.170	.63	.01368	.00100	.545	1794	388.821	28.737	1.90	126	1253.68	92.644
.180	1.25	.02388	.00169	.550	1725	397.519	29.380	1.95	114	1259.48	93.080
.190	2.71	.04288	.00316	.555	1720	406.131	30.017	2.00	103	1264.98	93.489
.210	10.7	.10989	.00811	.560	1695	414.649	30.644	2.10	90	1274.55	94.202
.219	22.9	.27785	.02052	.565	1705	423.163	31.276	2.20	79	1283.88	94.926
.220	57.5	.67985	.05024	.570	1712	431.711	31.907	2.30	69	1290.48	95.373
.225	64.9	.90585	.0728	.575	1719	440.289	32.541	2.4	62.0	1296.95	95.4560
.230	66.7	1.31485	.0971	.580	1715	448.874	33.176	2.5	55.0	1302.88	96.2903
.235	59.3	1.62985	.1204	.585	1712	457.441	33.809	2.6	48.0	1307.95	96.6710
.240	63.0	1.93568	.1438	.590	1708	465.971	34.439	2.7	43.0	1312.58	97.0073
.245	72.3	2.27385	.1688	.595	1682	474.426	35.064	2.8	39.0	1316.68	97.3113
.250	78.4	2.63868	.1944	.600	1646	482.796	35.683	2.9	35.0	1320.38	97.5838
.255	104	3.04668	.2266	.605	1647	491.079	36.295	3.0	31.0	1323.68	97.8277
.260	138	3.65168	.2698	.610	1635	499.264	36.902	3.1	28.0	1326.65	98.0383
.265	145	4.43918	.3288	.620	1602	515.669	38.098	3.2	22.6	1328.88	98.2179
.270	232	5.40168	.4051	.630	1570	531.329	39.278	3.3	19.2	1330.97	98.3724
.275	204	6.5716	.4857	.64	1544	546.899	40.421	3.4	16.6	1332.76	98.5067
.280	222	7.6366	.5644	.65	1511	562.176	41.558	3.5	14.6	1334.32	98.6288
.285	315	8.9791	.6638	.66	1488	577.159	42.657	3.6	13.5	1335.73	98.7238
.290	482	10.9716	.8109	.67	1456	591.863	43.744	3.7	12.3	1337.02	98.8192
.295	584	13.6366	1.0078	.68	1427	606.284	44.810	3.8	11.1	1338.19	98.9056
.300	514	16.3816	1.2107	.69	1402	620.429	45.855	3.9	10.3	1339.26	98.9847
.305	603	19.1761	1.4171	.70	1369	634.284	46.879	4.0	9.5	1340.25	99.0579
.310	689	22.4061	1.6558	.71	1344	647.849	47.882	4.1	8.7	1341.16	99.1252
.315	764	26.0366	1.9243	.72	1314	661.139	48.864	4.2	7.8	1341.98	99.1861
.320	838	30.0216	2.2188	.73	1290	674.159	49.826	4.3	7.1	1342.73	99.2412
.325	975	34.5341	2.552	.74	1260	686.909	50.769	4.4	6.50	1343.4141	99.291507
.330	1059	39.6191	2.928	.75	1235	699.384	51.691	4.5	5.90	1344.0341	99.337331
.335	1081	44.9691	3.323	.76	1211	711.614	52.595	4.6	5.38	1344.5941	99.378721
.340	1174	50.9366	3.721	.77	1185	723.594	53.480	4.7	4.88	1345.0991	99.416049
.345	1269	57.7141	4.117	.78	1159	735.314	54.346	4.8	4.50	1345.5641	99.450413
.350	1093	61.1191	4.517	.79	1134	746.779	55.194	4.9	4.10	1345.9841	99.481495
.355	1183	66.5531	4.919	.80	1109	757.994	56.023	5.0	3.83	1346.3906	99.511500
.360	1168	71.9366	5.316	.81	1085	768.964	56.834	6.0	1.75	1349.1806	99.717708
.365	1132	77.4366	5.723	.82	1060	779.694	57.627	7.0	.99	1350.5506	99.818965
.370	1181	83.2191	6.150	.83	1036	790.179	58.401	8.0	.60	1351.3456	99.877723
.375	1157	89.0641	6.582	.84	1013	800.419	59.158	9.0	.388	1351.8356	99.913939
.380	1120	94.7566	7.003	.85	998	810.434	59.899	10.0	.250	1352.1506	99.937221
.385	1298	100.3816	7.413	.86	988	820.224	60.622	11.0	.170	1352.3606	99.952742
.390	1298	106.7416	7.819	.87	967	829.799	61.330	12.0	.120	1352.5056	99.963459
.395	1149	111.5891	8.241	.88	926	839.164	62.022	13.0	.087	1352.6091	99.971108
.400	1429	118.0541	8.725	.89	904	848.334	62.700	14.0	.055	1352.6881	99.976956
.405	1644	125.7266	9.293	.90	891	857.329	63.365	15.0	.049	1352.7321	99.980199
.410	1751	134.2241	9.920	.91	880	866.184	64.019	16.0	.038	1352.7746	99.983414
.415	1776	143.0366	10.571	.92	869	874.929	64.665	17.0	.031	1352.8101	99.985964
.420	1767	151.8391	11.222	.93	858	883.564	65.304	18.0	.024	1352.8376	99.987997
.425	1693	160.4341	11.858	.94	847	892.08	65.934	19.0	.02088	1352.8596	99.989623
.430	1629	168.7691	12.473	.95	837	900.58	66.556	20.0	.01680	1352.8776	99.990953
.435	1663	177.0241	13.083	.96	828	908.79	67.168	25.0	.00618	1352.9328	99.995337
.440	1810	185.7066	13.725	.97	803	916.98	67.766	30.0	.00308	1352.9656	99.996718
.445	1922	195.0366	14.415	.98	785	926.84	68.355	35.0	.00160	1352.9871	99.997568
.450	2026	204.8566	15.140	.99	767	932.60	68.928	40.0	.00094	1352.9934	99.998037
.455	2057	215.0141	15.901	1.00	760	940.18	69.488	50.0	.00038	1352.9980	99.998525
.460	2066	225.3216	16.653	1.05	668	975.58	72.105	60.0	.00019	1352.9829	99.998736
.465	2048	235.6866	17.413	1.10	593	1007.10	74.435	80.0	.00007	1352.9895	99.999020
.470	2073	246.4891	18.167	1.15	539	1035.30	76.519	100.0	.00003	1352.9965	99.999082
.475	2044	256.881	18.921	1.20	485	1060.80	78.404	1000.0	.00000	1353.0000	100.000000
.480	2074	266.296	19.681	1.25	438	1083.80	80.109				
.485	1978	276.621	21.438	1.30	397	1104.75	81.652				
.490	1958	286.236	21.155	1.35	358	1123.63	83.047				
.495	1988	296.011	21.878	1.40	337	1141.08	84.331				
.500	1962	305.796	22.599	1.45	312	1157.23	85.530				
.505	1928	315.421	23.312	1.50	288	1172.23	86.639				
.510	1902	324.926	24.015	1.55	267	1186.18	87.665				
.515	1933	334.214	24.701	1.60	245	1198.98	88.611				
.520	1933	343.373	25.379	1.65	223	1210.68	89.475				

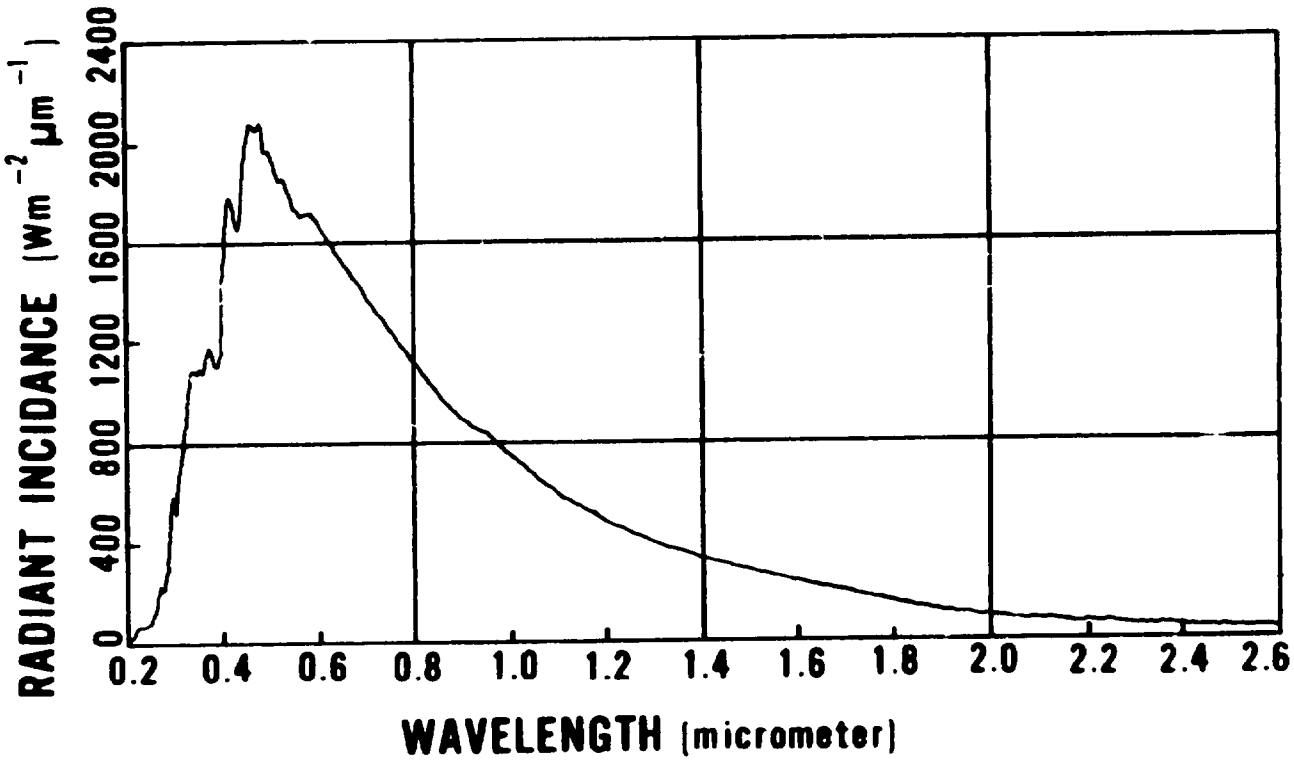

Fig. 1. The solar spectral radiant incidance (irradiance) NASA standard (Thekaekara).

Standard of solar constant is 135.3 mW cm^{-2} (1.940 calories cm^{-2} min^{-1}) with an error of ± 1%. The solar constant value of 139.5 mW cm^{-2} (2 cal cm^{-2} min^{-1}) proposed by Johnson in 1954 is about 3% higher than the new NASA Standard.[6] The wavelength range of 0.22 micrometer to 15.0 micrometers contains 99.98% of the solar energy out of which the 0.22- to 0.38-micrometer (ultraviolet) region contains 7.0%, the 0.38- to 0.72-micrometer (visible) region contains 41.86%, and the 0.72- to 15.0-micrometer (infrared) region contains 51.12% of the total solar energy.

The spectral or total solar radiant incidance E at a horizontal plane at any time at a given geographical location at a solar distance R is given by

$$E = E_o (R_o/R)^2 \cos z \qquad (1)$$

where E_o is the solar constant at normal incidence at the average solar distance R_o (one astronomical unit), and z is the solar zenith angle. The factor $(R_o/R)^2$ depends upon the position of the earth in its orbit around the sun. McCullough suggests that to a good approximation $(R_o/R)^2 = 1 + 2e \cos (2\pi D/365)$ where e is the eccentricity of the earth's orbit (0.01675) and D is the day of the year.[7] The annual variation of factor $(R_o/R)^2$, the inverse squared solar distance measured in astronomical units, is small as compared to the variations in cos z which is the principal factor determining the horizontal-plane solar radiant incidance. The zenith angle z may be expressed in terms of the astronomical coordinate variables using the spherical astronomy relation:[8]

$$\cos z = \sin \delta \sin \phi + \cos \delta \cos \phi \cos h, \qquad (2)$$

where δ is the declination, ϕ is the geographical coordinate latitude of the location, and h is the time of the day in hour angles.

The annual variation of daily totals of solar radiation in the absence of atmosphere at different latitudes is presented in Fig. 2 on a 3-coordinate graph. The vertical coordinates of the surface are proportional to the daily totals of incident solar energy for the corresponding latitude and season of the year. The terrestrial atmosphere attenuates the incoming solar radiation even under "clear" conditions due to scattering and absorption by atmospheric gaseous molecules and aerosols. Atmospheric transmission of electromagnetic radiation is a wavelength-dependent function. (This subject will be discussed in more detail in a later chapter.)

---

[6] F. S. Johnson, *J. Meteorol. 11*, 431 (1954).

[7] E. C. McCullough, *Arch. Met. Geophys. Biokl. Ser. B 16*, 129 (1968).

[8] I. I. Mueller and H. Eichhorn, *Spherical and Practical Astronomy*, Frederick Ungar Publishing Co., New York (1969).

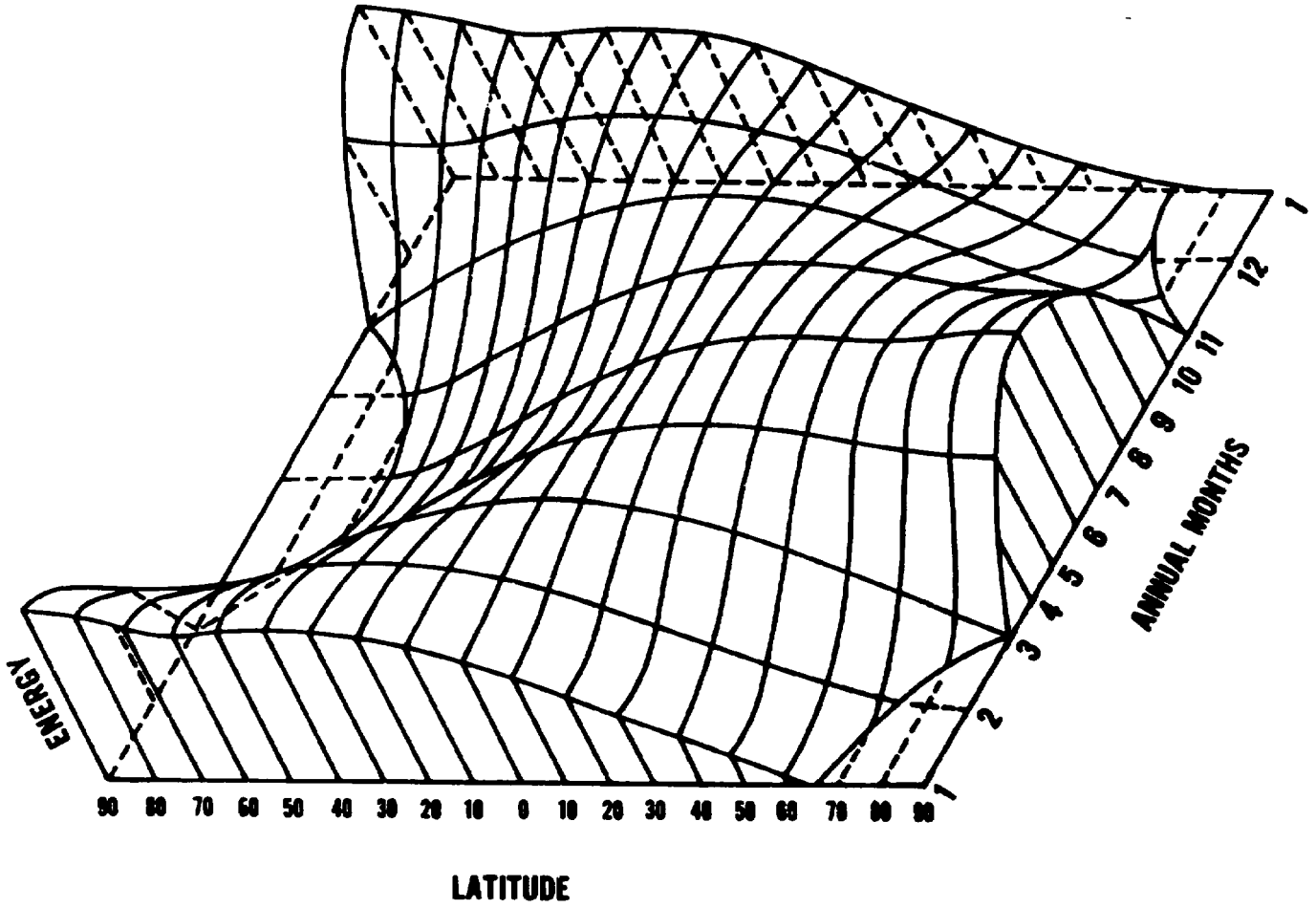

Fig. 2. The annual variation of insolation for different latitudes on the earth (adapted from Kondratyev).

In the presence of the terrestrial atmosphere, the spectral radiant incidance due to direct solar radiation is reduced while the atmospheric gases and aerosols produce diffuse sky radiation due to scattering of some of the direct solar radiation. The reduction of direct incoming solar radiation depends upon the optical path which the radiation has traveled within the terrestrial atmosphere. When the solar radiation is incident normally on the earth's surface, the optical air mass is unity. If the earth were flat and no refraction took place, the effect of radiation incident on any angle z from the normal would be to reduce the incident radiation by an air-mass factor equal to secant z. This is a good approximation until z approaches 80°. At greater zenith angles, the secant gives values which are increasingly too high because of errors due to atmospheric refraction, curvature of the earth, etc. The air mass m has been calculated by F. Kasten using corrections for the variations of refractive index.[9] Table II gives values of optical air mass as a function of solar altitude. In any transparent, homogeneous medium, the optical transmittance T through an optical path length R is given by

$$T_R = \exp(-\alpha R) \tag{3}$$

where α is the attenuation coefficient per unit optical path length.

For R = 1, $$T_1 = \exp(-\alpha), \tag{4}$$

therefore, $$T_R = T_1^R. \tag{5}$$

In the case of the earth's atmosphere, if T_1 is the atmospheric transmission for a unit air mass, then the atmospheric transmission T_m through a slant optical path involving air mass m will be given by

$$T_m = (T_1)^m . \tag{6}$$

The spectral radiant incidance (irradiance) E_λ due to the attenuation of the direct sunlight by the terrestrial atmosphere is given by

$$E_\lambda = E_{o\lambda} [T_{1\lambda}]^m , \tag{7}$$

where $E_{o\lambda}$ is the spectral radiant incidance for zero air mass, $T_{1\lambda}$ is the vertical, atmospheric transmittance for unit air mass, and m is the air mass between the sun and the point of incidence. The vertical, integral, atmospheric transmittance for unit mass for the visible range is 0.796. This is based upon the relation:[10]

[9] F. Kasten, "A New Table and Approximation Formula for the Relative Optical Air Mass," *Archiv für Meteorologie, Geophysik und Bioklimatologie, B-14*, 206 (1965).

[10] J. W. T. Walsh, *The Science of Daylight*, Macdonald & Co., London (1961).

Table II. Relative Optical Air Mass m(A) as a Function of Solar Altitude A.
Computed on the Basis of the ARDC Model Atmosphere, 1959 (F. Kasten)

A (deg)	m (A)	A (deg)	m (A)	A (deg)	m (A)	A (deg)	m (A)	A (deg)	m (A)	A (deg)	m (A)
0	36.2648	7.4	7.3589	12.3	4.5989	17.2	3.3467	24.2	2.4273	40	1.5535
0.5	31.3898	7.5	7.2707	12.4	4.5639	17.3	3.3283	24.4	2.4088	40.5	1.5376
1	26.3150	7.6	7.1845	12.5	4.5294	17.4	3.3102	24.6	2.3907	41	1.5222
1.5	22.4570	7.7	7.1003	12.6	4.4954	17.5	3.2923	24.8	2.3728	41.5	1.5072
2	19.4601	7.8	7.0179	12.7	4.4619	17.6	3.2745	25	2.3552	42	1.4926
2.5	17.0884	7.9	6.9375	12.8	4.4290	17.7	3.2570	25.2	2.3379	42.5	1.4784
3	15.1796	8	6.8587	12.9	4.3965	17.8	3.2397	25.4	2.3209	43	1.4646
3.1	14.8427	8.1	6.7817	13	4.3645	17.9	3.2225	25.6	2.3042	43.5	1.4511
3.2	14.5189	8.2	6.7064	13.1	4.3329	18	3.2056	25.8	2.2877	44	1.4380
3.3	14.2076	8.3	6.6327	13.2	4.3019	18.1	3.1888	26	2.2715	44.5	1.4252
3.4	13.9080	8.4	6.5605	13.3	4.2712	18.2	3.1722	26.2	2.2555	45	1.4128
3.5	13.6196	8.5	6.4899	13.4	4.2410	18.3	3.1558	26.4	2.2398	45.5	1.4007
3.6	13.3419	8.6	6.4207	13.5	4.2113	18.4	3.1396	26.6	2.2243	46	1.3888
3.7	13.0743	8.7	6.3530	13.6	4.1819	18.5	3.1236	26.8	2.2091	46.5	1.3773
3.8	12.8162	8.8	6.2866	13.7	4.1530	18.6	3.1076	27	2.1941	47	1.3661
3.9	12.5673	8.9	6.2216	13.8	4.1245	18.7	3.0919	27.2	2.1793	47.5	1.3552
4	12.3271	9	6.1579	13.9	4.0963	18.8	3.0763	27.4	2.1648	48	1.3445
4.1	12.0951	9.1	6.0955	14	4.0686	18.9	3.0609	27.6	2.1505	48.5	1.3341
4.2	11.8710	9.2	6.0343	14.1	4.0412	19	3.0457	27.8	2.1363	49	1.3240
4.3	11.6545	9.3	5.9743	14.2	4.0142	19.1	3.0306	28	2.1224	49.5	1.3141
4.4	11.4451	9.4	5.9154	14.3	3.9876	19.2	3.0157	28.2	2.1087	50	1.3045
4.5	11.2426	9.5	5.8577	14.4	3.9613	19.3	3.0009	28.4	2.0952	51	1.2859
4.6	11.0466	9.6	5.8011	14.5	3.9354	19.4	2.9863	28.6	2.0819	52	1.2682
4.7	10.8568	9.7	5.7456	14.6	3.9098	19.5	2.9719	28.8	2.0688	53	1.2514
4.8	10.6731	9.8	5.6911	14.7	3.8846	19.6	2.9576	29	2.0559	54	1.2354
4.9	10.4950	9.9	5.6376	14.8	3.8597	19.7	2.9434	29.2	2.0431	55	1.2202
5	10.3224	10	5.5851	14.9	3.8351	19.8	2.9294	29.4	2.0306	56	1.2057
5.1	10.1551	10.1	5.5336	15	3.8108	19.9	2.9155	29.6	2.0182	57	1.1918
5.2	9.9927	10.2	5.4829	15.1	3.7868	20	2.9017	29.8	2.0060	58	1.1787
5.3	9.8352	10.3	5.4332	15.2	3.7632	20.2	2.8746	30	1.9939	59	1.1662
5.4	9.6822	10.4	5.3844	15.3	3.7398	20.4	2.8481	30.5	1.9645	60	1.1543
5.5	9.5337	10.5	5.3365	15.4	3.7168	20.6	2.8220	31	1.9361	61	1.1430
5.6	9.3894	10.6	5.2894	15.5	3.6940	20.8	2.7965	31.5	1.9087	62	1.1322
5.7	9.2492	10.7	5.2431	15.6	3.6715	21	2.7714	32	1.8822	63	1.1220
5.8	9.1129	10.8	5.1976	15.7	3.6493	21.2	2.7469	32.5	1.8565	64	1.1123
5.9	8.9804	10.9	5.1529	15.8	3.6274	21.4	2.7227	33	1.8317	65	1.1031
6	8.8514	11	5.1089	15 9	3.6058	21.6	2.6991	33.5	1.8076	66	1.0944
6.1	8.7260	11.1	5.0657	16	3.5844	21 8	2.6758	34	1.7843	67	1.0862
6.2	8.6039	11.2	5.0232	16.1	3.5632	22	2.6530	34.5	1.7617	68	1.0784
6.3	8.4850	11.3	4.9814	16.2	3.5424	22.2	2.6306	35	1.7398	69	1.0710
6.4	8.3692	11.4	4.9403	16.3	3.5217	22.4	2.6087	35.5	1.7186	70	1.0640
6.5	8.2564	11.5	4.8999	16.4	3.5014	22.6	2.5871	36	1.6980	71	1.0575
6.6	8.1464	11.6	4.8602	16.5	3.4812	22.8	2.5659	36.5	1.6780	72	1.0513
6.7	8.0392	11.7	4.8210	16.6	3.4613	23	2.5450	37	1.6587	73	1.0456
6.8	7.9347	11.8	4.7825	16.7	3.4416	23.2	2.5245	37.5	1.6398	74	1.0402
6.9	7.8328	11.9	4.7446	16.8	3.4222	23.4	2.5044	38	1.6216	75	1.0352
7	7.7334	12	4.7073	16.9	3.4030	23.6	2.4846	38.5	1.6038	80	1.0154
7.1	7.6364	12.1	4.6706	17	3.3840	23.8	2.4652	39	1.5865	85	1.0038
7.2	7.5417	12.2	4.6345	17.1	3.3652	24	2.4461	39.5	1.5698	90	1.0000
7.3	7.4492										

$$T_{1v} = \Sigma E_{o\lambda} T_\lambda V_\lambda / \Sigma E_{o\lambda} V_\lambda , \qquad (8)$$

where T_{1v} is the integral, vertical, atmospheric transmittance for the visible solar radiation for unit air mass, V_λ is the spectral, luminous efficiency of radiation, and T_λ is the vertical, spectral transmittance of the atmosphere. The spectral atmospheric transmittance for a unit optical air mass T_λ is a variable function dependent upon the composition of the highly variable constituents of the atmosphere, namely water vapor, ozone, and aerosols at the time of measurement. Table III gives a typical set of atmospheric transmittance data based upon earlier measurements reported in the literature.[11] Figure 3 shows the spectral distribution of solar radiant incidance at sea level for one optical air mass.[12]

The spectral luminous efficiency V_λ for photopic vision (light-adapted vision) and V'_λ for scotopic vision (dark-adapted vision), is given in Table IV. These values are based upon a "standard" observer.[13] Interpolated values of spectral luminous efficiency at 1-nanometer intervals are available in the literature.[14] [15] An actual normal observer may have significantly different spectral luminous efficiency.[16]

During the period 1943-1947, Brown made worldwide photometric measurements of daytime and nighttime natural illumination as a function of solar altitude.[17] Figure 4 contains Brown's basic curves for horizontal luminous incidance (illuminance) as a function of solar and lunar altitude and various phases of the moon. These curves give average luminous incidance levels for "clear" environments. Table V gives values of average luminous incidance in footcandles for the entire range of solar altitudes from -90° to +90°. At a particular geographic location, the altitude of the sun is calculated using the relation,

$$A = \sin^{-1} [\sin \delta \sin \phi + \cos \delta \cos \phi \cos h]. \qquad (9)$$

---

[11] J. W. T. Walsh, *The Science of Daylight*, Macdonald & Co., London (1961).

[12] S. L. Valley, *Handbook of Geophysics and Space Environments*, McGraw-Hill, New York (1965).

[13] *International Lighting Vocabulary*, Third Edition, International Commission on Illumination (CIE), Paris (1970).

[14] Y. Le Grand, *Light, Colour and Vision*, translated by R. W. G. Hunt, J. W. T. Walsh, and F. R. W. Hunt, Chapman and Hall Ltd., London (1968).

[15] J. W. T. Walsh, *Photometry*, Third Edition, Constable & Company Ltd., London (1958).

[16] Y. Le Grand, *Loc. cit.*

[17] D. R. E. Brown, *Natural Illumination Charts*, Report No. 374-1, Department of the Navy, Bureau of Ships, Washington, D. C. (1952).

Table III. Vertical Atmospheric Transmittance for a Unit Optical Air Mass

WAVELENGTH (MICROMETER)	TRANSMITTANCE	WAVELENGTH (MICROMETER)	TRANSMITTANCE
0.36	0.489	0.56	0.797
0.37	0.516	0.57	0.800
0.38	0.547	0.58	0.801
0.39	0.575	0.59	0.804
0.40	0.600	0.60	0.813
0.41	0.624	0.61	0.822
0.42	0.644	0.62	0.830
0.43	0.663	0.63	0.843
0.44	0.685	0.64	0.853
0.45	0.703	0.65	0.862
0.46	0.718	0.66	0.869
0.47	0.733	0.67	0.877
0.48	0.746	0.68	0.883
0.49	0.759	0.69	0.824
0.50	0.768	0.70	0.888
0.51	0.777	0.71	0.884
0.52	0.783	0.72	0.789
0.53	0.788	0.73	0.860
0.54	0.795	0.74	0.905
0.55	0.796	0.75	0.838

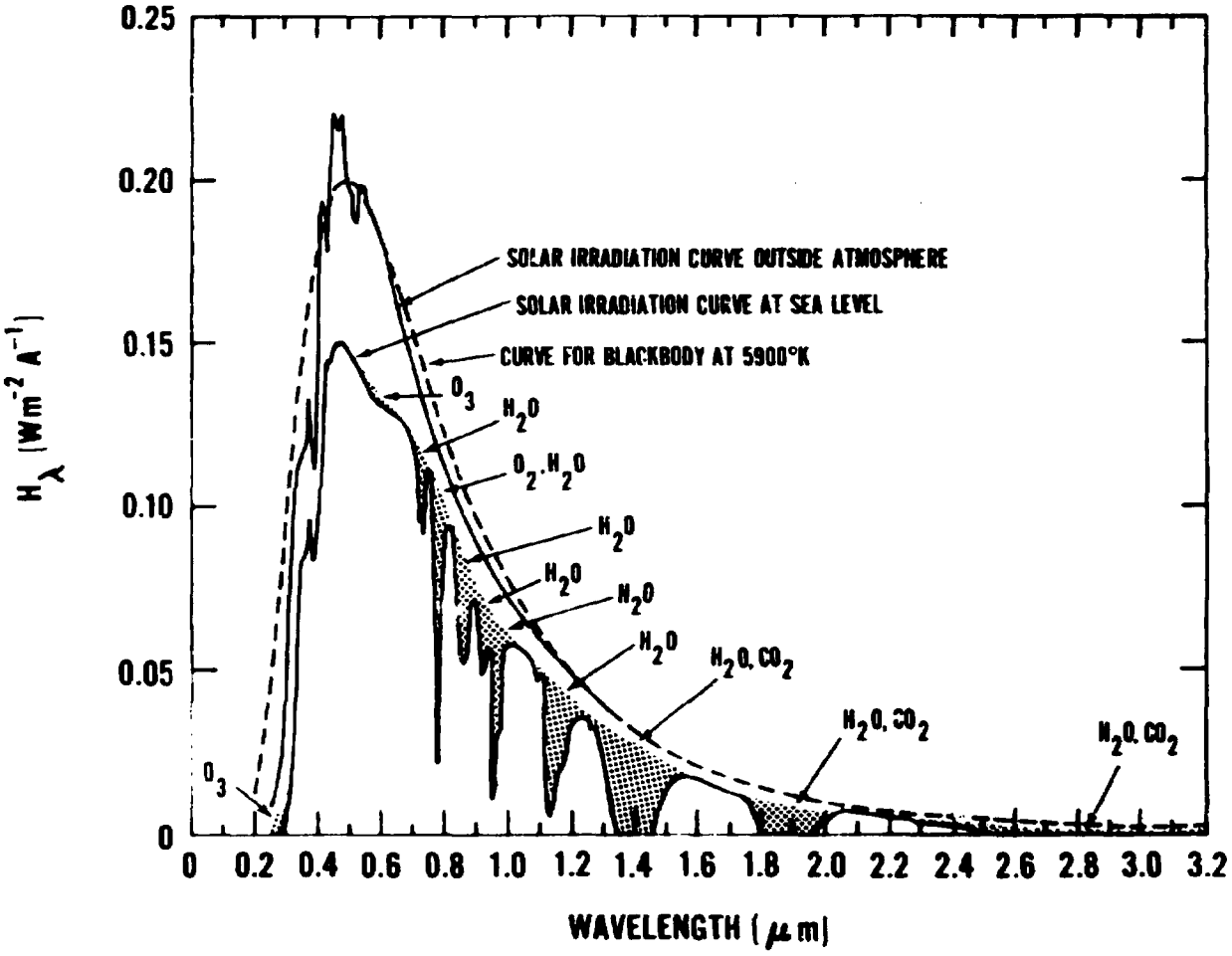

Fig. 3. The solar spectral radiant incidance (irradiance) at sea level for one air mass absorption by atmospheric constituents is indicated by shaded areas (Valley).

Table IV. Spectral Luminous Efficiency for the CIE Standard Observer
(From International Lighting Vocabulary)

WAVELENGTH (NANOMETERS)	LUMINOUS EFFICIENCY FOR PHOTOPIC VISION V_λ	LUMINOUS EFFICIENCY FOR SCOTOPIC VISION V'_λ
380	0.000 0	0.000 589
390	0.000 1	0.002 209
400	0.000 4	0.009 29
410	0.001 2	0.034 84
420	0.004 0	0.096 6
430	0.011 6	0.199 8
440	0.023	0.328 1
450	0.038	0.455
460	0.060	0.567
470	0.091	0.676
480	0.139	0.793
490	0.208	0.904
500	0.323	0.982
510	0.503	0.997
520	0.710	0.935
530	0.862	0.811
540	0.954	0.650
550	0.995	0.481
560	0.995	0.328 8
570	0.952	0.207 6
580	0.870	0.121 2
590	0.757	0.065 5
600	0.631	0.033 15
610	0.503	0.015 93
620	0.381	0.007 37
630	0.265	0.003 335
640	0.175	0.001 497
650	0.107	0.000 677
660	0.061	0.000 312 9
670	0.032	0.000 148 0
680	0.017	0.000 071 5
690	0.008 2	0.000 035 33
700	0.004 1	0.000 017 80
710	0.002 1	0.000 009 14
720	0.001 05	0.000 004 78
730	0.000 52	0.000 002 546
740	0.000 25	0.000 001 379
750	0.000 12	0.000 000 760
760	0.000 06	0.000 000 425
770	0.000 03	0.000 000 241
780	0.000 015	0.000 000 139

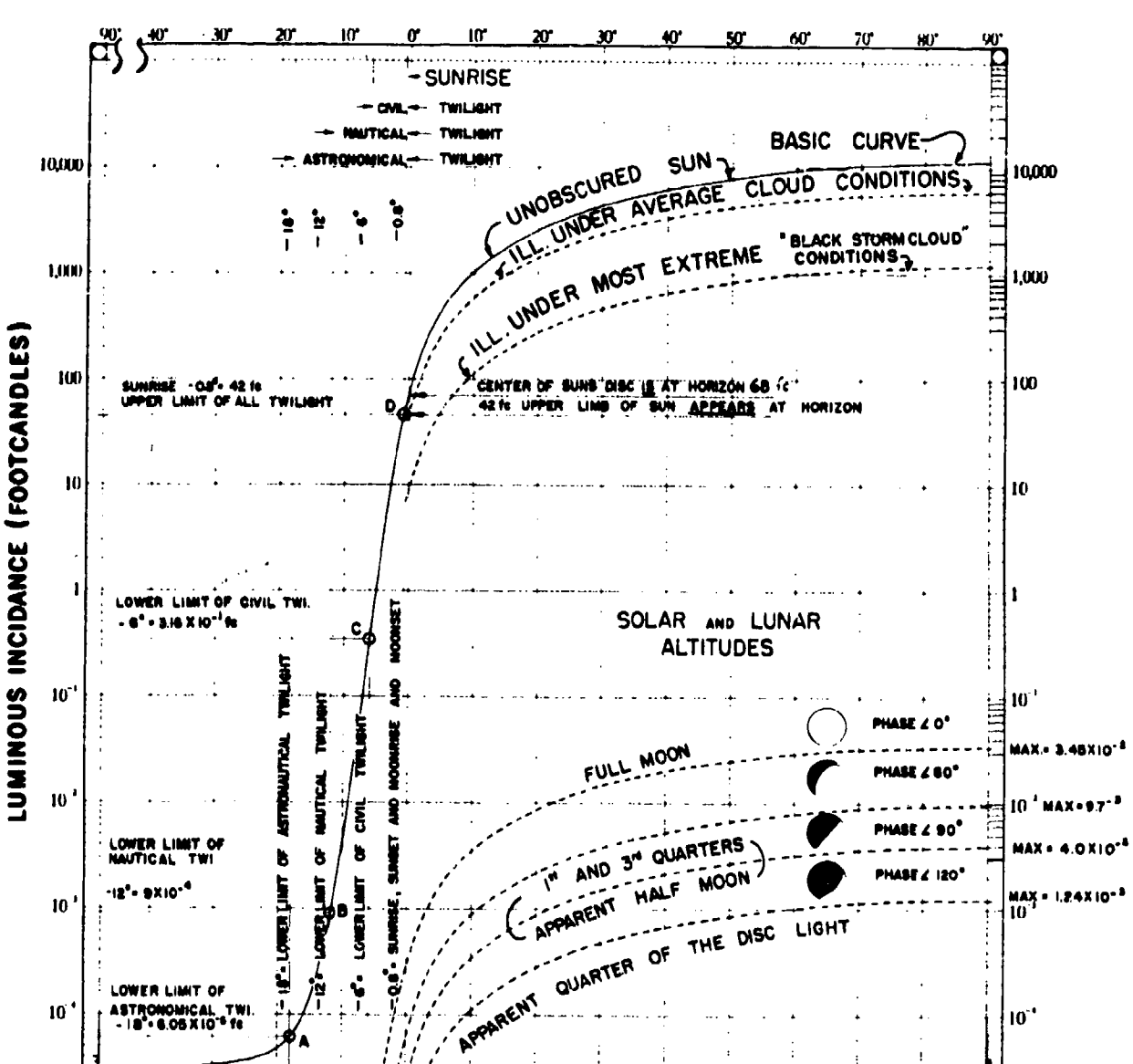

Fig. 4. Natural luminous incidance (illuminance) as a function of solar and lunar altitude and for various phases of the moon as measured by Brown.

Table V. Horizontal Luminous Incidance for Various Solar Altitudes (Brown)

-90°	2.80×10⁻⁴	-20°	4.77×10⁻³	-10°	4.30×10⁻²	0°	6.80	10°	1015	20°	2540	30°	4370	40°	6200	50°	7900	60°	9450
-89°		.9	481	.9	4.73	.1	71.9	.1	1028	.1	2555	.1	4390	.1	6220	.1	7920	.1	9460
-88°		.8	4.86	.8	5.20	.2	76.0	.2	1040	.2	2575	.2	4410	.2	6230	.2	7940	.2	9470
-87°		.7	4.90	.7	5.73	.3	80.3	.3	1053	.3	2595	.3	4430	.3	6250	.3	7950	.3	9480
-86°		.6	4.95	.6	6.32	.4	84.8	.4	1068	.4	2610	.4	4450	.4	6270	.4	7970	.4	9500
-85°		.5	500	.5	6.97	.5	89.3	.5	1082	.5	2625	.5	4460	.5	6290	.5	7990	.5	9510
-84°		.4	505	.4	7.70	.6	94.2	.6	1096	.6	2645	.6	4480	.6	6300	.6	8000	.6	9520
-83°		.3	511	.3	8.50	.7	99.3	.7	1103	.7	2660	.7	4500	.7	6320	.7	8020	.7	9530
-82°		.2	516	.2	9.40	.8	105	.8	1123	.8	2675	.8	4520	.8	6340	.8	8040	.8	9540
-81°		.1	522	.1	1.04×10⁻¹	.9	110	.9	1136	.9	2690	.9	4540	.9	6350	.9	8050	.9	9550
-80°		-19°	528	-9°	1.16	1°	116	11°	1150	21°	2705	31°	4560	41°	6370	51°	8070	61°	9570
-79°		.9	534	.9	1.28	.1	121	.1	1162	.1	2725	.1	4580	.1	6390	.1	8080	.1	9580
-78°		.8	541	.8	1.43	.2	128	.2	1178	.2	2745	.2	4600	.2	6410	.2	8100	.2	9600
-77°	2.80×10⁻³	.7	548	.7	1.57	.3	134	.3	1193	.3	2760	.3	4620	.3	6420	.3	8120	.3	9610
-76°	2.81×10⁻³	.6	555	.6	1.74	.4	140	.4	1205	.4	2780	.4	4640	.4	6440	.4	8140	.4	9620
-75°		.5	562	.5	1.93	.5	148	.5	1220	.5	2795	.5	4660	.5	6460	.5	8160	.5	9630
-74°		.4	570	.4	2.13	.6	155	.6	1235	.6	2810	.6	4680	.6	6480	.6	8180	.6	9640
-73°		.3	578	.3	2.37	.7	161	.7	1250	.7	2830	.7	4700	.7	6490	.7	8190	.7	9660
-72°		.2	587	.2	2.63	.8	168	.8	1262	.8	2845	.8	4710	.8	6510	.8	8210	.8	9670
-71°		.1	595	.1	2.93	.9	175	.9	1275	.9	2860	.9	4730	.9	6530	.9	8220	.9	9680
-70°	2.81×10⁻³	-18°	605	-8°	3.25	2°	183	12°	1290	22°	2875	32°	4750	42°	6540	52°	8240	62°	9690
-69°	2.82	.9	615	.9	3.62	.1	191	.1	1303	.1	2895	.1	4770	.1	6560	.1	8260	.1	9700
-68°	2.83	.8	625	.8	4.02	.2	199	.2	1315	.2	2910	.2	4790	.2	6580	.2	8270	.2	9710
-67°		.7	636	.7	4.49	.3	206	.3	1329	.3	2930	.3	4810	.3	6590	.3	8290	.3	9720
-66°	2.83	.6	647	.6	5.00	.4	215	.4	1342	.4	2945	.4	4830	.4	6610	.4	8310	.4	9730
-65°	2.84	.5	660	.5	5.60	.5	222	.5	1356	.5	2960	.5	4850	.5	6630	.5	8330	.5	9750
-64°		.4	673	.4	6.27	.6	231	.6	1370	.6	2980	.6	4870	.6	6640	.6	8340	.6	9760
-63°	2.84	.3	686	.3	7.01	.7	239	.7	1385	.7	3000	.7	4880	.7	6660	.7	8360	.7	9770
-62°	2.85	.2	700	.2	7.88	.8	248	.8	1400	.8	3015	.8	4900	.8	6670	.8	8380	.8	9780
-61°	2.85	.1	715	.1	8.85	.9	256	.9	1415	.9	3035	.9	4920	.9	6690	.9	8400	.9	9790
-60°	2.86	-17°	730	-7°	10⁻¹	3°	263	13°	1430	23°	3050	33°	4940	43°	6710	53°	8410	63°	9800
-59°	2.86	.9	747	.9	1.12	.1	274	.1	1446	.1	3070	.1	4960	.1	6730	.1	8430	.1	9810
-58°	2.87	.8	765	.8	1.26	.2	282	.2	1460	.2	3090	.2	4980	.2	6750	.2	8440	.2	9820
-57°	2.87	.7	783	.7	1.41	.3	290	.3	1475	.3	3105	.3	4990	.3	6760	.3	8460	.3	9830
-56°	2.88	.6	803	.6	1.58	.4	298	.4	1490	.4	3125	.4	5010	.4	6780	.4	8480	.4	9840
-55°	2.88	.5	823	.5	1.77	.5	307	.5	1504	.5	3145	.5	5030	.5	6800	.5	8490	.5	9850
-54°	2.89	.4	845	.4	1.98	.6	316	.6	1518	.6	3165	.6	5050	.6	6810	.6	8510	.6	9860
-53°	2.90	.3	869	.3	2.23	.7	324	.7	1532	.7	3180	.7	5070	.7	6830	.7	8530	.7	9870
-52°	2.91	.2	895	.2	2.51	.8	333	.8	1545	.8	3200	.8	5080	.8	6850	.8	8540	.8	9880
-51°	2.92	.1	924	.1	2.81	.9	342	.9	1560	.9	3215	.9	5100	.9	6870	.9	8560	.9	9890
-50°	2.93	-16°	957	-6°	3.16	4°	350	14°	1575	24°	3230	34°	5120	44°	6880	54°	8580	64°	9900
-49°	2.94	.9	990	.9	3.53	.1	359	.1	1590	.1	3250	.1	5140	.1	6900	.1	8600	.1	9910
-48°	2.95	.8	1.02×10⁻⁰	.8	3.97	.2	368	.2	1604	.2	3265	.2	5160	.2	6920	.2	8610	.2	9920
-47°	2.96	.7	106	.7	4.47	.3	377	.3	1618	.3	3285	.3	5170	.3	6930	.3	8630	.3	9930
-46°	2.97	.6	110	.6	5.01	.4	386	.4	1635	.4	3305	.4	5190	.4	6950	.4	8650	.4	9940
-45°	2.98	.5	114	.5	5.61	.5	396	.5	1650	.5	3320	.5	5210	.5	6970	.5	8670	.5	9950
-44°	2.99	.4	118	.4	6.30	.6	404	.6	1665	.6	3340	.6	5230	.6	6980	.6	8680	.6	9960
-43°	3.00	.3	123	.3	7.08	.7	414	.7	1680	.7	3360	.7	5250	.7	7000	.7	8700	.7	9970
-42°	3.01	.2	128	.2	7.94	.8	424	.8	1695	.8	3380	.8	5260	.8	7010	.8	8710	.8	9980
-41°	3.02	.1	134	.1	8.90	.9	432	.9	1710	.9	3395	.9	5280	.9	7030	.9	8730	.9	9990
-40°	3.04	-15°	1.40	-5°	1.00	5°	442	15°	1725	25°	3410	35°	5300	45°	7050	55°	8740	65°	10000
-39°	3.06	.9	146	.9	1.11	.1	452	.1	1740	.1	3430	.1	5320	.1	7060	.1	8750	66°	10100
-38°	3.08	.8	1.52	.8	1.24	.2	462	.2	1755	.2	3460	.2	5340	.2	7080	.2	8770	67°	10200
-37°	3.10	.7	159	.7	1.38	.3	472	.3	1770	.3	3475	.3	5350	.3	7100	.3	8780	68°	10300
-36°	3.12	.6	167	.6	1.54	.4	482	.4	1785	.4	3495	.4	5370	.4	7120	.4	8800	69°	10400
-35°	3.14	.5	175	.5	1.72	.5	492	.5	1805	.5	3510	.5	5390	.5	7130	.5	8820	70°	10480
-34°	3.17	.4	1.83	.4	1.93	.6	501	.6	1820	.6	3530	.6	5410	.6	7150	.6	8840	71°	10570
-33°	3.20	.3	1.92	.3	2.13	.7	512	.7	1835	.7	3550	.7	5420	.7	7170	.7	8850	72°	10650
-32°	3.23	.2	202	.2	2.37	.8	522	.8	1855	.8	3570	.8	5440	.8	7190	.8	8860	73°	10720
-31°	3.27	.1	2.12	.1	2.60	.9	533	.9	1870	.9	3585	.9	5460	.9	7200	.9	8880	74°	10800
-30°	3.32	-14°	224	-4°	2.92	6°	543	16°	1885	26°	3600	36°	5480	46°	7220	56°	8890	75°	10870
-29°	3.36	.9	235	.9	3.23	.1	554	.1	1900	.1	3620	.1	5500	.1	7240	.1	8900	76°	10930
-28°	3.42	.8	248	.8	3.61	.2	566	.2	1915	.2	3640	.2	5510	.2	7250	.2	8920	77°	11000
-27°	3.48	.7	262	.7	3.96	.3	577	.3	1930	.3	3660	.3	5530	.3	7270	.3	8940	78°	11060
-26°	3.56	.6	276	.6	4.38	.4	587	.4	1945	.4	3680	.4	5550	.4	7290	.4	8950	79°	11110
-25°	3.66	.5	292	.5	4.84	.5	599	.5	1960	.5	3700	.5	5570	.5	7310	.5	8970	80°	11180
-24°	3.78	.4	308	.4	5.34	.6	610	.6	1975	.6	3720	.6	5590	.6	7320	.6	8980	81°	11220
-23°	3.94	.3	327	.3	5.90	.7	621	.7	1990	.7	3740	.7	5600	.7	7340	.7	8990	82°	11280
-22°	4.14	.2	347	.2	6.48	.8	633	.8	2005	.8	3760	.8	5620	.8	7360	.8	9010	83°	11310
-21°	4.41	.1	368	.1	7.10	.9	642	.9	2020	.9	3775	.9	5640	.9	7370	.9	9030	84°	11350
		-13°	392	-3°	7.80	7°	653	17°	2045	27°	3790	37°	5660	47°	7390	57°	9040	85°	11380
		.9	415	.9	8.55	.1	664	.1	2060	.1	3810	.1	5680	.1	7410	.1	9060	86°	11420
		.8	444	.8	9.35	.2	676	.2	2075	.2	3830	.2	5700	.2	7420	.2	9070	87°	11450
		.7	473	.7	10.2	.3	687	.3	2090	.3	3850	.3	5710	.3	7440	.3	9090	88°	11470
		.6	504	.6	11.1	.4	698	.4	2105	.4	3870	.4	5730	.4	7460	.4	9100	89°	11490
		.5	540	.5	12.1	.5	710	.5	2130	.5	3890	.5	5750	.5	7480	.5	9120	90°	11500
		.4	568	.4	13.1	.6	720	.6	2145	.6	3910	.6	5770	.6	7490	.6	9130		
		.3	620	.3	14.3	.7	732	.7	2160	.7	3930	.7	5790	.7	7510	.7	9140		
		.2	665	.2	15.5	.8	743	.8	2180	.8	3950	.8	5810	.8	7530	.8	9160		
		.1	716	.1	16.7	.9	754	.9	2195	.9	3965	.9	5820	.9	7540	.9	9170		
		-12°	772	-2°	180	8°	763	18°	2210	28°	3980	38°	5840	48°	7560	58°	9180		
		.9	832	.9	195	.1	776	.1	2225	.1	4000	.1	5860	.1	7580	.1	9200		
		.8	900	.8	210	.2	788	.2	2245	.2	4020	.2	5880	.2	7590	.2	9210		
		.7	972	.7	22.7	.3	800	.3	2260	.3	4040	.3	5890	.3	7610	.3	9230		
		.6	1.05×10⁻¹	.6	244	.4	811	.4	2275	.4	4060	.4	5910	.4	7630	.4	9240		
		.5	1.14	.5	26.2	.5	823	.5	2290	.5	4080	.5	5930	.5	7640	.5	9250		
		.4	1.24	.4	28.2	.6	835	.6	2310	.6	4100	.6	5950	.6	7660	.6	9270		
		.3	1.35	.3	30.2	.7	848	.7	2330	.7	4120	.7	5970	.7	7680	.7	9280		
		.2	1.46	.2	32.4	.8	859	.8	2345	.8	4140	.8	5990	.8	7690	.8	9300		
		.1	1.59	.1	34.6	.9	871	.9	2360	.9	4160	.9	6000	.9	7710	.9	9310		
		-11°	1.74	-1°	37.0	9°	882	19°	2375	29°	4160	39°	6020	49°	7730	59°	9320		
		-.9	1.88	-.9	39.5	.1	895	.1	2390	.1	4200	.1	6040	.1	7750	.1	9340		
		.8	2.03	.8	42.1	.2	907	.2	2405	.2	4220	.2	6060	.2	7760	.2	9350		
		.7	2.25	.7	44.7	.3	921	.3	2425	.3	4240	.3	6080	.3	7780	.3	9360		
		.6	2.46	.6	47.6	.4	935	.4	2440	.4	4260	.4	6090	.4	7800	.4	9370		
		.5	2.68	.5	50.6	.5	949	.5	2455	.5	4280	.5	6110	.5	7820	.5	9390		
		.4	2.94	.4	53.8	.6	962	.6	2470	.6	4300	.6	6130	.6	7330	.6	9400		
		.3	3.23	.3	57.2	.7	975	.7	2485	.7	4320	.7	6150	.7	7850	.7	9410		
		.2	3.55	.2	60.5	.8	989	.8	2505	.8	4340	.8	6160	.8	7870	.8	9430		
		-.1	3.90	-.1	64.2	.9	1000	.9	2520	.9	4350	.9	6180	.9	7880	.9	9440		

A is the altitude, δ the declination, ϕ the latitude, and h the time of the day in hour angles. *The Nautical Almanac, The Air Almanac,* and the *American Ephemeris and Nautical Almanac* issued by the Nautical Almanac Office of the United States Naval Observatory, Washington, D. C., are yearly publications containing the celestial coordinates of the sun and the moon and other useful astronomical data.

A very useful summary of solar-radiation observations for the major meteorological observation stations in the United States has been published by Atlas and Charles.[18] The vertical, atmospheric transmittance for various horizontal, visible ranges and other data are presented.

2. **Twilight Radiation.** The radiation scattered by the atmosphere when the sun is just below the horizon is called twilight radiation. The twilight period separates the interval between daytime and nighttime conditions of illumination. There are three periods into which the twilight interval is subdivided according to the general levels of illuminance. These are called the civil, nautical, and astronomical twilight periods. The civil twilight period is defined as the time interval between the instant when the apparent altitude of the upper solar limb is at 0° (astronomical horizon) and when the center of the solar disk is at -6°. Under the average, civil twilight conditions, there is enough illuminance to perform normal daytime activities. The nautical twilight period prevails when the apparent solar altitude is between 0° (upper limb) and -12° (center of solar disk). When the solar depression is between 9° and 12°, the illuminance is reduced considerably and, consequently, the horizontal, visible range is reduced to less than 400 meters. The brighter planets and stars begin to be visible in the sky from sea level. The astronomical twilight period extends during the interval when the apparent solar altitude is between 0° and -18°. When the solar depression is between 12 and 18 degrees below the horizon, there is insignificant illuminance for visual purposes but just too much scattered solar radiant incidance for proper astronomical observations. The actual conditions of ground-level illuminance during the twilight period will generally depend on the optical state of the atmosphere. According to another scheme, the twilight period is subdivided into three periods of civil, nautical, and astronomical twilight when the solar depression is between $0° - 6°$, $6° - 12°$, and $12° - 18°$, respectively. The duration of twilight at any place depends upon the apparent angular velocity of the sun and, hence, on the geographical latitude of the location and the time of the year. Tables of sunrise, sunset, and twilight are published in the literature.[19]

---

[18] R. A. Atlas and B. N. Charles, *Summary of Solar Radiation Observations*, The Boeing Company, Aerospace Division, Seattle, Wash., Document D2-90577-112 (1964), AD 889157.

[19] *Supplement to the American Ephemeris for 1946*, U. S. Government Printing Office, Washington, D. C.

During the transition between day and night through the twilight period, the illuminance at the earth's surface varies by a factor of almost a billion from about 1.15×10^4 footcandles in the daytime to about 5×10^{-5} footcandles at night as shown in Fig. 4 for a "clear" atmosphere. Since the variation of illuminance at the earth's surface during the twilight period is very rapid, the absolute quantitative measurements are comparatively much harder to make. The twilight spectra are highly variable in spectral composition and relative strengths of spectral lines with time as the shadow of the earth varies with time thus changing both the excited and attenuating layers of the lower atmosphere. However, twilight phenomena have attracted worldwide attention through the ages. A number of workers have recently published extensive literature on the studies of twilight phenomena.[20-25]

The twilight spectra are dominated by emissions from ionized molecular nitrogen (band heads at 3914 A and 4278 A), sodium D lines (at 5896 A and 5890 A), and atomic oxygen lines (at 5577 A, 6300 A, and 6364 A) in the visible spectrum and the helium emission (at 10830 A) and molecular oxygen O_2 (bands at 1.27 and 1.58 micrometers) emissions in the infrared region. Since the 1.27-micrometer radiation is reabsorbed by the atmospheric oxygen in the lower atmosphere, this band is observed only in high-altitude twilight spectra. Figure 5 shows some low-resolution twilight spectra recorded by Rozenberg,[26] and Fig. 6 shows a high-resolution twilight spectrum by Chamberlain.[27] These spectra are characteristically different from the daylight or nightglow spectra in that certain features are found in twilight spectra which are either absent or much different in the nightglow or solar spectra. Most of the twilight emissions are caused by the resonance scattering or fluorescence while the atmosphere is directly irradiated by the solar radiation. (The processes of excitation whereby atmospheric atoms or molecules absorb solar radiation which is subsequently released or re-emitted as atmospheric radiation will be discussed later.)

---

[20] J. W. Chamberlain, *Physics of the Aurora and Airglow*, Academic Press, New York (1961).

[21] J. A. Ratcliffe, *Physics of the Upper Atmosphere*, Academic Press, New York (1960).

[22] B. M. McCormac and A. Omholt, editors, *Atmospheric Emissions*, Van Nostrand Reinhold Company, New York (1969).

[23] B. M. McCormac, editor, *The Radiating Atmosphere*, Springer-Verlag New York, Inc., New York (1971).

[24] G. V. Rozenberg, *Twilight*, Plenum Press, New York (1966).

[25] M. F. Ingham, "The Spectrum of the Airglow," *Scientific American* 226, 78 (1972).

[26] G. V. Rozenberg, *Loc. cit.*

[27] J. W. Chamberlain, *Loc. cit.*

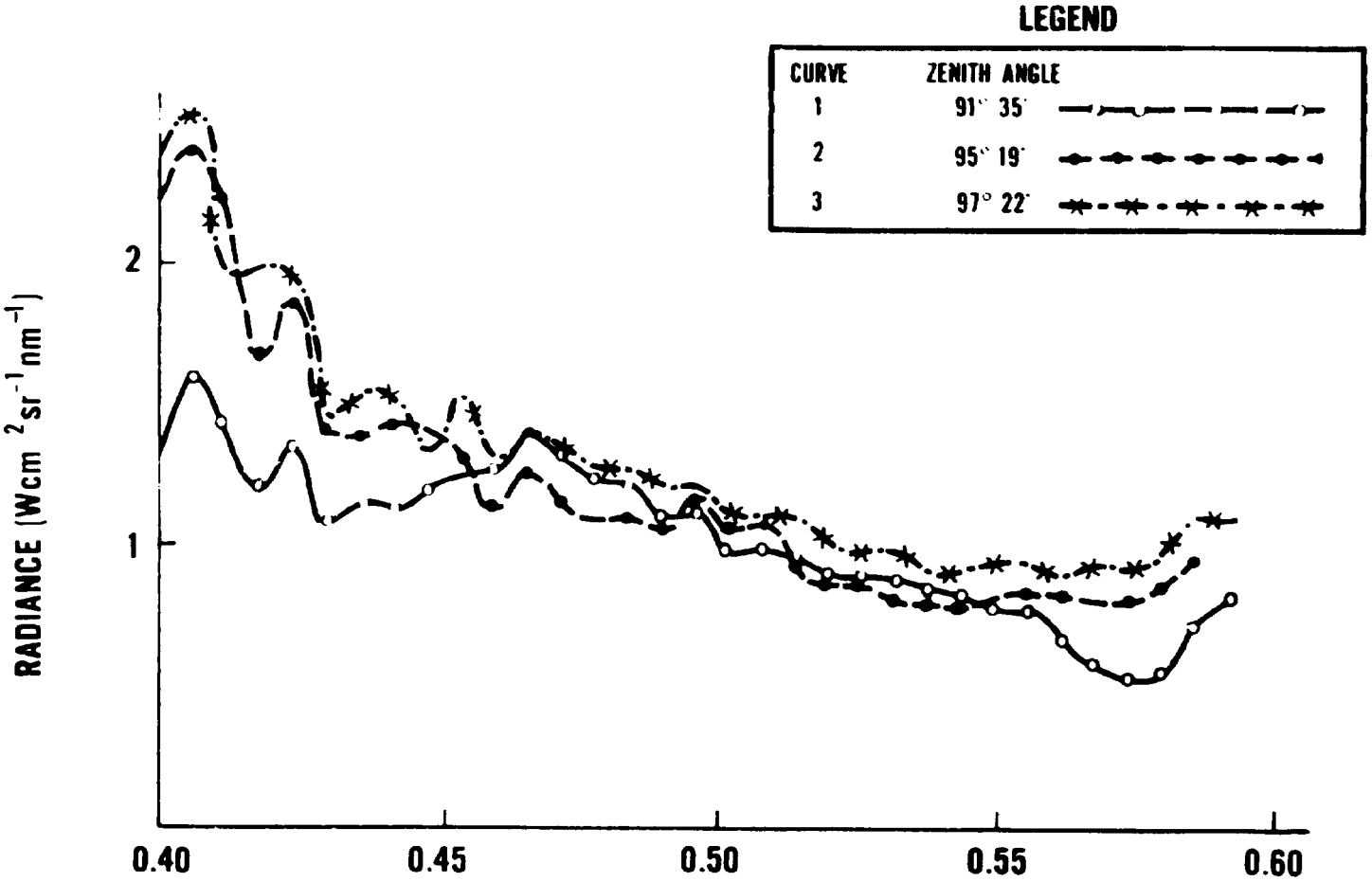

Fig. 5. Some low resolution twilight radiant sterance spectra of the zenith sky for three solar zenith angles. The ordinate axis numbers are to be multiplied by 10^{-12} for curve 1, x 10^{-14} for curve 2, and x 10^{-15} for curve 3 (Rozenberg).

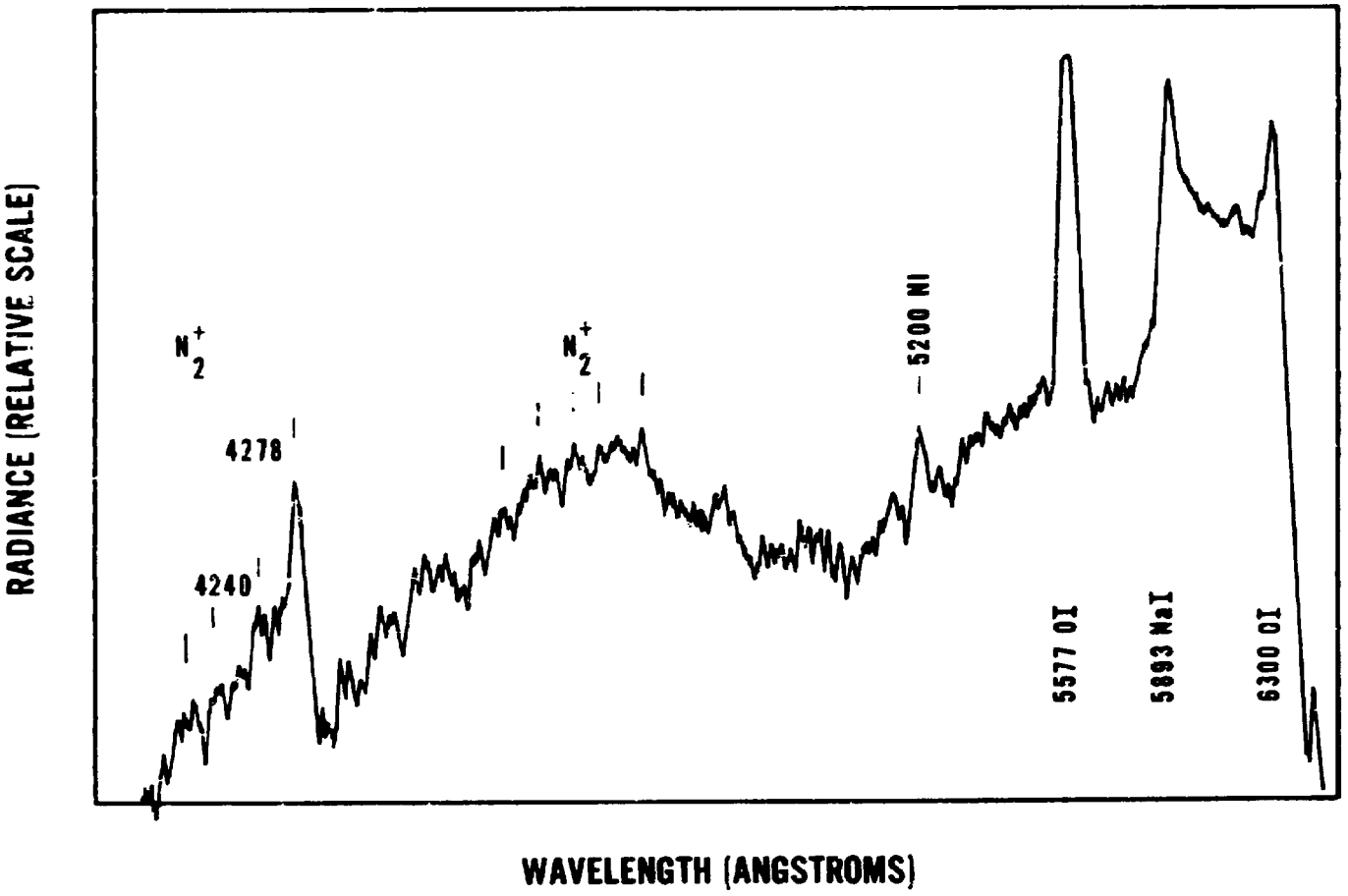

Fig. 6. A high-resolution twilight spectrum (from Chamberlain).

3. **Nighttime Radiation.** When the sun is more than 18 degrees below the celestial horizon, the earth's surface and the lower atmosphere do not receive any direct solar radiation. Yet, even on a moonless night, there is a faint amount of diffuse radiation reaching the earth's surface. The nighttime radiation is composed of the following components:

(a) The integrated stellar radiation originating from the distant stars.

(b) The zodiacal radiation which is solar radiation scattered by the interplanetary dust.

(c) The nightglow (or night airglow) originating in the upper terrestrial atmosphere due to the interaction of the solar radiation on gaseous atoms and molecules. The excitation energy is later released as the nightglow radiation.

(d) The integrated nebular radiation from the distant gaseous nebulae.

(e) The auroral emissions which are often visible at high latitudes.

(f) The lunar radiation which is the solar radiation reflected by the moon.

All radiation originating either in the extra-terrestrial space or in the upper terrestrial atmosphere is scattered and attenuated by the lower atmosphere before reaching sea level. Knowedge of the characteristics of nighttime radiation is important to the atmospheric physicist or aeronomer who is interested in the optical, physical, and chemical processes in the atmosphere. The spectra of the nighttime radiation provide essential clues to the nature of these processes at different heights in the terrestrial atmosphere as well as in the extra-terrestrial space.

a. **Nightglow.** A number of authoritative and exhaustive treatises[28-32] and

---

[28] J. W. Chamberlain, *Physics of the Aurora and Airglow*, Academic Press, New York (1961).

[29] J. A. Ratcliffe, *Physics of the Upper Atmosphere*, Academic Press, New York (1960).

[30] B. M. McCormac and A. Omholt, editors, *Atmospheric Emissions*, Van Nostrand Reinhold Company, New York (1969).

[31] B. M. McCormac, editor, *The Radiating Atmosphere*, Springer-Verlag New York Inc., New York (1971).

[32] G. V. Rozenberg, *Twilight*, Plenum Press, New York (1966).

excellent review articles[33-41] have been published recently on various measurements and theories of the excitation processes which may be responsible for various components of nighttime radiation. The problem of exactly how various nightglow emissions are produced and exactly at what height in the atmosphere is still not completely resolved. There are multiple excitation and de-excitation processes which are responsible for atmospheric emissions under different dynamic conditions of the terrestrial atmosphere. The complexity of the nightglow emissions is due to the variability of the concentration and composition of atmospheric constituents (atoms, molecules, and ions) as well as the energy of the extra-terrestrial photons or other particles which interact with atmospheric particles at various heights above sea level in the presence of a variable electromagnetic field.

The major processes of excitation whereby energy may be absorbed by an atmospheric atom or molecule and later released as nightglow radiation are briefly described here:

(1) Resonance scattering—the process in which an atom absorbs incident, radiant energy and later emits radiation of the same wavelength.

(2) Fluorescence—the process in which an atom absorbs radiation of one wavelength and emits radiation of a longer wavelength.

(3) Chemical association—the process by which atoms and molecules combine and undergo chemical change resulting in the release of radiative energy.

---

[33] M. F. Ingham, "The Spectrum of the Airglow," *Scientific American 226*, 78 (1972).

[34] F. E. Roach, "The Light of the Night Sky: Astronomical, Interplanetary and Geophysical," *Space Science Reviews 3*, 512 (1964).

[35] F. E. Roach, "The Nightglow," *Advances in Electronics 18*, 1 (1963).

[36] V. I. Krassovsky and N. N. Shefov, "Airglow," *Space Science Reviews 4*, 176 (1965).

[37] S. M. Silverman, "Night Airglow Phenomenology," *Space Science Reviews 11*, 341 (1970).

[38] J. F. Noxon, "Day Airglow," *Space Science Reviews 8*, 92 (1968).

[39] D. M. Hunten, "Spectroscopic Studies of the Twilight Airglow," *Space Science Reviews 6*, 493 (1967).

[40] A. L. Broadfoot and K. R. Kendall, "The Airglow Spectrum, 3100-10,000 A," *Jour. Geophy. Res., Space Phys. 73*, 426 (1968).

[41] V. I. Krassovosky, N. N. Shefov, and V. I. Yarin, "Atlas of the Airglow Spectrum 3000-12400 A," *Planetary Space Sci 9*, 883 (1962).

(4) Ionic reaction–the process in which ionized gaseous molecules recombine with available electrons resulting in dissociative recombinations with consequent release of radiation.

(5) Photo-dissociation (or radiative dissociation)–the process in which a molecule may absorb radiation resulting in one or more atoms in an excited state with subsequent de-activation and re-emission of radiation.

(6) Particle collision–the process in which an energetic particle collides with atmospheric atoms or molecules resulting in a change of internal energy of the participants and subsequent release of radiation.

(7) Transfer of excitation–the process in which excitation energy may be transferred to another atom or molecule leaving the latter in an excited state with subsequent emission of radiation.

Figure 7 shows a high-resolution airglow spectrum from 310 nm to 1000 nm, recorded by Broadfoot and Kendall at the Kitt Peak Observatory, Arizona, at an altitude of 2080 meters.[42] The prominent features of this spectrum are the oxygen OI 5577 A, OI 6300-6364 A, Sodium Na I 5893 A (unresolved doublet 5890-5896 A), and the hydroxyl OH emissions spread almost all over the entire spectrum but quite dominant beyond the visual cutoff at about 7200 A. The other important features are the atmospheric oxygen molecular bands (Herzberg) from about 3140 A to 4840 A and the contamination due to mercury lines Hg 4358 A and 5461 A from artificial lights on the ground–a common problem in the United States even in "remote" locations. There is an absorption band system, starting at 7619 A, due to the atmospheric oxygen O_2. Figure 8 shows some low-resolution, total night-sky radiant sterance (radiance) spectra due to the entire hemispheric radiation recorded by Vatsia, Stich, and Dunlap at ground level for various lunar phases.[43] These spectra cover the spectral range from 450 nm to 1950 nm. Curve 1 corresponds to the total, moonless-night-sky radiation consisting of the nightglow (airglow), the zodiacal radiation, the integrated stellar radiation, and the nebular radiation. Curves 2, 3, and 4 are due to the radiation represented in curve 1 plus contributions from the solar radiation as reflected by the moon for various phases. In addition to the prominent emission features of OI 5577, 6300-64 A, Na I 5893, and OH emissions between 7200-19500 A, there are characteristic absorption bands due to the constituents of the lower atmosphere, chiefly atmospheric molecular oxygen, water

[42] A. L. Broadfoot and K. R. Kendall, "The Airglow Spectrum, 3100-10,000 A," *Jour. Geophy. Res., Space Phys.* 73, 426 (1968).

[43] M. L. Vatsia, U. K. Stich, and D. Dunlap, "Night Sky Radiant Sterance from 450 nm to 2000 nm," *J. Opt. Soc. Am.* 59, 483 (1969); also Technical Report ECOM-7022, Night Vision Laboratory, Visionics Technical Area, Fort Belvoir, Virginia (1972).

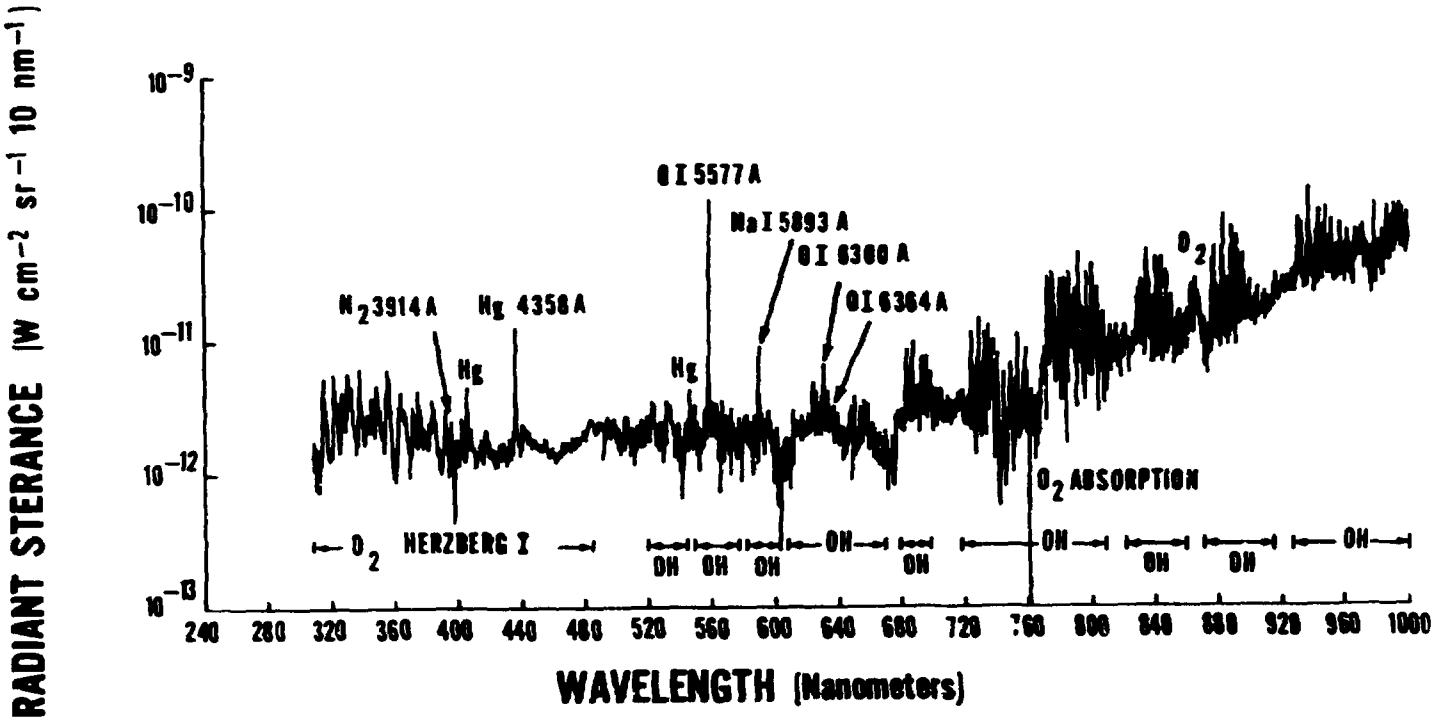

Fig. 7. Night sky spectral radiant sterance at Kitt Peak Observatory (adapted from Broadfoot and Kendall).

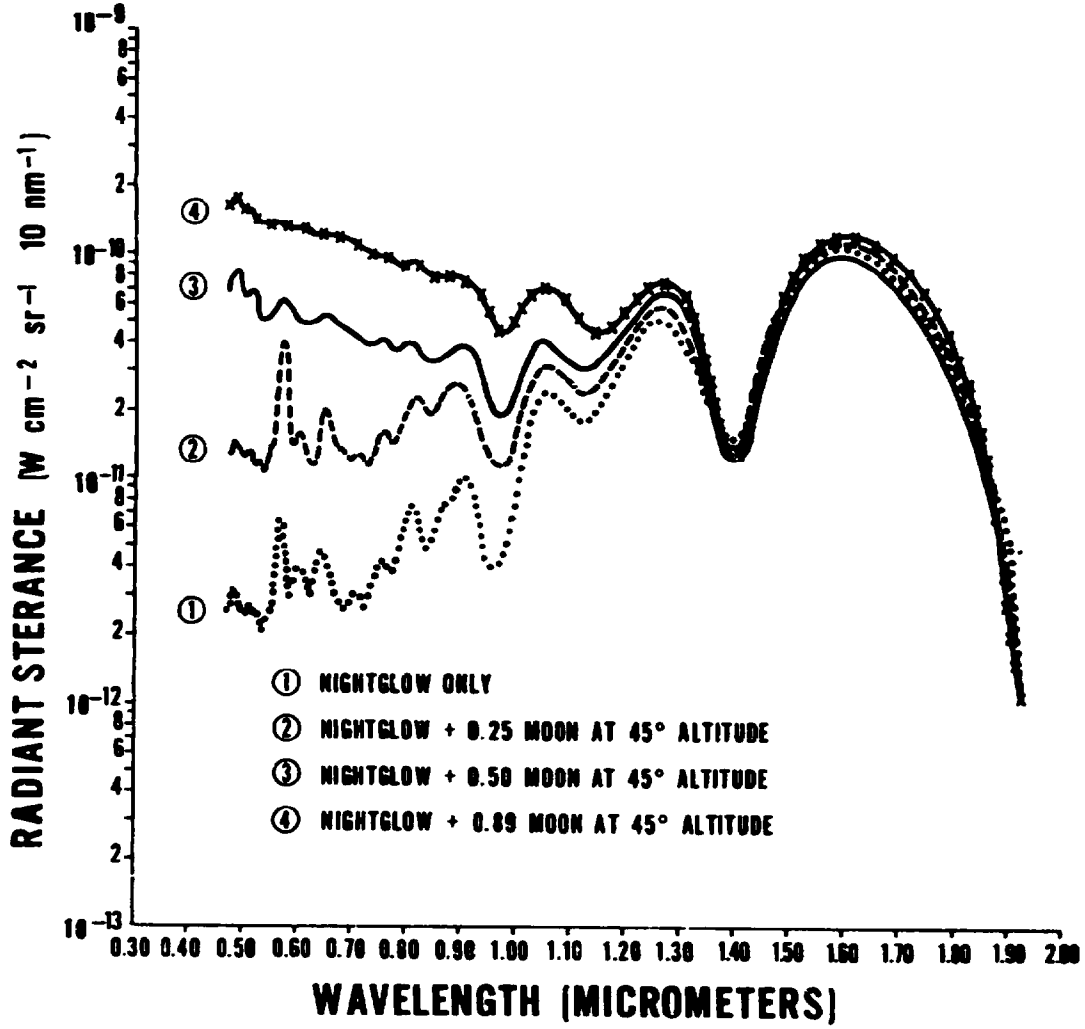

Fig. 8. Night sky spectral radiant sterance for various phases of the moon as measured by Vatsia, Stich, and Dunlap.

vapor, and carbon dioxide at about 0.72, 0.76, 0.78, 0.84, 0.94, 1.13, 1.38, and 1.85 micrometers (compare Fig. 3). The individual, sharp features of the atmospheric airglow emissions are quite prominent until the solar-radiation contribution from the larger illuminated lunar fraction becomes overwhelming. The lunar contribution to the integral, nighttime radiation decreases rapidly beyond the visible-radiation, cutoff wavelength and becomes almost insignificant beyond 1.35 μm for all phases of the moon. In the visible spectral range, however, the lunar-radiation increases the ground-level radiant incidance by a factor of up to 700 for the full moon.

The excitation processes for the prominent atmospheric emissions constituting the nightglow are discussed here. Further details may be found in the literature.[44-57] Figure 9 shows an atomic oxygen OI energy-level diagram indicating various quantum mechanical energy states and the observed emission lines. The green OI 5577 A emission line represents a transition from the $^1S_0$ state to the $^1D_2$ state, and the red lines OI 6300 A and OI 6364 A result from the transitions between the $^1D_2$ state and the $^3P_2$

---

[44] J. W. Chamberlain, *Physics of the Aurora and Airglow*, Academic Press, New York (1961).

[45] J. A. Ratcliffe, *Physics of the Upper Atmosphere*, Academic Press, New York (1960).

[46] B. M. McCormac and A. Omholt, editors, *Atmospheric Emissions*, Van Nostrand Reinhold Company, New York (1969).

[47] B. M. McCormac, editor, *The Radiating Atmosphere*, Springer-Verlag New York Inc., New York (1971).

[48] G. V. Rozenberg, *Twilight*, Plenum Press, New York (1966).

[49] M. F. Ingham, "The Spectrum of the Airglow," *Scientific American 226*, 78 (1972).

[50] F. E. Roach, "The Light of the Night Sky: Astronomical, Interplanetary and Geophysical," *Space Science Reviews 3*, 512 (1964).

[51] F. E. Roach, "The Nightglow," *Advances in Electronics 18*, 1 (1963).

[52] V. I. Krassovsky and N. N. Shefov, "Airglow," *Space Science Reviews 4*, 176 (1965).

[53] S. M. Silverman, "Night Airglow Phenomenology," *Space Science Reviews 11*, 341 (1970).

[54] J. F. Noxon, "Day Airglow," *Space Science Reviews 8*, 92 (1968).

[55] D. M. Hunten, "Spectroscopic Studies of the Twilight Airglow," *Space Science Reviews 6*, 493 (1967).

[56] A. L. Broadfoot and K. R. Kendall, "The Airglow Spectrum, 3100-10,000 A," *Jour. Geophy. Res., Space Phys. 73*, 426 (1968).

[57] V. I. Krassovsky, N. N. Shefov, and V. I. Yarin, "Atlas of the Airglow Spectrum 3000-12400 A," *Planetary Space Sci 9*, 883 (1962).

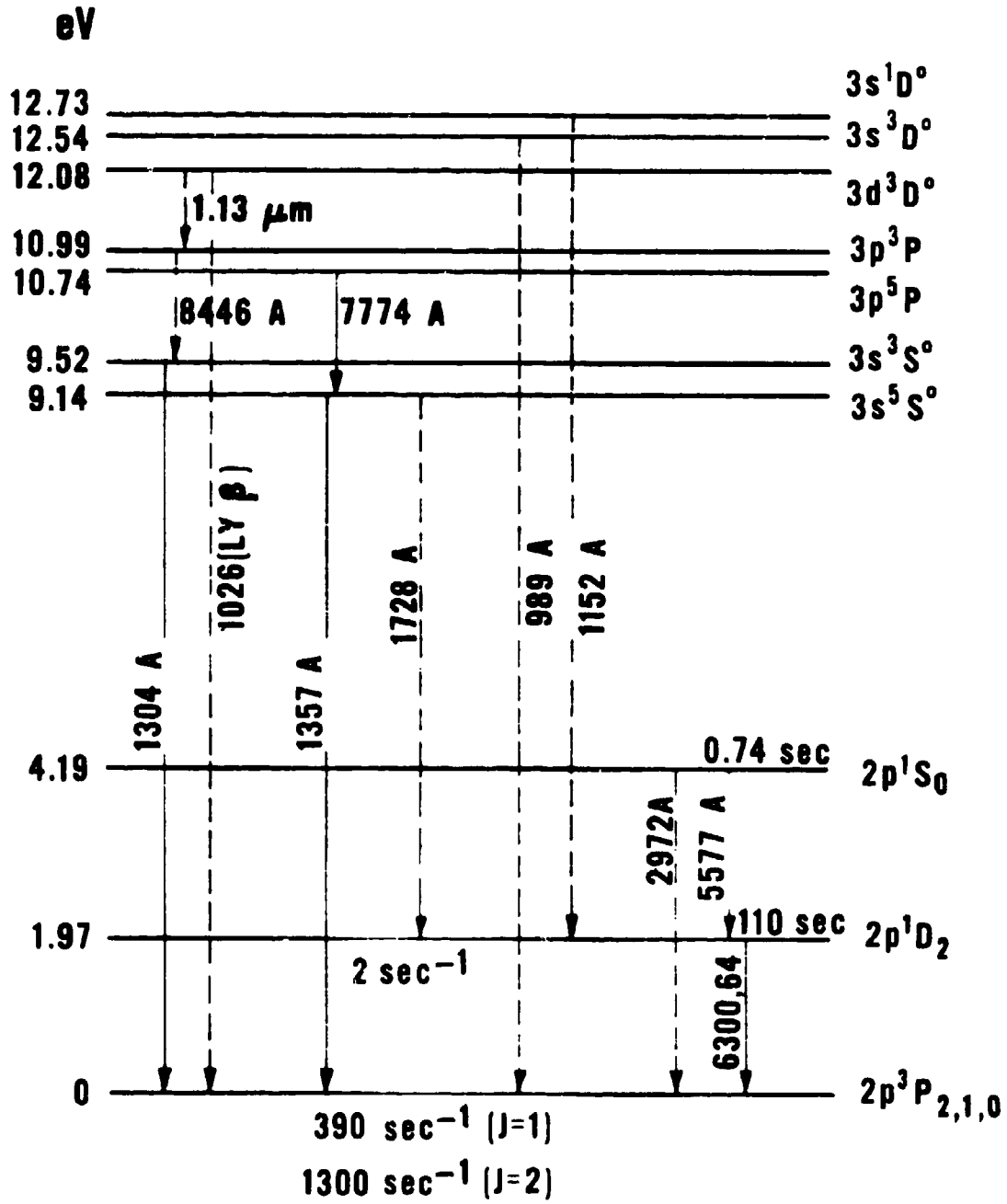

Fig. 9. Atomic oxygen (OI) energy levels.

and $^3P_1$ states, respectively. Some of the proposed excitation mechanisms for OI emissions follow:

$$3\,O \rightarrow O_2 + O\,(^1S) + 0.95\ eV \tag{10}$$

$$O_2^+ + e^- \rightarrow O + O\,(^1D) + 4.99\ eV \tag{11}$$

$$\rightarrow 2\,O\,(^1D) + 3.03\ eV \tag{12}$$

$$\rightarrow O + O\,(^1S) + 2.78\ eV \tag{13}$$

$$\rightarrow O\,(^1D) + O\,(^1S) + 0.82\ eV \tag{14}$$

$$NO^+ + e^- \rightarrow N + O\,(^1D) + 0.80\ eV. \tag{15}$$

The excitation process represented by equation (10) is the Chapman process, a chemical association process, while those represented by equations (11) through (15) are ionic dissociative recombinations. The Chapman process is considered to be the predominant process for the 5577 A emission at about 100-km altitude while the OI 6300/6364 A doublet is emitted in the F layer at about 300-km altitude as a consequence of the ionic recombination processes.

The Meinel vibration rotation bands of hydroxyl radical OH are thought to be due to the chemical recombination process suggested by Bates and Nicolet:

$$O_3 + H \rightarrow OH^* + O_2^*\ (+3.34\ eV). \tag{16}$$

Krassovsky and Shefov suggest the alternate process for OH emissions:

$$O_2^* + H \rightarrow OH^* + O. \tag{17}$$

The sodium Na D lines at night are believed to be a result of the processes:

$$Na\,O + O \rightarrow Na(^2P) + O_2 \tag{18}$$

and

$$Na\,H + O \rightarrow Na(^2P) + OH. \tag{19}$$

Krassovsky and Shefov have proposed the excitation process for the emission of the green continuum due to the reaction:

$$NO + O \rightarrow NO_2 + h\nu\,. \tag{20}$$

Table VI contains the main nightglow emissions, the emitter level energy state, the altitude of occurrence, the photon exitance in rayleighs* and equivalent photon sterance in Watts/cm^2-sr, and the excitation process for each.

---

*The rayleigh is a unit of airglow emission rate named after the fourth Lord Rayleigh (R. J. Strutt). One rayleigh corresponds to the emission rate of 10^6 photons per second per cm^2 (column) from a volume source of radiation (see Chamberlain, *Physics of the Aurora and Airglow*, *Appendix II*, Academic Press, New York, 1961). The photon-integrated emission E measured in rayleighs is defined:

$$E_R = 1\ R = 10^6 \text{ photons } s^{-1}\ cm^{-2} \text{ (column)}. \tag{21}$$

The photon sterance (earlier called radiance or intensity) L_p of the volume source of radiation emitting at the rate of one rayleigh will be:

$$L_p = (10^6/4\pi) \text{ photons } s^{-1}\ cm^{-2}\ sr^{-1}. \tag{22}$$

For monochromatic radiation of wavelength λ, the photon sterance in the equivalent energy units will be:

$$L_p(\lambda) = (10^6/4\pi)\,(hc/\lambda)\ s^{-1}\,cm^{-2}\ sr^{-1}, \tag{23}$$

$h = 6.6256 \times 10^{-34}\ W\ s^2$ (Planck constant),

$c = 2.9979 \times 10^{18}\ A\ s^{-1}$ (Speed of light).

The substitution of the values of the Planck constant h and the speed of light c in equation (23) gives

$$L_p(\lambda) = (1.5806 \times 10^{-10}) / \lambda(A)\ W\ cm^{-2}\ sr^{-1} \tag{24}$$

where $\lambda(A)$ is wavelength expressed in angstroms.

For a volume source with emission rate of R/A (rayleighs per angstrom), the corresponding photon sterance (radiance) will be given by

$$L_\lambda = (R/A)\,(1.5806 \times 10^{-10})/\lambda(A)\ W\ cm^{-2}\ sr^{-1}\ A^{-1}. \tag{25}$$

In general, the photon emission in rayleighs can be expressed in the equivalent energy units using the relation:

$$1\ R_\lambda = 10^6\,(hc/\lambda)\ s^{-1}\,cm^{-2}, \tag{26}$$

or

$$1\ R_\lambda = 1.9863 \times 10^{-9}/\lambda(A)\ W\ cm^{-2} \tag{27}$$

where $\lambda(A)$ is the wavelength in angstroms.

Table VI. Major Nightglow Emissions (Adapted from McCormac)

WAVELENGTH (MICROMETERS)	EMITTER STATE	EXCITATION PROCESS	ALTITUDE (km)	PHOTON EMISSION (RAYLEIGH)	PHOTON STERANCE ($W\ cm^{-2}\ sr^{-1}$)
0.5577	$O(^1S)$	C, I	908300	250	7.08×10^{-12}
0.5 - 0.65 (CONTINUUM)	NO_2	C	90	1	2.85×10^{-14}
0.5393	$Na(^2P)$	C	92	20 - 150	$5.36 - 40.23 \times 10^{-13}$
0.6300 0.6364	$O(^1D)$	I	300	10 - 500	2.5×10^{-13} TO 1.25×10^{-12}
0.7619 BAND	$O_2(^1\Sigma)$	C	80	6,000	1.24×10^{-10}
0.55 - 4.4	OH	C	90	4,500,000	3.56×10^{-8}

b. Moonlight. The luminous incidance (illuminance) on the earth due to the solar radiation reflected by the moon goes through variations determined by the altitude and phase of the moon. The relative, integral, luminous sterance (luminance) of the moon as a function of lunar phase angle has been experimentally measured by Russel[58] and Rougier.[59] Tables VIIa and VIIb and Fig. 10 show the relative, luminous sterance of the moon as a function of the phase angle. The phase angle is the angle subtended by the sun and the earth as observed from the moon. The phase angle is negative for the waxing moon and positive for the waning moon. The phase angle φ can be computed from the *Nautical Almanac* from the longitudes of the sun and the moon. The phase angle is 180° minus the absolute difference between the longitudes of the sun and the moon at a particular time. The fraction of the moon illuminated and seen from the earth is also listed in the *Nautical Almanac*. The fraction of area of the lunar disk that is illuminated is equal to the illuminated fraction of the diameter perpendicular to the line of cusps. The fraction of the moon illuminated as a function of the phase angle φ is given by the relation:

$$F = (1 + \cos \varphi)/2. \tag{28}$$

The luminous incidance (illuminance) of the moon has been reported by Brown.[60] The full moon at the zenith produces a luminous incidance (illuminance) of about 3.4×10^{-2} footcandles on a horizontal plane at sea level under clear atmospheric conditions. For a zenith angle z and a lunar phase angle φ, the horizontal, sea level, lunar luminous incidance (illuminance) will be given by the relation:

$$E = L(\varphi)\, E_0\, (T_1)^{m-1}\,, \tag{29}$$

where E is luminous incidance on a sea level horizontal plane, $L(\varphi)$ is the lunar luminance phase function (from Fig. 10), E_0 is the sea level horizontal luminous incidance when the full moon is at the zenith, T_1 is the vertical atmospheric transmittance for a unit optical mass ($T_1 = 0.796$), and m is the atmospheric optical air mass. The air mass m equals secant z where z is the lunar zenith angle. This is a good approximation until z approaches over 80 degrees. Accurately computed values of the optical air mass for various values of the altitude angle are given in Table II.

---

[58] H. N. Russel, *Astrophysical Jour.* *43*, 103 (1916).

[59] G. Rougier, *Ann. Obs. Strasbourg* *2*, 205 (1933).

[60] D. R. E. Brown, *Natural Illumination Charts*, Report No. 374-1, Department of the Navy, Bureau of Ships, Washington, D. C. (1952).

Table VIIa. The Relative Radiant Sterance of the Moon as a Function of Phase Angle Based Upon Russel's Measurements

PHASE-ANGLE	BEFORE FULL MOON		AFTER FULL MOON	
	STERANCE	MAGNITUDE	STERANCE	MAGNITUDE
0°	100	0.00	100	0.00
10	81.7	0.22	81.7	0.22
20	66.7	0.44	64.3	0.48
30	54.0	0.67	50.6	0.74
40	43.6	0.90	38.7	1.03
50	35.3	1.13	29.9	1.31
60	28.3	1.37	23.3	1.58
70	21.9	1.65	18.0	1.86
80	16.1	1.98	13.6	2.17
90	11.5	2.35	10.0	2.50
100	7.73	2.78	7.18	2.88
110	5.15	3.22	4.92	3.27
120	3.10	3.77	3.19	3.74
130	1.75	4.39	1.90	4.30
140	0.88	5.14	1.02	4.98
150	0.37	6.09	0.44	5.89

Table VIIb. The Relative Radiant Sterance of the Moon as a Function of Phase Angle Based Upon Rougier's Measurements

PHASE-ANGLE	BEFORE FULL MOON		AFTER FULL MOON	
	STERANCE	MAGNITUDE	STERANCE	MAGNITUDE
0	100	0.00	100	0.00
10	78.7	0.26	75.9	0.30
20	60.3	0.55	58.6	0.58
30	46.6	0.83	45.3	0.86
40	35.6	1.12	35.0	1.14
50	27.5	1.40	27.3	1.41
60	21.1	1.69	21.1	1.69
70	16.1	1.98	15.6	2.02
80	12.0	2.30	11.1	2.39
90	8.24	2.71	7.80	2.77
100	5.60	3.15	5.81	3.09
110	3.77	3.56	4.05	3.48
120	2.49	4.01	2.61	3.96
130	1.51	4.55	1.58	4.50
140			0.93	5.08
150			0.46	5.84

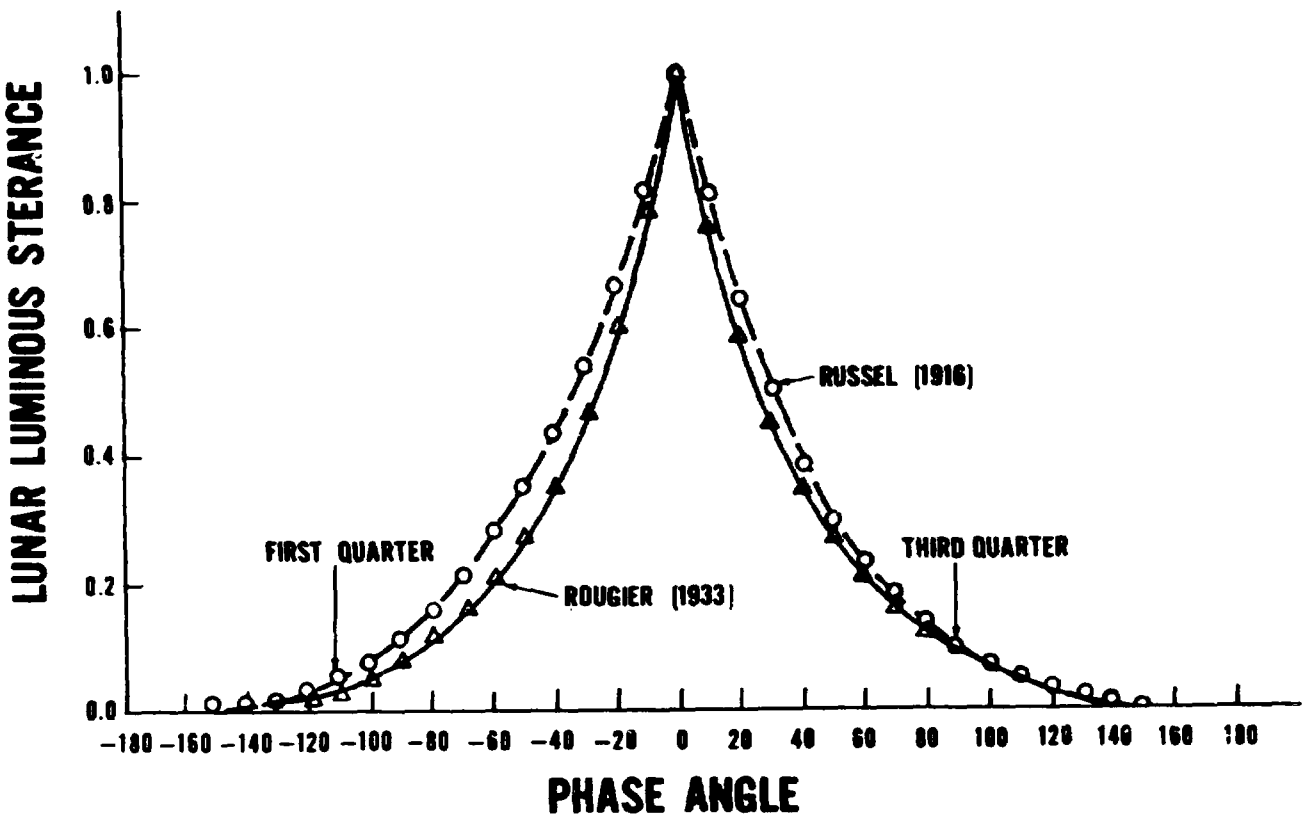

Fig. 10. The relative radiant sterance of the moon as a function of phase angle after Russel and Rougier measurements.

The geocentric coordinates of the moon can be calculated for any geographical location for any time with the following relations:

$$\cos z = \sin A = \sin \delta \sin \phi + \cos \delta \cos \phi \cos h \tag{2}$$

$$\sin Z = (\cos \delta \sin h)/\sin z \tag{30}$$

where z, A, Z, δ, and h are the zenith distance, altitude, azimuth, declination, and hour angle of the moon, respectively, and ϕ is the geographical latitude of the location. To compute the apparent altitude of the moon from the surface of the earth, one has to apply a parallax correction. The parallax is the difference of altitude or zenith distance of a celestial body as seen from the surface and the center of the earth respectively. The parallax angle equals the angle subtended by the earth's radius at the center of the celestial body. The apparent altitude A′ is given by:[61]

$$A' = A - p \tag{31}$$

$$\sin p = \sin \pi \cos A \tag{31a}$$

where p is the parallax angle and π is the equatorial horizontal parallax (H.P.) of the moon (tabulated at hourly intervals in the *Nautical Almanac*). There is no parallax in azimuth, of course.

The spectral radiant incidance (irradiance) due to the radiation from the moon as well as the low-level radiation from nightglow, and zodiacal and integrated stellar radiation varies considerably as the proportion of moonlight is added to the low-level, nighttime radiation. Figure 11 shows nighttime radiation spectra for various altitudes of the moon during the same night recorded by Vatsia, Stich, and Dunlap at Lake Montauban, Canada.[62] The relative heights of the airglow spectral emissions over the general level of the continuum vary as the contribution due to the lunar radiation increases. The spectral line profiles are determined by the resolution of the spectroradiometer.

---

[61] William Chauvenet, *A Manual of Spherical and Practical Astronomy*, Volume 1, p. 103, 5th edition, Dover Publications, Inc., New York (1960).

[62] M. L. Vatsia, U. K. Stich, and D. Dunlap, "Night Sky Radiant Sterance from 450 nm to 2000 nm," *J. Opt. Soc. Am.* 59, 483 (1969); also Technical Report ECOM-7022, Night Vision Laboratory, Visionics Technical Area, Fort Belvoir, Virginia (1972).

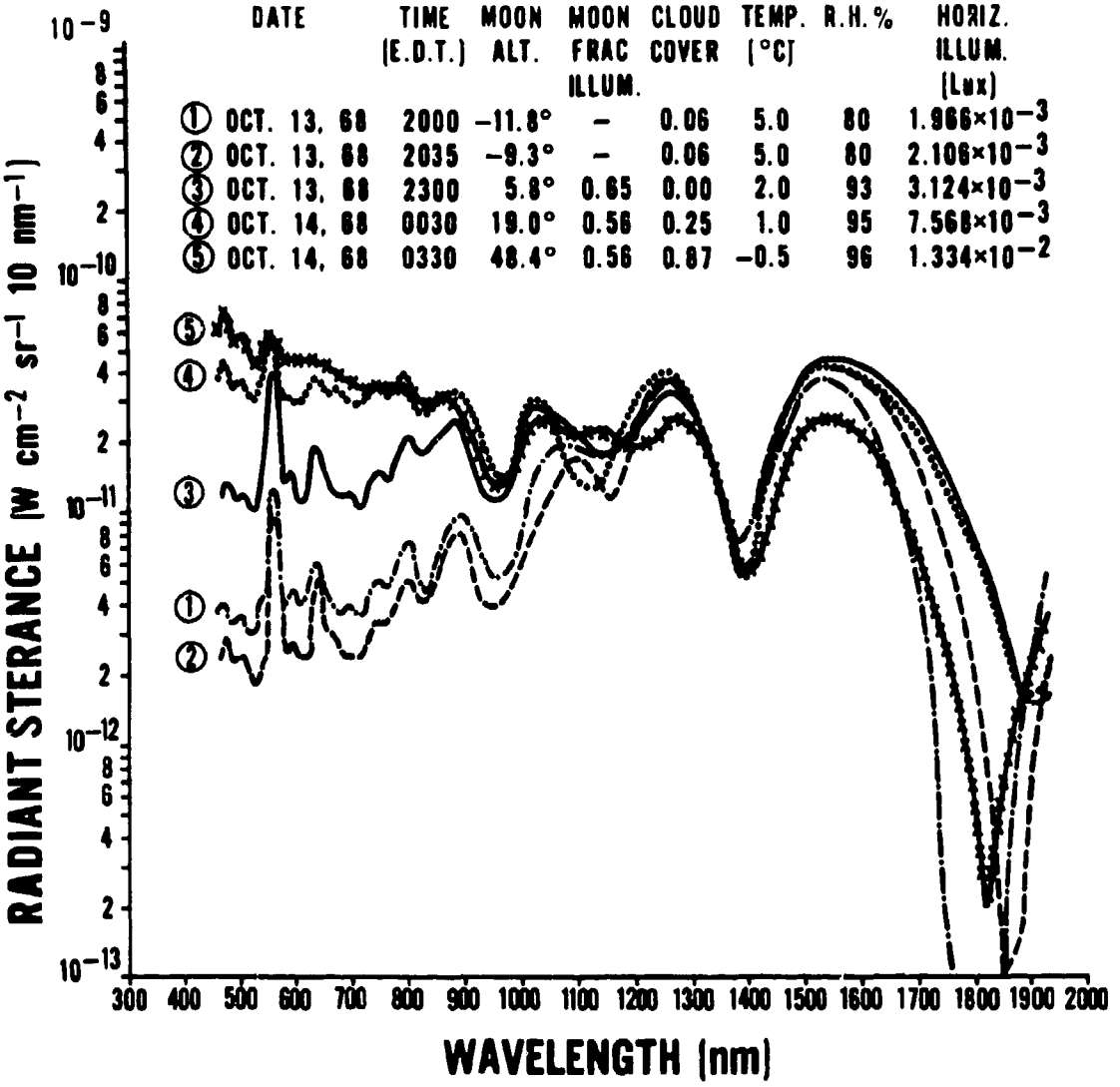

Fig. 11. Night sky radiant sterance spectra for various altitudes of the moon as measured by Vatsia, Stich and Dunlap.

II. ATMOSPHERIC TRANSMISSION

4. The Terrestrial Atmosphere. There are a large number of publications which contain extensive treatises on various features of the terrestrial atmosphere.[63-71] Only those properties of the atmosphere which influence the propagation of electromagnetic radiation in the wavelength range from 0.2 micrometer to 15.0 micrometers will be reviewed here. The composition of the permanent atmospheric constituents varies with height above sea level as shown in Figs. 12 and 13. For all practical purposes, the proportions of the four permanent gases–nitrogen, oxygen, argon, and carbon dioxide (which constitute 99.997% of the dry atmosphere up to 90 kilometers)–are generally considered to be constant up to a height of 90 kilometers. However, the concentration of carbon dioxide does vary slightly and the water vapor content of the atmosphere can vary up to 4%, but it is generally between 0.1 and 1.0%. Table VIII lists the major, permanent constituents of the atmosphere. The principal, man-made atmospheric pollutants which can have a significant influence on the atmospheric transmission are the oxygen compounds (CO, CO_2, O_3), nitrogen compounds (NO, NO_2, NH_3), halogens, hydrocarbons, aldehydes, and aerosols. The concentration of the man-made pollutants is highly variable. Ozone (O_3) is an important constituent of the atmosphere, but it is distributed nonuniformly between 10 and 40 kilometers above the earth's surface with a sharp peak between 20 and 30 kilometers.

A temperature-altitude profile in the atmosphere is caused by the physical interactions between the solar radiation and the atmospheric constituents and the earth's surface. The temperature-altitude profile is a variable with latitude and season. Mean annual temperature-altitude profiles based upon large measurements averaged over

---

[63] K. Ya. Kondratyev, *Radiation in the Atmosphere*, Academic Press, New York (1969).

[64] S. L. Valley, *Handbook of Geophysics and Space Environments*, McGraw-Hill, New York (1965).

[65] R. M. Goody, *Atmospheric Radiation*, Oxford University Press, London (1964).

[66] *U. S. Standard Atmosphere*, 1962, and *U. S. Standard Atmosphere Supplements*, 1966, U. S. Government Printing Office, Washington, D. C. 20402.

[67] H. Riehl, *Introduction to the Atmosphere*, McGraw-Hill Book Company, New York (1965).

[68] S. K. Mitra, *The Upper Atmosphere*, The Asiatic Society, Calcutta (1952).

[69] H. S. W. Massey and R. L. F. Boyd, *The Upper Atmosphere*, Philosophical Library, New York (1958).

[70] R. W. Fairbridge, *The Encyclopedia of Atmospheric Sciences and Astrogeology*, Reinhold Publishing Corporation, New York (1967).

[71] *Handbook of Geophysics*, Revised Edition, The MacMillan Company, New York (1961).

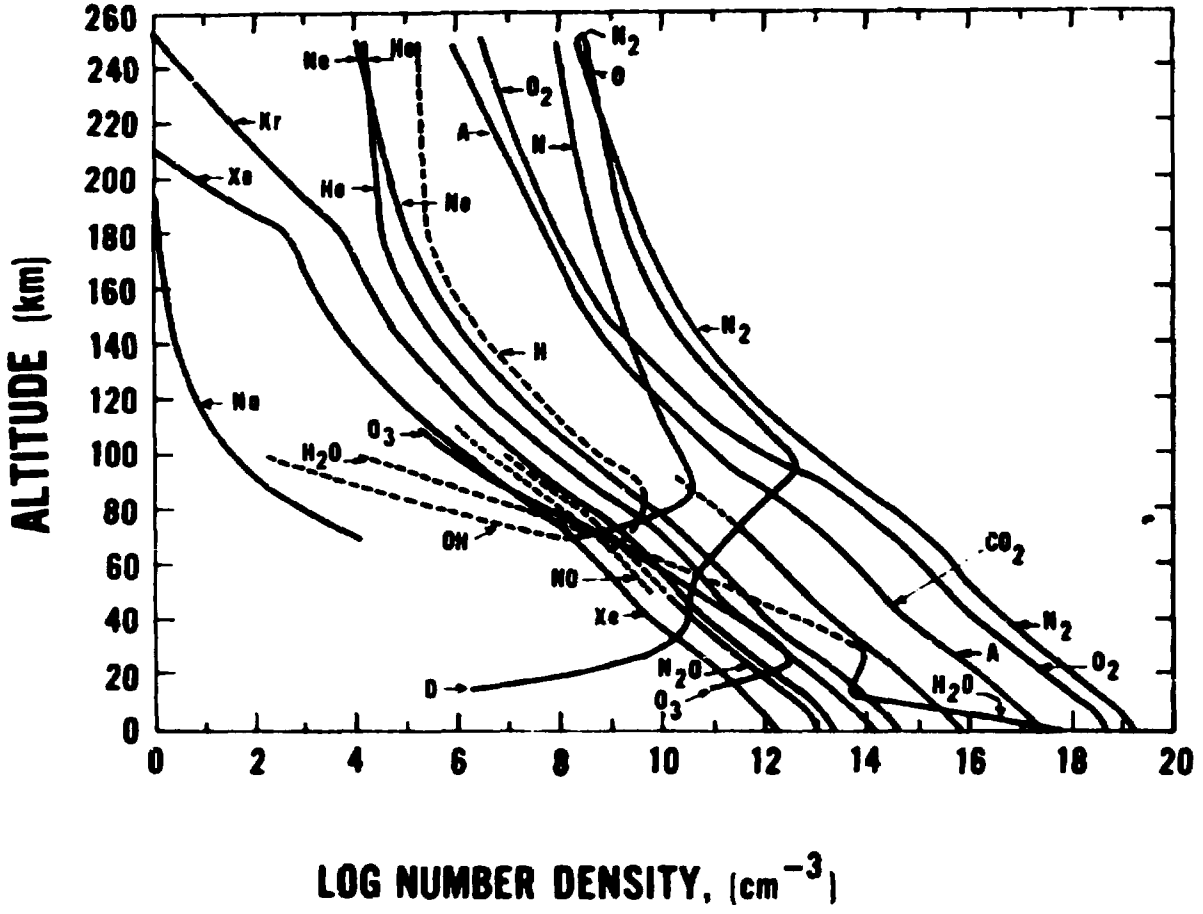

Fig. 12. Vertical distribution of atmospheric constituents from 0 to 250 kilometers (Valley).

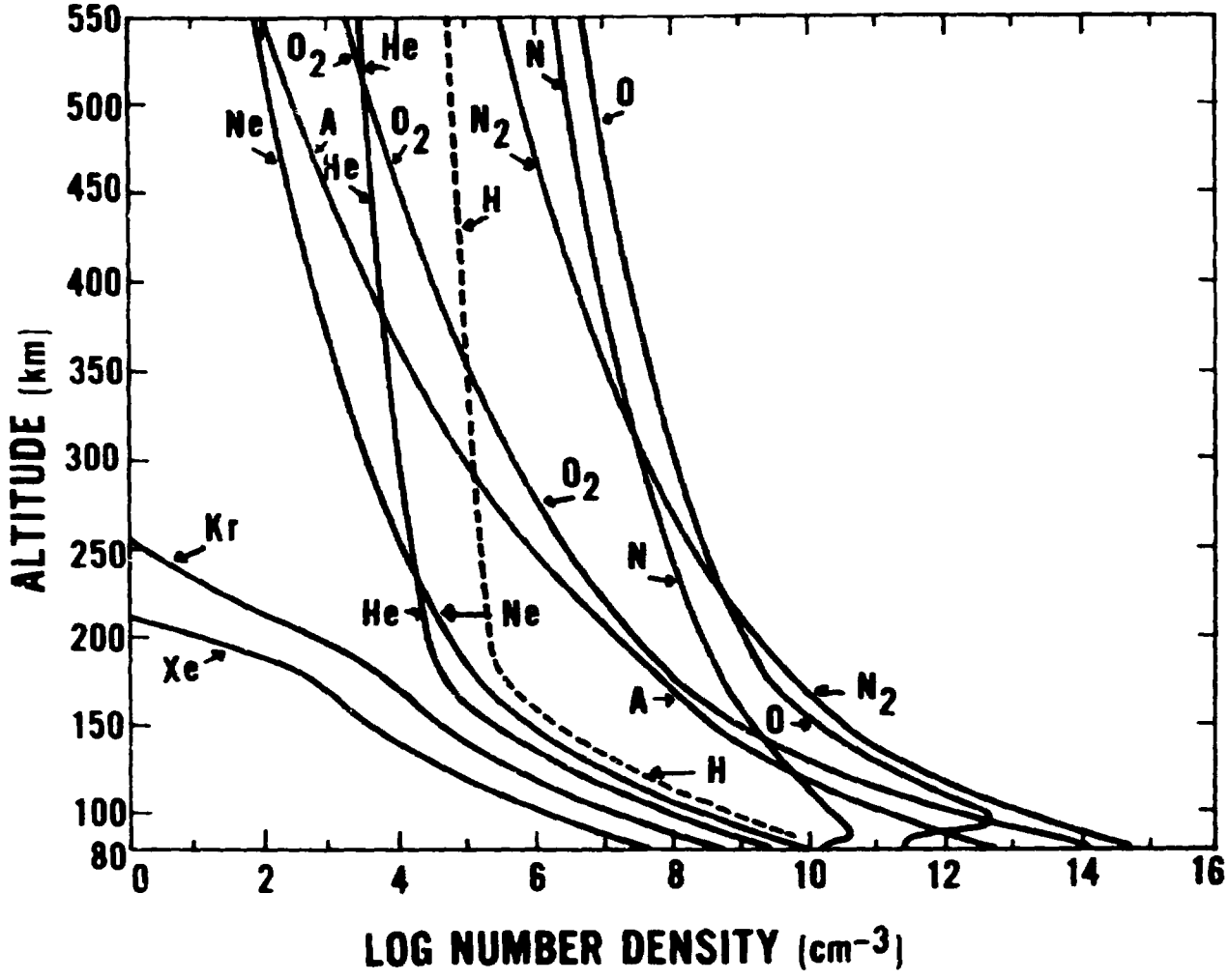

Fig. 13. Vertical distribution of atmospheric constituents from 80 to 500 kilometers (Valley).

Table VIII. Composition of the Atmosphere (Dry)
Up to About 90 km

CONSTITUENT	PER CENT BY VOLUME	PER CENT BY WEIGHT	REDUCED THICKNESS* (atm-cm, STP)
NITROGEN (N_2)	78.088	75.527	6.2434×10^5
OXYGEN (O_2)	20.949	23.143	1.5750×10^5
ARGON (A)	0.93	1.282	7.436×10^3
CARBON DIOXIDE (CO_2)	0.03	4.56×10^{-2}	2.40×10^2
NEON (Ne)	1.8×10^{-3}	1.25×10^{-3}	1.44×10^1
HELIUM (He)	5.24×10^{-4}	7.24×10^{-5}	4.19
METHANE (CH_4)	1.4×10^{-4}	7.25×10^{-5}	1.12
KRYPTON (Kr)	1.14×10^{-4}	3.30×10^{-4}	9.11×10^{-1}
NITROUS OXIDE (N_2O)	5×10^{-5}	7.6×10^{-5}	4.0×10^{-1}
XENON (Xe)	8.6×10^{-6}	3.90×10^{-5}	6.9×10^{-2}
HYDROGEN (H_2)	5×10^{-5}	3.48×10^{-6}	4.0×10^{-1}
WATER VAPOR (AVERAGE)	0.1 - 1		$10^3 - 10^4$

ONE atm-cm, STP, IS AN AMOUNT OF GAS EQUIVALENT TO A COLUMN 1 cm IN HEIGHT AT 760 mm PRESSURE AND 0° C.

periods of several decades have been adopted for various latitudes and reported in the literature.[72] Figure 14 shows the temperature-altitude profile up to 100 kilometers for the U. S. Standard Model Atmosphere, 1962.

The terrestrial atmosphere is subdivided into five shells—troposphere, stratosphere, mesosphere, thermosphere, and ionosphere. The lowest shell of the atmosphere in which temperature decreases with altitude at an approximate rate of 6.5° C/km or 3.6° F/kft is called the troposphere (named from the Greek word "tropos" meaning turn). This is the mixing layer of the atmosphere. The atmosphere is mainly heated by convective heat transfer from the ground. At the tropopause, there is no further decrease in the temperature with increasing altitude. The altitude of the tropopause varies from 6 to 18 kilometers. High wind speeds and the highest cirrus clouds dominate at the tropopause. The second shell is called the stratosphere because there is stratification, or layering, without rapid mixing. There is an increase in temperature with increase in altitude until there is no further increase at the stratopause. The absorption of the solar ultraviolet radiation by ozone produces higher temperatures in the upper strata of the stratosphere. The third shell is called the mesosphere (the middle sphere) where the temperature decreases with increasing altitude. The lapse rate is approximately half of the troposphere, namely 3° C/km. The mesopause has the minimum temperature in the terrestrial atmosphere which is about -90° C. The fourth atmospheric shell, called the thermosphere, is characterized by an increase in temperature with an increase in altitude. The outermost shell called the ionosphere contains a sufficiently large density of electrons and ionized atomic oxygen and nitrogen. The ionosphere plays a major role in the propagation of radio waves and in the production of airglow and auroral emissions. The outermost region of the ionosphere wherein molecular escape from the earth is significant is called the exosphere. The height of the exosphere is thought to be about 1000 kilometers.

For the purpose of transmission of electromagnetic radiation through the atmosphere, it is a fortunate coincidence of nature that a major part of the ultraviolet radiation is absorbed by ozone in the stratosphere and that the major constituents of the atmosphere, the molecules of nitrogen and oxygen, are transparent to the visible and most of the near infrared radiation. Near the earth's surface, the principal absorbers for the infrared radiation are water vapor (H_2O) and carbon dioxide (CO_2). Water vapor is highly variable in concentration in the atmosphere because the humidity of air fluctuates widely with geographical location, season, and time. Most of the water vapor is confined to the troposphere.

---

[72] *U. S. Standard Atmosphere*, 1962, and *U. S. Standard Atmosphere Supplements*, 1966, U. S. Government Printing Office, Washington, D. C. 20402.

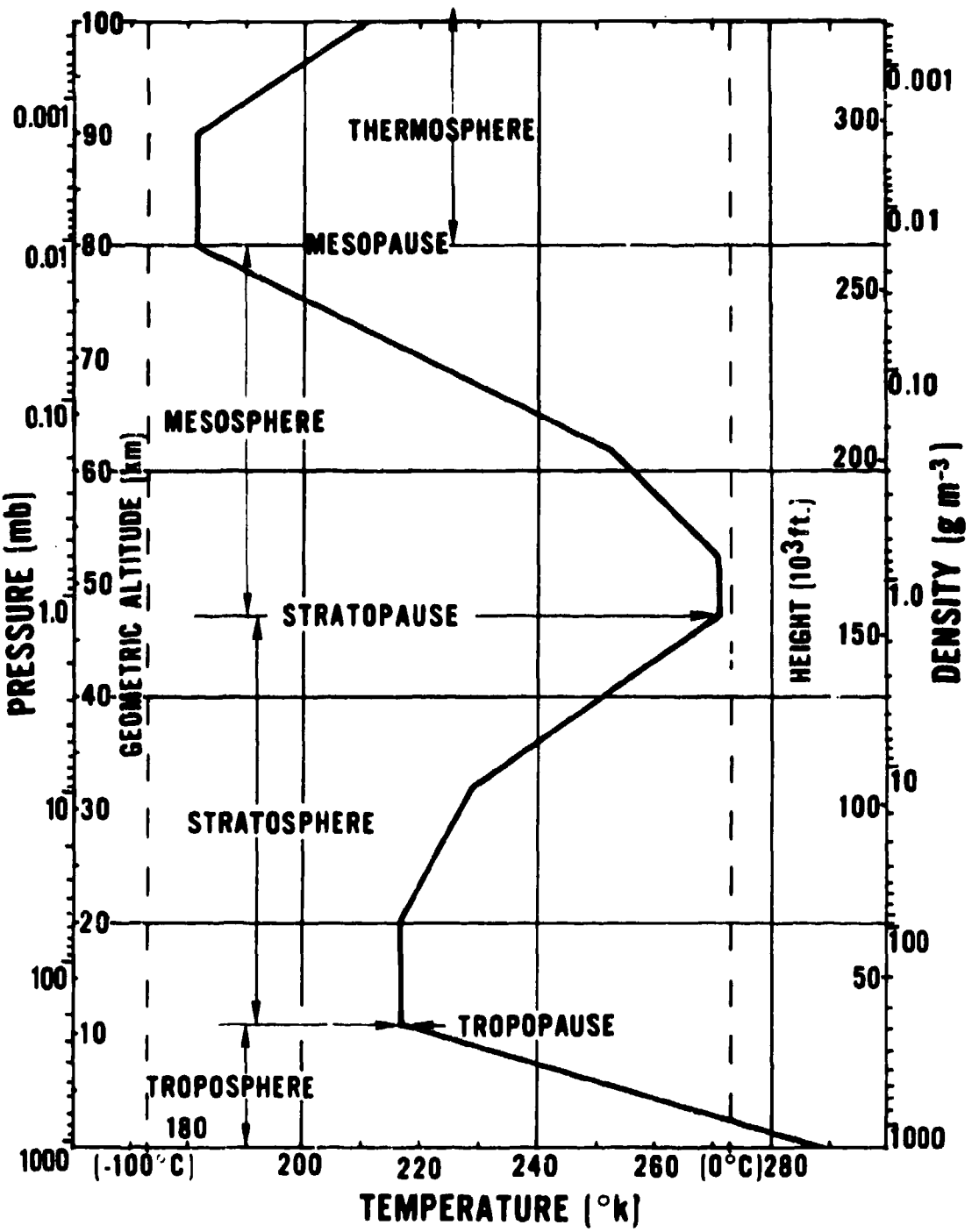

Fig. 14. Temperature-altitude profile to 100 km for U. S. standard atmosphere, 1962 (Valley).

5. **Atmospheric Attenuation and Emission.** The interactions between electromagnetic radiation and matter may be classified either as attenuation (extinction) or emission of radiation by matter. If there is a net increase in the radiant flux along the direction of propagation, we have emission; if there is a decrease in the radiant flux, we have attenuation. Attenuation of electromagnetic radiation by matter is caused by atsorption or scattering or both. Scattering is due to diffraction, reflection, refraction, or a combination of these effects. For a general and more extensive treatment, the reader should consult extensive literature on this subject.[73] [74] [75]

The fundamental law of attenuation is known as the Lambert, Beer, or Bouger law. It states that for monochromatic radiation the attenuation process is linearly proportional to the intensity of radiation and the amount of attenuating matter provided that the physical state (i.e. pressure, temperature, composition) of the matter remains constant. There are some cases in which Lambert's law does not apply; the photon density required for nonlinear effects is extremely high, such as in high-power lasers. If the inter-molecular distances and forces are fixed, then Lambert's law applies.

If the spectral intensity I_λ of a monochromatic parallel beam of radiation is changed by an amount dI_λ due to attenuation by matter after traversing a length dx of the optical medium along the direction of propagation, then

$$dI_\lambda = -\alpha_\lambda \, I_\lambda \, dx. \tag{32}$$

Similarly, for the emission process, the change in intensity of the emitted radiation corresponding to a source function J_λ is given by

$$dI_\lambda = +\alpha_\lambda \, J_\lambda \, dx. \tag{33}$$

The constant of proportionality α_λ is called the attenuation (extinction) coefficient (per unit length). If the attenuation coefficient α' is expressed per unit mass, equation (32) will be written as

$$dI_\lambda = -\alpha'_\lambda \, \rho(x) \, I_\lambda \, dx, \tag{34}$$

---

[73] K. Ya. Kondratyev, *Radiation in the Atmosphere*, Academic Press, New York (1969).

[74] R. M. Goody, *Atmospheric Radiation*, Oxford University Press, London (1964).

[75] D. Anding, *Band-Model Methods for Computing Atmospheric Molecular Absorption*, Report No. 7142-21-T, Willow Run Laboratories, The University of Michigan, Ann Arbor, Michigan (1967).

where $\rho(x)$ is the density of the medium at the point of consideration. From equation (32), we note that the product ($\alpha\, dx$) is dimensionless. This is known as the (differential) optical path or optical thickness,

$$d\tau_\lambda = \alpha_\lambda\, dx. \tag{35}$$

For a general interaction between radiation and matter involving both attenuation and emission, from equations (32), (33), and (35), one obtains the change in intensity,

$$-dI_\lambda = I_\nu\ d\tau_\lambda - J_\lambda\ d\tau_\lambda, \tag{36}$$

and thus

$$-(dI_\lambda/d\tau_\lambda) = I_\lambda - J_\lambda. \tag{37}$$

Equation (37) is the general equation of transfer; the left-hand side being a differential along the direction of propagation. This equation is used to solve radiative, heat-transfer problems.

If we integrate equations (32) and (34) for a homogeneous, non-radiating medium from $x = o$ to $x = X$, the transmitted intensity I_λ is given by

$$I_\lambda = I_{o\lambda} \exp\left[-\int_o^X \alpha_\lambda\, dx \right] \tag{38}$$

or

$$I_\lambda = I_{o\lambda} \exp\left[-\int_o^X \alpha'_\lambda\, \rho(x)\, dx \right], \tag{39}$$

where $I_{o\lambda}$ is the incident intensity at $x = o$.

The transmittance T and absorptance A of the medium are defined by the relations:

$$T_\lambda = I_\lambda / I_{o\lambda}, \tag{40}$$

$$A_\lambda = 1 - T_\lambda. \tag{41}$$

In the real atmosphere, the attenuation coefficient may vary from point to point along an arbitrary slant optical path. However, in a stable atmosphere under

specified representative conditions, one can define average atmospheric parameters and, hence, the average attenuation coefficient at various layers above the point of observation. Various atmospheric models have been proposed with increasing accuracy as better observational data are obtained.[76] [77] [78] The total atmospheric transmittance T_λ for j layers of a particular model atmosphere can be computed from equations (38) and (39):

$$T_\lambda = \exp\left[-\sum_j \alpha_{\lambda j} \Delta x_j \right] . \tag{42}$$

For a homogeneous optical path of length R having an attenuation coefficient α_λ for monochromatic radiation of wavelength λ, the atmospheric transmittance is given by

$$T_\lambda = \exp\left[-\alpha_\lambda R \right] . \tag{42a}$$

In general, the attenuation coefficient α_λ is the sum of an absorption coefficient k_λ and a scattering coefficient σ_λ:

$$\alpha_\lambda = k_\lambda + \sigma_\lambda . \tag{43}$$

The terrestrial atmosphere is composed of gaseous molecules and aerosols. The total atmospheric attenuation coefficient α_λ is the sum of absorption and scattering coefficients for molecules and aerosols; thus

$$\alpha_\lambda = k_{m\lambda} + \sigma_{m\lambda} + k_{a\lambda} + \sigma_{a\lambda} , \tag{44}$$

where the subscripts m and a indicate molecule and aerosol respectively. Each of these coefficients is wavelength dependent.

The optical transmittance per unit distance of a medium T is sometimes expressed in terms of the optical density or opacity of the medium using the relations:

---

[76] *U. S. Standard Atmosphere*, 1962, and *U. S. Standard Atmosphere Supplements*, 1966, U. S. Government Printing Office, Washington, D. C. 20402.

[77] L. Elterman, *Vertical Attenuation Model with Eight Surface Meteorological Ranges 2 to 13 Kilometers*, AFCRL-70-0200, Environ. Res. Paper No. 318, U. S. Air Force Cambridge Research Laboratories, Bedford, Massachusetts (1970).

[78] R. A. McClatchey, R. W. Fenn, J. E. A. Selby, F. W. Volz, and J. S. Garing, *Optical Properties of the Atmosphere (Revised)*, AFCRL-71-0279, Environ. Res. Paper No. 354, Air Force Cambridge Research Laboratories, Bedford, Massachusetts (1971).

Density, $D = \log_{10} (T)^{-1}$, (45)

Opacity, $O = T^{-1}$, (46)

or $D = \log_{10} O$, (47)

$O = 10^{D}$ (48)

thus $T = 10^{-D}$. (49)

The attenuation coefficient α may be written in terms of the optical density D. Remembering that the atmospheric transmittance for a unit optical path length from equation (42a) is given by

$$T_1 = e^{-\alpha_1} \tag{50}$$

and a comparison of equations (49) and (50) gives

$$e^{\alpha} = 10^{D}, \tag{51}$$

and $\alpha = D \ln 10$, (52)

or $\alpha = 2.3025851 \times D.$ (53)

The attenuation coefficient α can also be expressed in terms of decibels (db) using the relation:

$$10 \log_{10} [I_0/I] = db, \tag{54}$$

or $10 \log_{10} O = db$. (55)

Therefore, $10 D = db$, (56)

thus $D = 0.1$ db. (57)

Comparison of equations (53) and (57) gives

$$\alpha = 0.2305851 \text{ db}, \tag{58}$$

or attenuation loss in

$$\text{db/km} = 4.3367936\,\alpha\,(\text{km}^{-1}). \tag{58a}$$

A comparison of equations (49) and (57) gives the relation between transmittance T and the signal loss in db per unit distance:

$$T = 10^{-0.1\,\text{db}} \tag{59}$$

6. **Outdoor, Horizontal, Long-Path Atmospheric Transmittance.** Due to the unsteadiness of the real atmospheric optical environment, it is rather difficult to make successful and reliable measurements of atmospheric spectral transmittance. In a relatively clear and stable atmospheric optical environment, the atmospheric turbulence may introduce small-scale variations in atmospheric transmittance. However, over long, outdoor, horizontal, optical paths involving haze, fog, and large concentrations of smoke and dust aerosols, large-scale fluctuations in atmospheric transmittance are added due to space and time variations in the optical thickness of the medium caused by rapid movements of haze, fog, or dust banks in the optical path. In order to make reliable atmospheric optical measurements, the following parameters should be measured at as many locations as practical along the optical path:

(a) Atmospheric spectral transmittance.

(b) Geometry of the optical path with respect to the surface terrain and the surroundings.

(c) Ambient air temperature at a number of altitudes below, at, and above the optical path.

(d) Atmospheric pressure at a number of relevant locations.

(e) Relative humidity at a number of altitudes.

(f) Number and size distributions of atmospheric aerosols at a number of relevant points.

(g) Concentration of any abnormal atmospheric constituents in the optical path such as smoke, dust, exhaust fumes, and chemical effluents.

(h) Measurement of refractive indices of all types of aerosols encountered in the optical path.

(i) Chemical analysis of any abnormal gases in the optical path.

Due to the enormity of this task, it is no wonder that just a few teams of workers have been successful in making atmospheric transmittance measurements throughout the world. There is still an acute shortage of measurement data on the spectral transmission through heavy haze, fog, dust, and smoke environment. A set of spectroradiometers with large input apertures and optimized cooled sensitive detectors to measure the entire spectrum simultaneously (such as Fourier spectroradiometers) would be an ideal instrument system for atmospheric transmittance measurements.

A summary of the major, outdoor, horizontal, long-path atmospheric spectral transmittance measurements is presented in Table IX. Gebbie *et al.* made their measurements about 30 meters above the sea surface on the east coast of Scotland over optical path lengths of 2 and 4 kilometers.[79] Rock salt and lithium fluoride prisms were used in the spectrograph. The detector was a vacuum thermocouple. Most of their measurements were made under clear and stable atmospheric environments.

From 1952 to 1955, the French Institute of Optics group lead by Arnulf made atmospheric transmission measurements near the sea at St. Inglevert and near the Paris airport through haze and fog. Unfortunately, their haze spectra still remain unpublished in 1972, but they did publish their fog-transmission spectra.[80] They used ranges of 50, 100, 200, 600, and 1200 meters to measure transmission of quite-dense optical paths involving haze and various types of fogs. They measured fog droplet size and number spectra and calculated spectral transmittance using Mie theory calculations. The aerosol spectra measurements and spectral transmittance measurements both had a number of stated errors mainly due to the method of collection of aerosols and inhomogeneity of fog layers.

The spectral transmission measurements by the Naval Research Laboratory group of Taylor and Yates were made at three sea level ranges of 0.3, 5.5, and 16.25 kilometers under good visibility and stable atmospheric environmental conditions.[81] Yates and Taylor also made atmospheric transmission measurements at an altitude of about 3 kilometers above sea level through a horizontal optical path length of 27.7 km

---

[79] H. A. Gebbie, W. R. Harding, C. Hilsum, A. Pryce, and V. Roberts, "Atmospheric Transmission in the 1 to 14 Micron Region," *Proc. Roy. Soc. A 206*, 87 (1951).

[80] A. Arnulf, J. Bricard, E. Curé, and C. Veret, "Transmission by Haze and Fog in the Spectral Region 0.35 to 10 Microns," *J. Opt. Soc. Amer.* 47, 491 (1957).

[81] J. H. Taylor and H. W. Yates, "Atmospheric Transmission in the Infrared," *J. Opt. Soc. Amer.* 47, 223 (1957).

Table IX. Major Horizontal Long-Path Atmospheric Transmittance Measurements

WAVELENGTH	OPTICAL PATH	OPTICAL ENVIRONMENT	REFERENCE
1 TO 14 μm	2.07, 4.09 km	CLEAR, STABLE	GEBBIE et al. [a] [1951]
0.35 TO 10 μm	50 TO 1200 m	HAZE, FOG, VARIABLE	ARNULF et al. [b] [1957]
0.5 TO 15 μm	0.3, 5.5, 16.25 km 27.7 km	CLEAR, LIGHT HAZE " " "	TAYLOR & YATES [c] [1957] YATES & TAYLOR [d] [1960]
0.56 TO 10.7 μm	25 km	CLEAR, LIGHT HAZE	STREETE [e] [1968]
0.59 TO 12 μm	1.3, 2.6 km	HAZE	FILIPPOV et al. [f][g] [1969]
0.63 μm LASER 3.5 μm LASER 10.6 μm LASER	2.6 km	HAZE, RAIN, SNOW	CHU & HOGG [h] [1968]

(a) H. A. Gebbie, W. R. Harding, C. Hilsum, A. Price, and V. Roberts, "Atmospheric Transmission in the 1 to 14 Micron Region," *Proc. Roy. Society A206*, 87 (1951).

(b) A. Arnulf, J. Bricard, E. Cure, and C. Veret, "Transmission by Haze and Fog in the Spectral Region 0.35 to 10 Microns," *J. Opt. Soc. Amer.* 47, 491 (1957).

(c) J. H. Taylor and H. W. Yates, "Atmospheric Transmission in the Infrared," *J. Opt. Soc. Amer.* 47, 223 (1957).

(d) H. W. Yates and J. H. Taylor, *Infrared Transmission of the Atmosphere*, NRL Report 5453, U. S. Naval Research Laboratory, Washington, D. C. (1960).

(e) J. L. Streete, "Infrared Measurements of Atmospheric Transmission at Sea Level," *J. Opt. Soc. Amer.* 7, 1545 (1958).

(f) V. L. Filippov, L. M. Artem'yeva and S. O. Mirumyants, "Spectral Attenuation of Infrared Radiation in Winter Haze," Izvestiya, Academy of Science, U.S.S.R., *Atmospheric and Oceanic Physics (English Translation)* 5, 521 (1969).

(g) V. L. Filippov and S. O. Mirumyants, "The Spectral Transparency of the Atmospheric Boundary Layer to Infrared Radiation," Izvestiya, Academy of Science, U.S.S.R., *Atmospheric and Oceanic Physics (English Translation)* 5, 742 (1969).

(h) T. S. Chu and D. C. Hogg, "Effects of Precipitation on Propagation at 0.63, 3.5, and 10.6 Microns," *The Bell System Technical Journal*, 722 (1968).

between two mountain peaks—Mauna Loa and Mauna Kea in Hawaii.[82] The transmission spectra covering the spectral range 0.5 to 15 μm were recorded through a variety of amounts of precipitable water vapor 0.11 to 38 cm in the optical path.

Streete made the atmospheric transmission measurements through a 25-km-long optical path about 10 meters above the Atlantic Ocean water surface at Cape Kennedy, Florida.[83] He used an NaCl prism spectroradiometer with a thermocouple detector to study transmission of radiation in the 0.56 to 10.7 μm range from six carbon arc searchlights, each with a 150-cm-diameter aperture. His measurements covered a precipitable water vapor range from 21.5 cm to 43.3 cm in the 25-km optical path.

The Russian work performed over a period of several months during 1967-68 and reported by Filippov *et al.* contains atmospheric transmittance spectra from 0.59 μm to 12 μm recorded at the Zvenigorod Scientific Station of the Institute of Atmospheric Physics, Moscow.[84] [85] The measurements were conducted on a 1300-m horizontal, optical path under typical Moscow winter and summer environments involving clear, haze, haze mixed with snow, and dense haze conditions corresponding to meteorological visible ranges of 1.5 km to 20 km. The precipitable water-vapor content of the optical path ranged from 0.047 cm to 3.5 cm.

The measurements made at the Bell System Laboratory, Holmdel, New Jersey, and reported by Chu and Hogg were made with very narrow band coherent radiation sources; namely, an He-Ne laser operating at 0.63 μm, an He-Xe laser operating at 3.5 μm, and a CO_2 laser operating at 10.6 μm.[86] The optical path, 2.6 km in length, passed over a terrain containing grassy and plant nursery land partially planted and plowed with a few asphalt and dirt roadways. Atmospheric transmittance through haze, light fog, rain, and snow was studied at the three wavelengths. Chu and Hogg concluded

---

[82] H. W. Yates and J. H. Taylor, *Infrared Transmission of the Atmosphere*, NRL Report 5453, U. S. Naval Research Laboratory, Washington, D. C. (1960).

[83] J. L. Streete, "Infrared Measurements of Atmospheric Transmission at Sea Level," *J. Opt. Soc. Amer.* 7, 1545 (1958).

[84] V. L. Filippov, L. M. Artem'yeva, and S. O. Mirumyants, "Spectral Attenuation of Infrared Radiation in Winter Haze," Izvestiya, Academy of Science, U.S.S.R., *Atmospheric and Oceanic Physics (English Translation)* 5, 521 (1969).

[85] V. L. Filippov and S. O. Mirumyants, "The Spectral Transparency of the Atmospheric Boundary Layer to Infrared Radiation," Izvestiya, Academy of Science, U.S.S.R., *Atmospheric and Oceanic Physics (English Translation)* 5, 742 (1969).

[86] T. S. Chu and D. C. Hogg, "Effects of Precipitation on Propagation at 0.63, 3.5, and 10.6 Microns," *The Bell System Tech. Jour.* 722 (1968).

that the attenuation due to haze (called light fog by them) was up to one order of magnitude less at 10.6 μm compared to that at 0.63 μm; attenuation due to fog at 10.6 μm exceeded 40 db per km (Transmittance, $T = 10^{-4}$ per km). The attenuation in rain at 0.63 μm is less than 20 db per km (Transmission, $T = 10^{-2}$ per km). For the sake of convenience of the reader and for comparison, some of the major worldwide atmospheric transmittance measurements are presented here.

Figure 15 shows a sea-level spectrum of solar radiant incidance (irradiance) with spectra of the "infrared active" atmospheric gases recorded individually in the laboratory. The intensities of the spectral lines for individual gases are approximately relative to the concentration of each gas in the vertical atmospheric path. This figure is based on the work performed at Ohio State University.[87] Carbon monoxide (CO) has only a fairly weak absorption band at about 4.8 μm. Methane (CH_4) has two absorption bands at 3.2 μm and 7.8 μm. Nitrous Oxide (N_2O) has two strong absorption bands at 4.7 μm and 7.8 μm; the latter almost coincides with the absorption band of methane. Ozone (O_3) has a strong absorption band at 9.6 μm and another at 14 μm. Carbon dioxide (CO_2) has three very strong absorption bands centered at 2.7, 4.3, and 15 μm. HDO, the rare isotopic form of water, which has an abundance of 1/3355 in H_2O, has a very conspicuous absorption band at 3.67 μm and another at 7.13 μm; whereas, the important absorption bands of water vapor (H_2O) are centered at 1.14, 1.38, 1.88, 2.7, 3.2, and 6.3 μm.

Figure 16 presents an atmospheric transmission spectrum based upon the measurements of Gebbie *et al.*[88] The precipitable water vapor in the path was 1.7 cm. The average transmittance in the 3-4 μm band is about 0.90 compared to about 0.75 in the 8-12 μm band.

Figures 17a through c present atmospheric transmission spectra through fog at various stages of evolution and stability. These spectra are based upon the work of Arnulf *et al.*[89] To our knowledge, this is the only outdoor work ever reported in the worldwide literature for the spectral transmittance of fog. There were a number of sources of probable error and inaccuracy in this work as stated by the authors. The need for more work with improved instrumentation in order to obtain better accuracy and reliability is obvious.

---

[87] J. N. Howard, "The Transmission of the Atmosphere in the Infrared," *Proc. IRE*, 47, 1451 (1959).

[88] H. A. Gebbie, W. R. Harding, C. Hilsum, A. Pryce, and V. Roberts, "Atmospheric Transmission in the 1 to 14 Micron Region," *Proc. Roy. Soc. A 206*, 87 (1951).

[89] A. Arnulf, J. Bricard, E. Cure, and C. Veret, "Transmission by Haze and Fog in the Spectral Region 0.35 to 10 Microns," *J. Opt. Soc. Amer.* 47, 491 (1957).

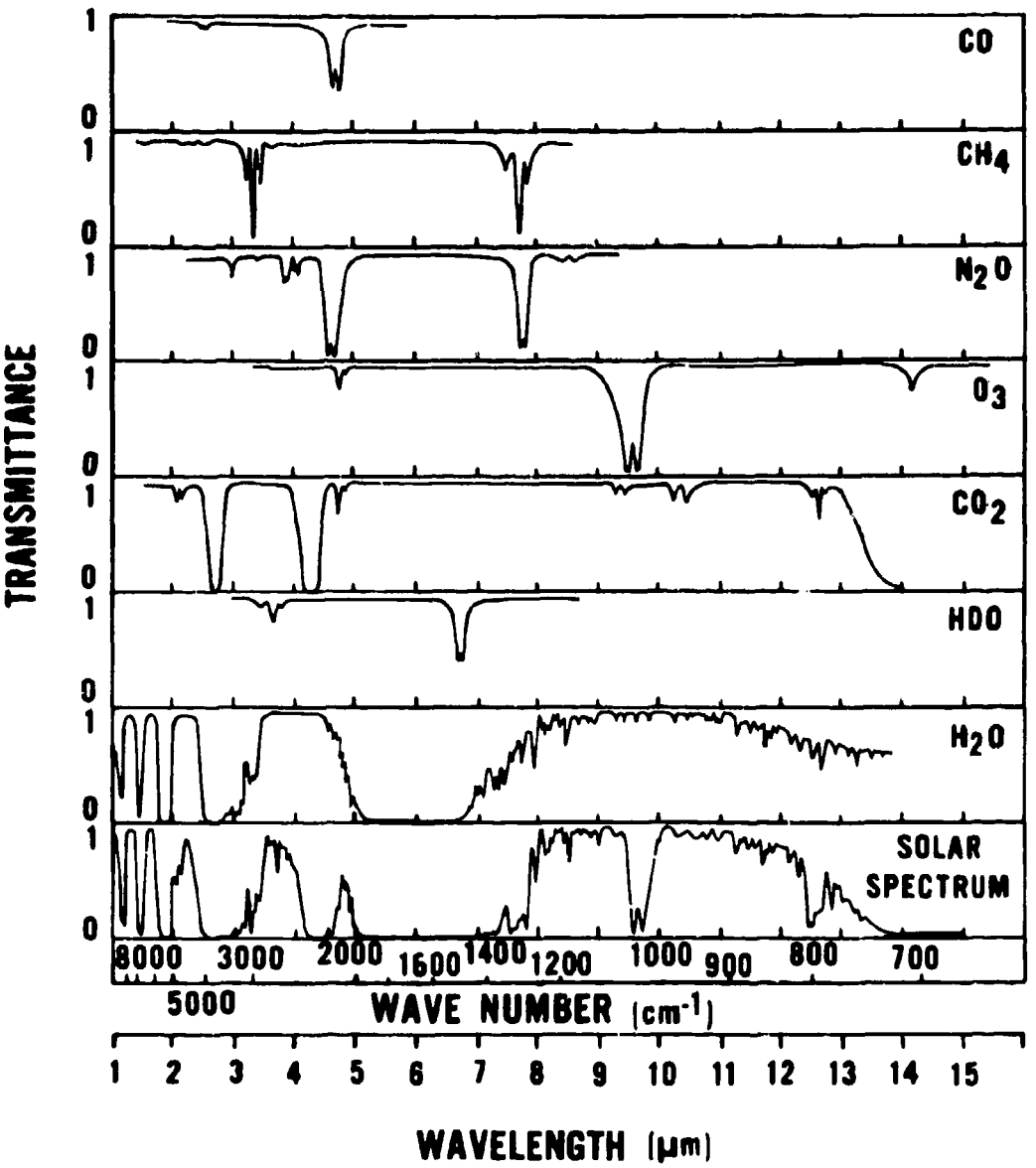

Fig. 15. Spectral transmittance of atmospheric gases (laboratory measurements) and the solar radiant incidance spectrum (Valley).

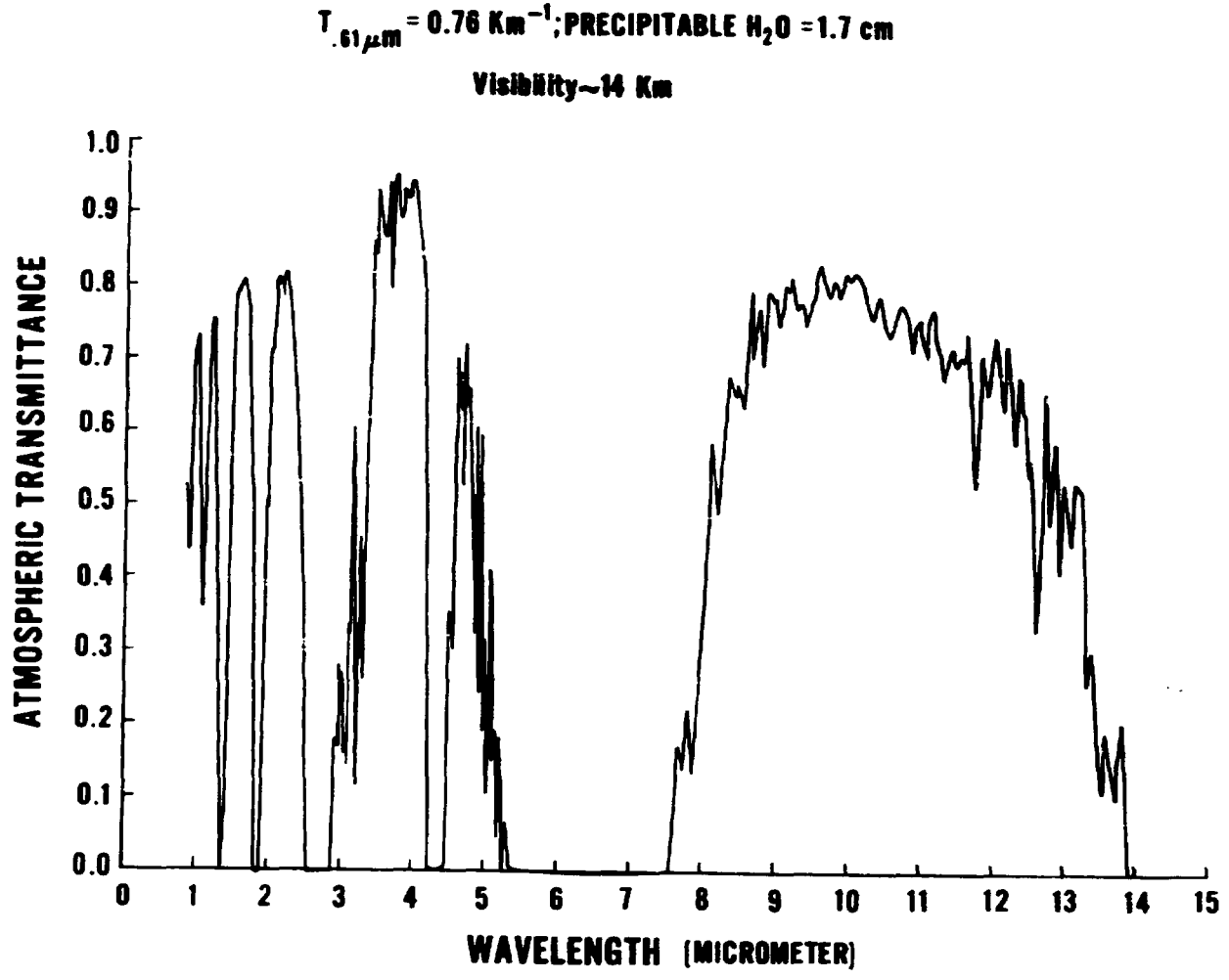

Fig. 16. Spectrum of atmospheric transmittance for 2.07 km optical path containing 1.7 cm of precipitable water vapor based upon Gebbie *et al.* measurements.

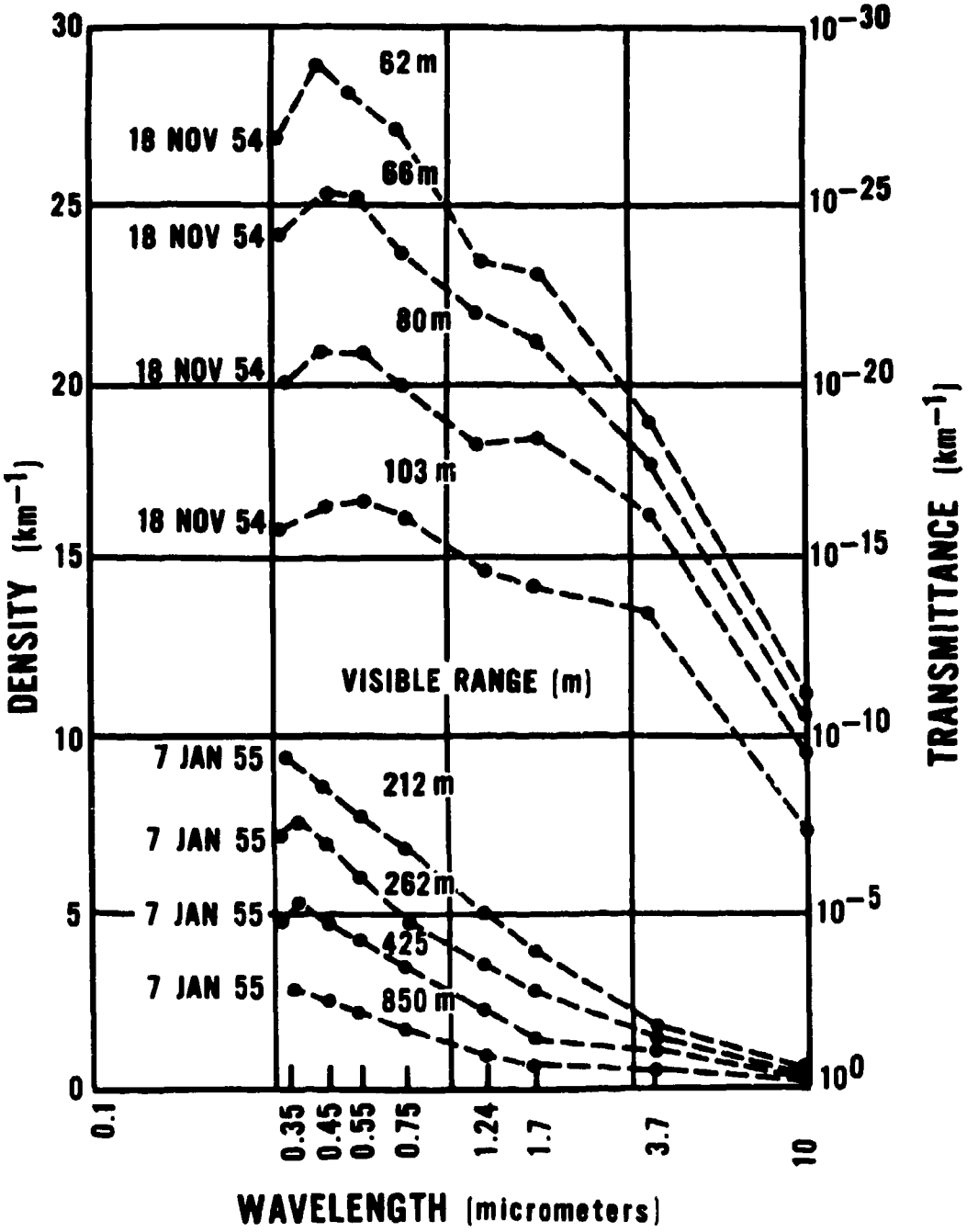

Fig. 17a. Atmospheric transmittance spectra for selective fogs as measured by Arnulf *et al.*

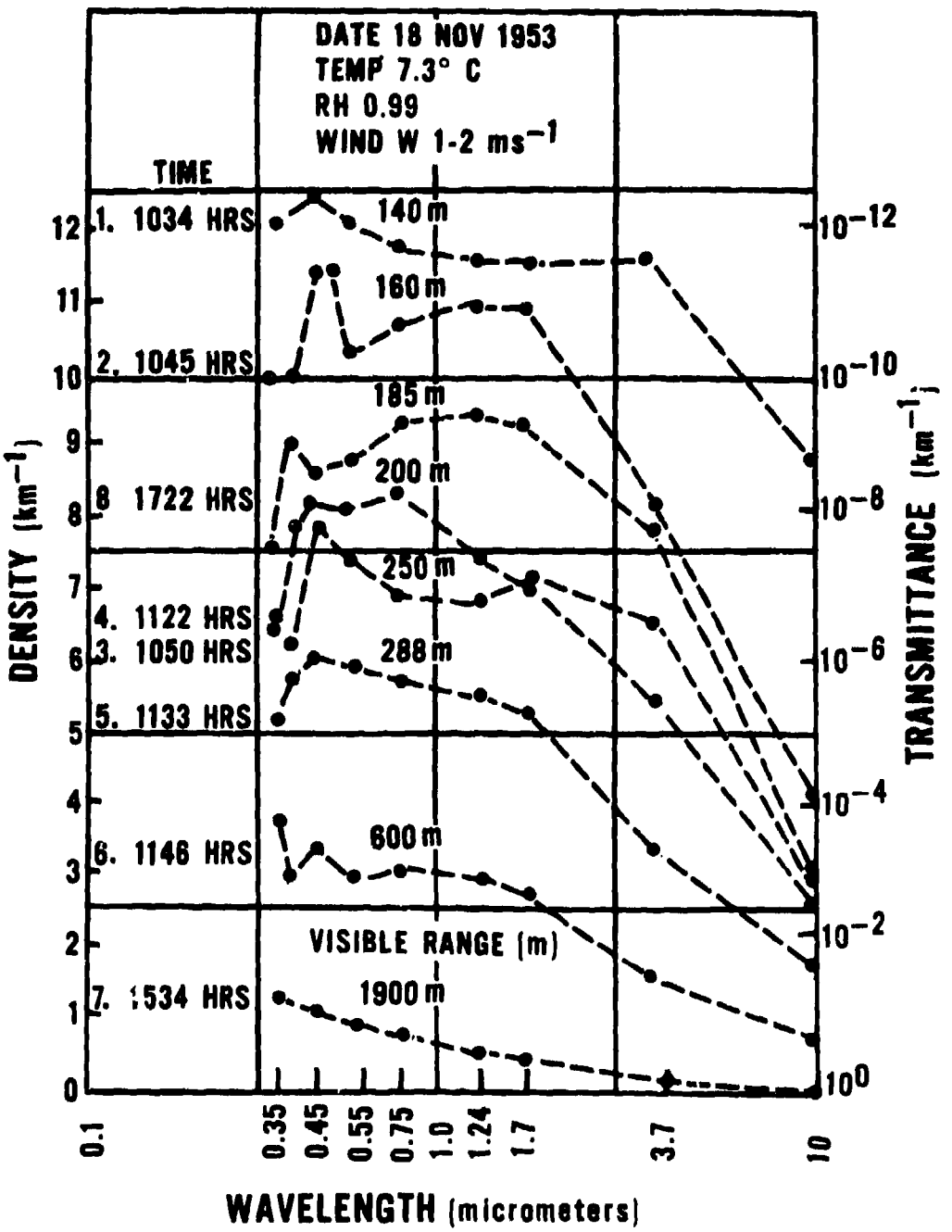

Fig. 17b. Atmospheric transmittance spectra for evolving fogs as measured by Arnulf *et al.*

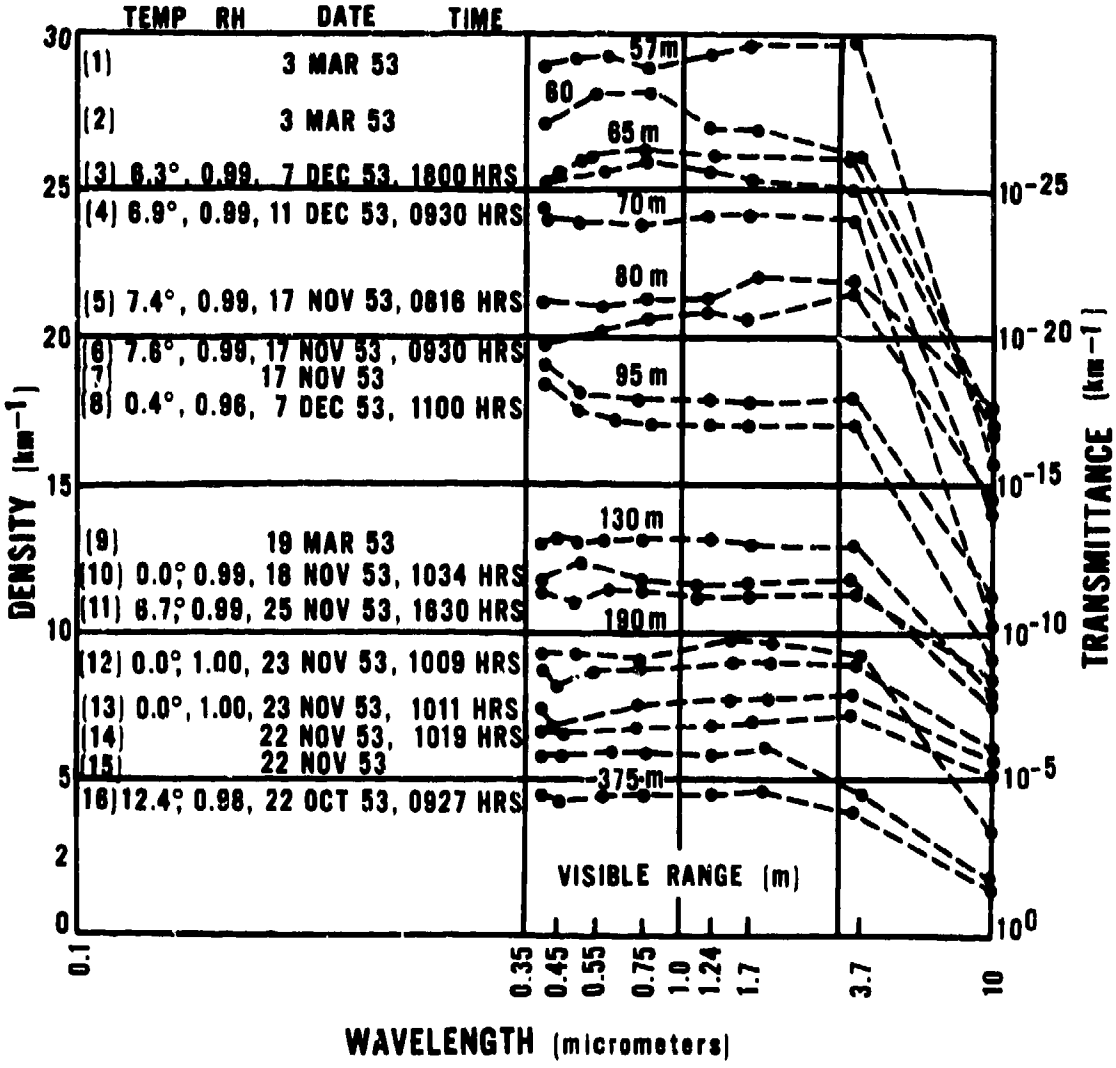

Fig. 17c. Atmospheric transmittance spectra for stable fogs, Type 1, as measured by Arnulf *et al.*

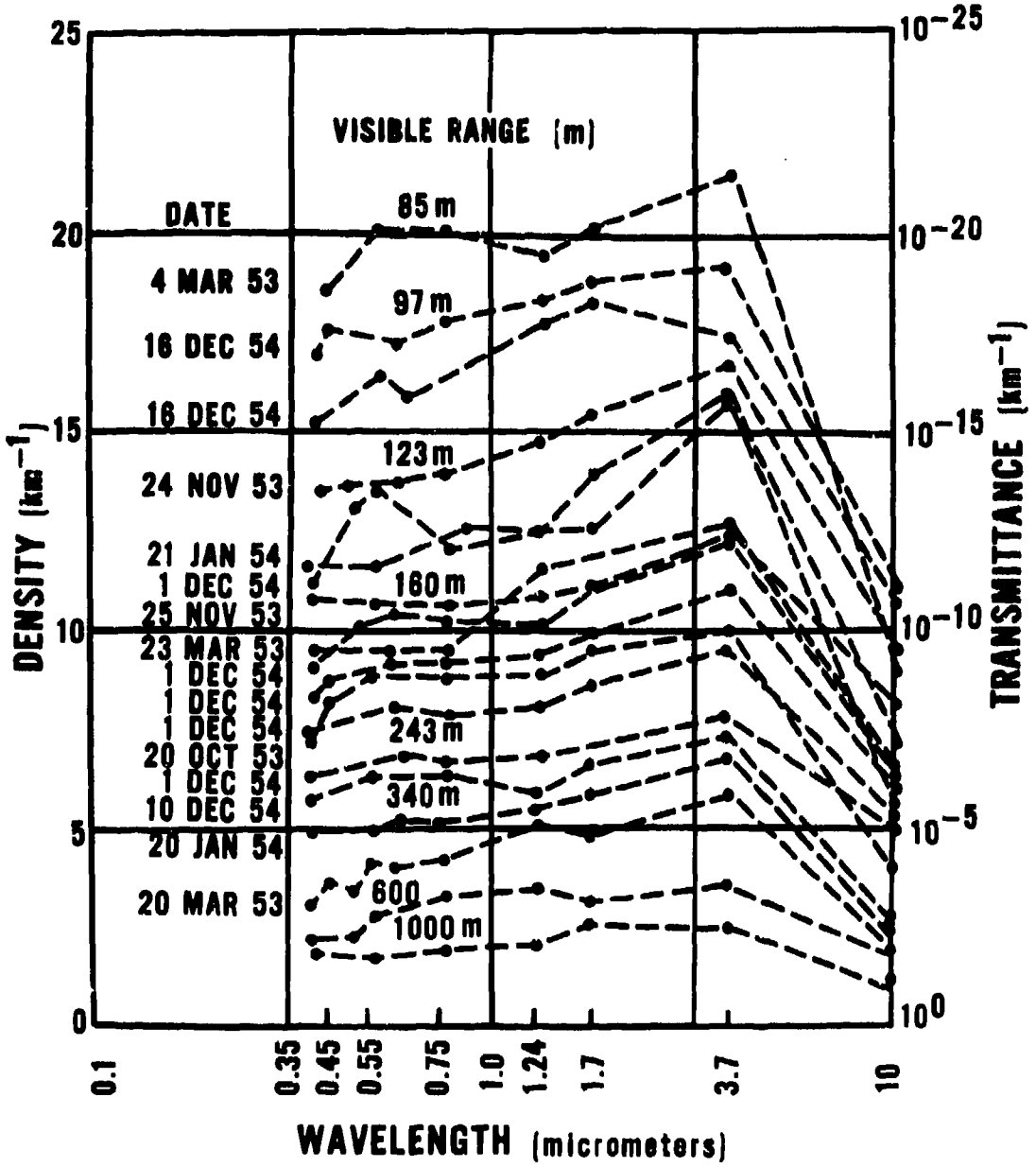

Fig. 17d. Atmospheric transmittance spectra for stable fogs, Type 2, as measured by Arnulf *et al.*

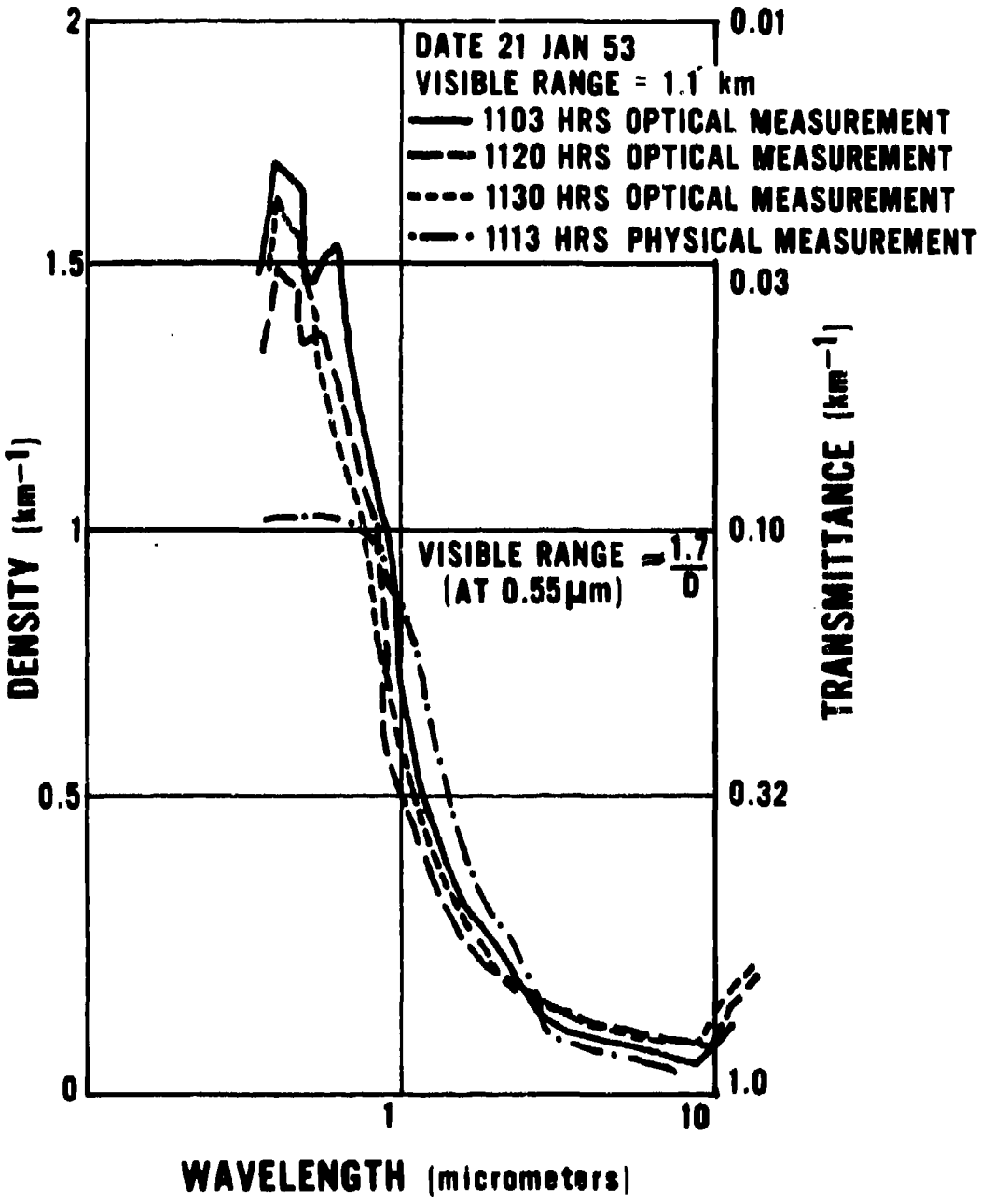

Fig. 17e. Atmospheric transmittance spectra for haze as measured by Arnulf *et al.*

Figures 18 and 19 present atmospheric transmittance spectra based upon the work of Taylor and Yates who used optical ranges of 0.3, 5.5, 16.2, and 27.7 km with the precipitable water vapor content of 0.11, 1.37, 5.2, and 20 cm respectively. Their work has the best accuracy, reliability, and spectral resolution ($\lambda/\Delta\lambda = 300$), but most of this study was limited to clear and stable atmospheric conditions.[90] [91]

Figure 20 contains atmospheric transmittance spectra recorded on a 25-km optical path by Streete for various amounts of precipitable water vapor ranging from 21.5 cm to 43.3 cm.[92] In this study, the optical path was over the Atlantic Ocean at varying heights above the water surface with occasional sprays of mist tossed up into the optical path by ocean waves. Streete used Fowle's spectroscopic method to compute the amount of precipitable water instead of using values of temperature and relative humidity at a number of points along the optical path.[93] The HDO absorption band at 3.67 μm in the Yates and Taylor data was used to determine the relation between transmittance and precipitable water vapor. This method assumes that the atmospheric optical environments under which the two measurements of Taylor-Yates and Streete were conducted were identical. This procedure may have introduced a considerable inaccuracy in the determination of the precipitable water vapor content of the optical path. McCoy has also analyzed this problem and has come to the same conclusion.[94]

Figures 21 and 22 present ten atmospheric transmittance spectra recorded by Filippov and Mirumyants for various amounts of precipitable water vapor ranging from 0.105 cm to 3.5 cm on 1.3 km or 2.6 km long optical paths near Moscow.[95] Figure 23 shows the spectral variation of attenuation coefficients in the 0.59 μm to 12 μm range

---

[90] J. H. Taylor and H. W. Yates, "Atmospheric Transmission in the Infrared," *J. Opt. Soc. Amer.* 47, 223 (1957).

[91] H. W. Yates and J. H. Taylor, *Infrared Transmission of the Atmosphere*, NRL Report 5453, U. S. Naval Research Laboratory, Washington, D. C. (1960).

[92] J. L. Streete, "Infrared Measurements of Atmospheric Transmission at Sea Level," *J. Opt. Soc. Amer.* 7, 1545 (1958).

[93] F. E. Fowle, "The Spectroscopic Determination of Aqueous Vapor," *The Astrophysical Journal, 35*, 149 (1912), also "The Determination of Aqueous Vapor above Mount Wilson," *The Astrophy. Jour. 37*, 367 (1913).

[94] J. H. McCoy, *Atmospheric Absorption of Carbon Dioxide Laser Radiation Near Ten Microns*, Technical Report 2476-2, The Ohio State University, Columbus, Ohio (1968).

[95] V. L. Filippov and S. O. Mirumyants, "The Spectral Transparency of the Atmospheric Boundary Layer to Infrared Radiation," Izvestiya, Academy of Science, U.S.S.R., *Atmospheric and Oceanic Physics (English Translation) 5*, 742 (1969).

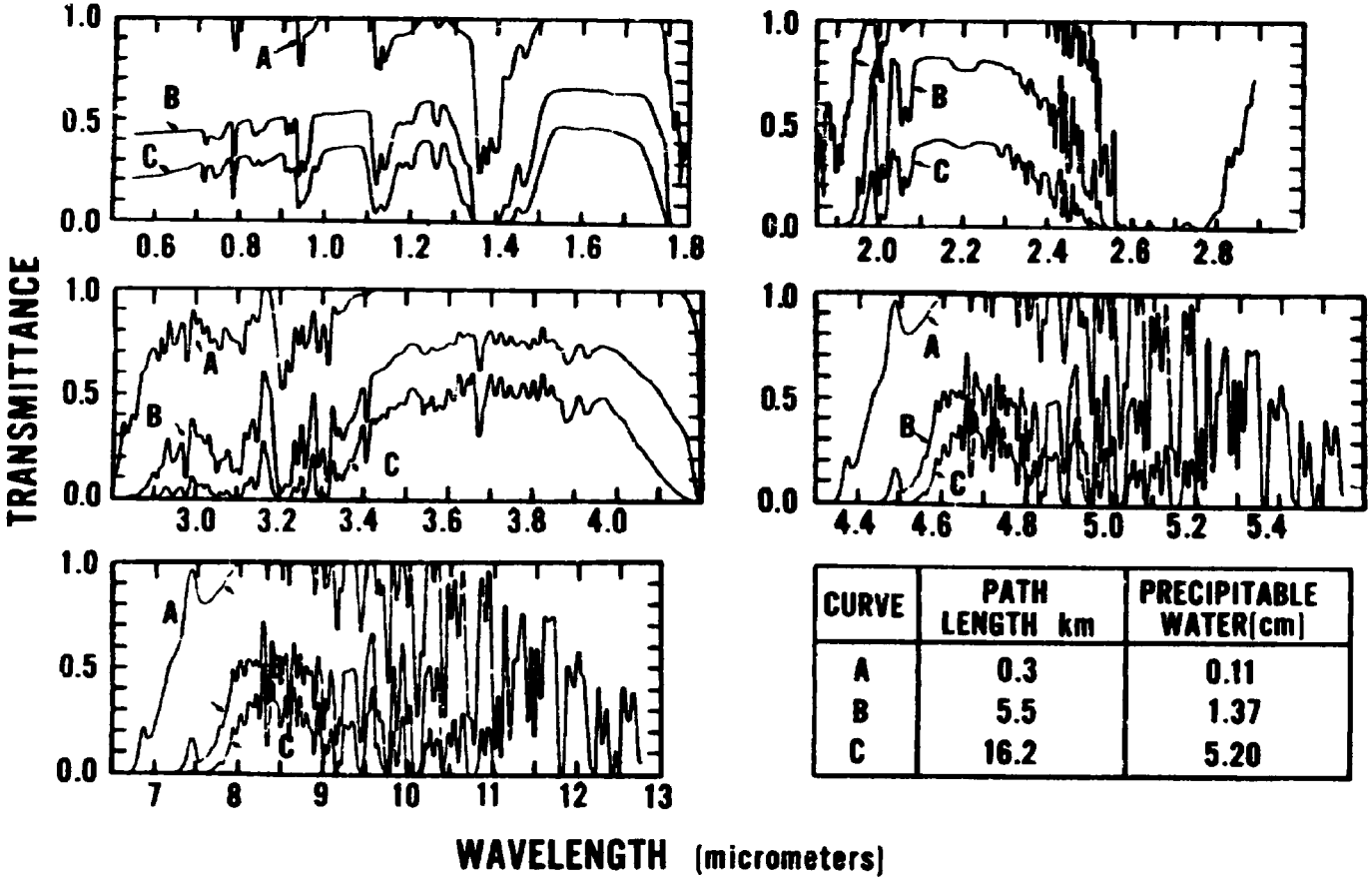

CURVE	PATH LENGTH km	PRECIPITABLE WATER(cm)
A	0.3	0.11
B	5.5	1.37
C	16.2	5.20

Fig. 18. Atmospheric transmittance spectra recorded by Taylor and Yates over 0.3, 5.5 and 16.2 km long optical paths.

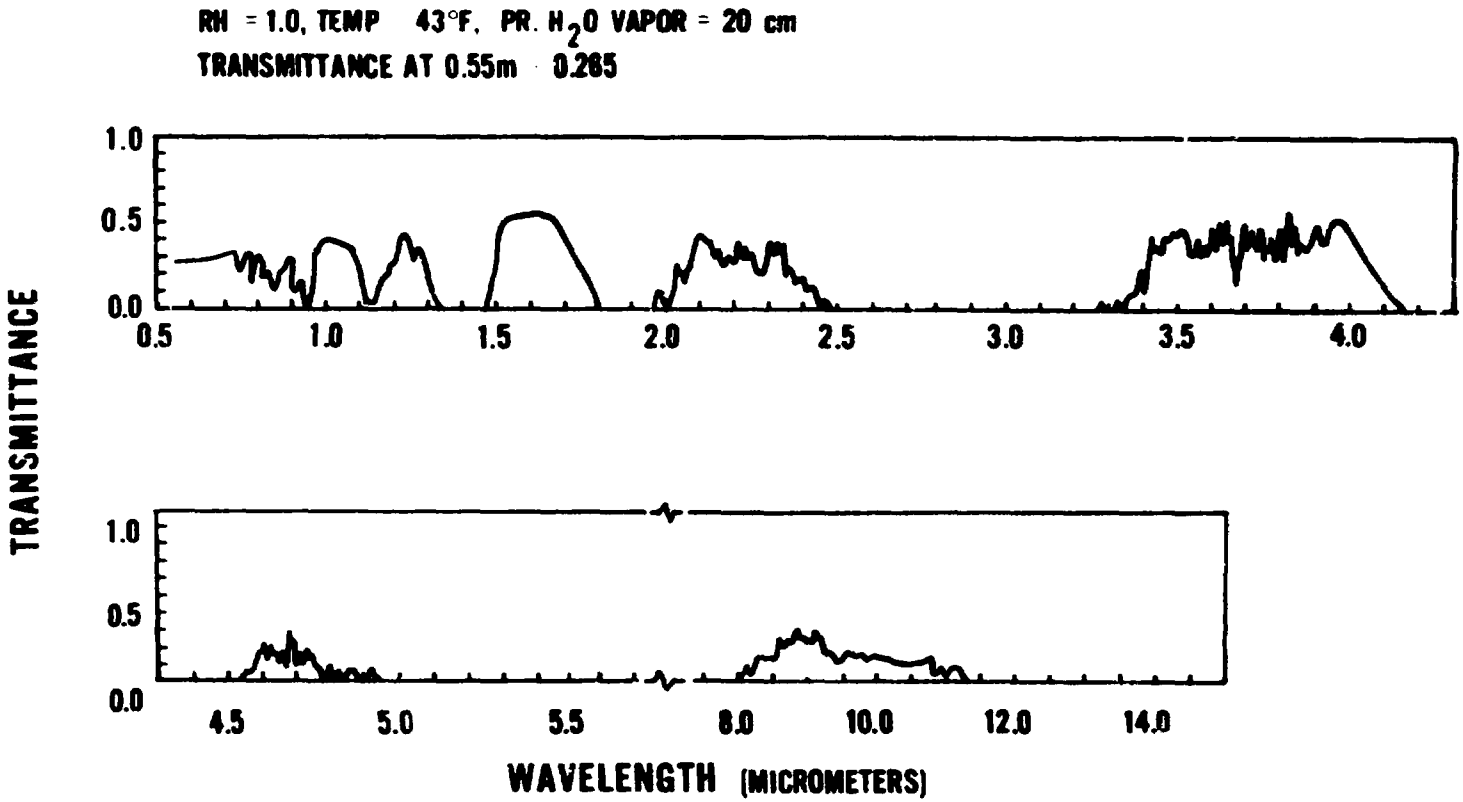

Fig. 19. Atmospheric transmittance spectrum recorded by Yates and Taylor on a 27.7 km optical path with 20 cm precipitable water vapor.

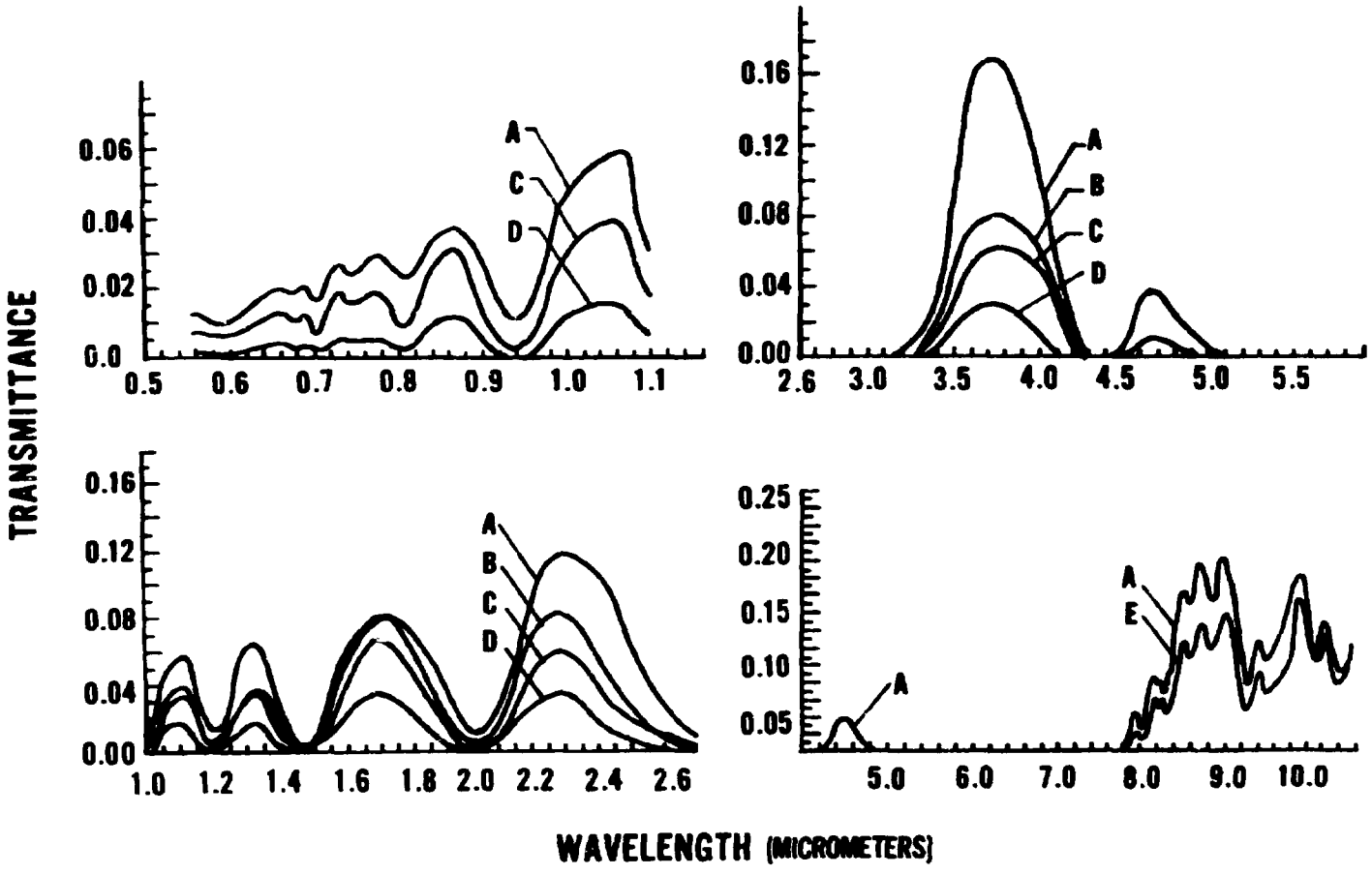

Fig. 20. Atmospheric transmittance spectra for various amounts of precipitable water vapor in 25 km optical path: (A) 21.5 cm, (B) 25.4 cm, (C) 36.2 cm, (D) 43.3 cm, and (E) 26.7 cm, recorded by Streete.

CURVE	DATE, TIME	OPTICAL PATH LENGTH (km)	PRE-CIPIT-ABLE WATER w,cm	ATMOS-PHERIC TRANS-MITTANCE	TEMP °C	RELA-TIVE HUMID-ITY (%)
A	17 MAY, 1968 1100	1.3	0.105	0.68	−21.0	75
B	18 APRIL, 1968 1000	1.3	0.27	0.72	−2.1	46
C	14 APRIL, 1968 1500	1.3	0.53	0.75	+4.6	66
D	24 APRIL, 1968 0800	1.3	1.05	0.79	+9.5	88
E	9 APRIL, 1968 1700	1.3	0.78	0.74	+14	50

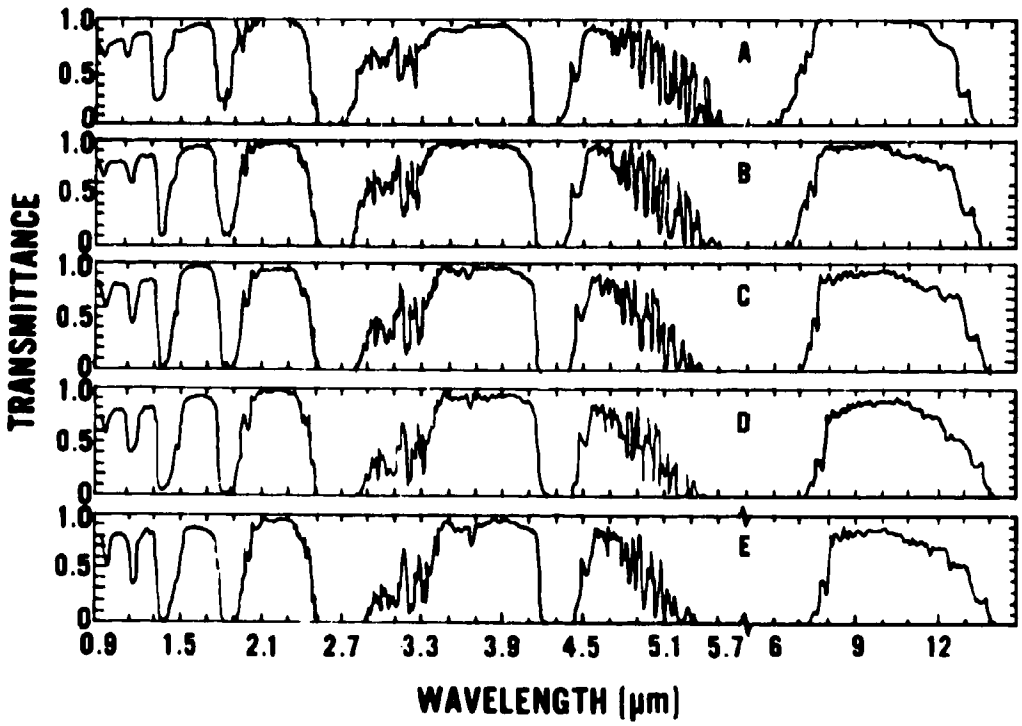

Fig. 21. Atmospheric transmittance spectra for various amounts of precipitable water vapor: (A) 0.105 cm, (B) 0.27 cm, (C) 0.53 cm, (D) 1.05 cm, and (E) 0.78 cm, recorded by Filippov *et al.*

CURVE	DATE, TIME	OPTICAL PATH LENGTH (km)	PRE-CIPIT-ABLE WATER w,cm	ATMOS-PHERIC TRANS-MITTANCE	TEMP C	RELA-TIVE HUMID-ITY (%)
A	11 AUG., 1968 2000	1.3	1.55	0.85	+15.2	90
B	8 OCT., 1967 1345	2.6	2.05	0.92	+10.7	81
C	10 AUG., 1968 1830	2.6	2.47	0.92	+20	54.5
D	11 AUG., 1968 1800	2.6	3.0	0.85	+15.7	86
E	13 AUG., 1968 2030	2.6	3.5	0.90	+15.4	96

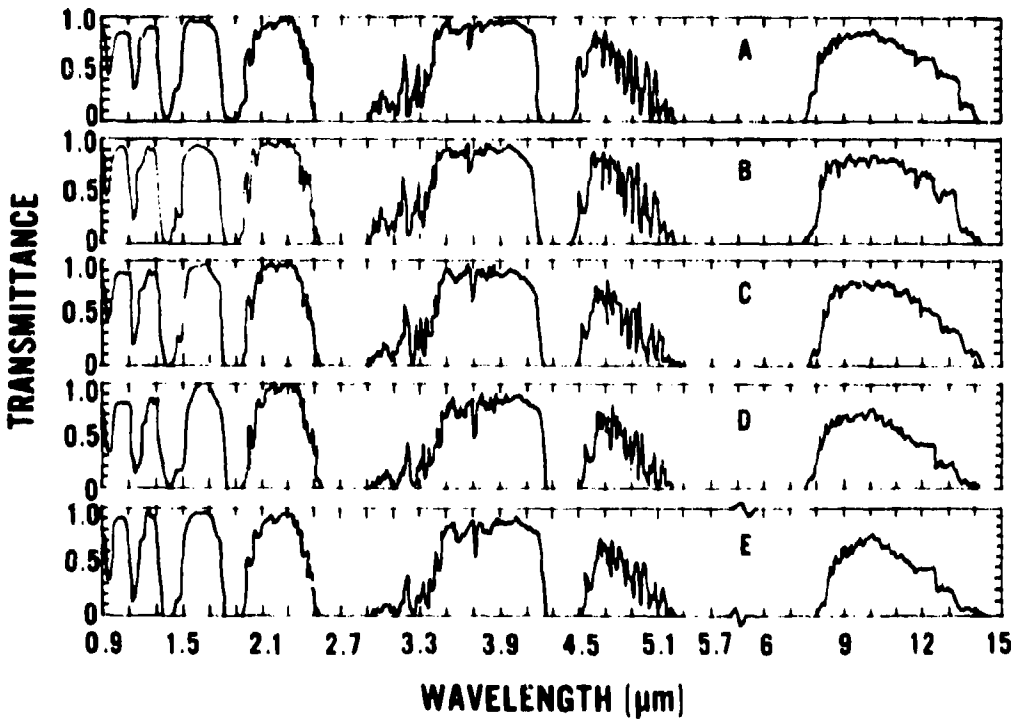

Fig. 22. Atmospheric transmittance spectra for various amounts of precipitable water vapor: (A) 1.55 cm, (B) 2.05 cm, (C) 2.47 cm, (D) 3.0 cm, and (E) 3.5 cm, recorded by Filippov *et al.*

MEASUREMENT NO.	S_M, km	t, C	RH°,	AMOUNT OF H20 VAPOR w. pr. cm.	DATE AND TIME	REMARKS
262	1.97	-30.0	90	0 053	23 JAN 1968, 1740 HRS	HAZE AND WIDELY SPACED SNOW
157	3.18	-14.5	89	0 297	25 DEC 1967, 1600 HRS	SAME
233	2.6	-30.0	82	0.047	24 JAN 1968, 1200 HRS	DENSE HAZE
208	2.70	-22.0	82	0.100	21 " " 1610 HRS	SAME
196	7.5	-18.0	85	0.144	20 " " 1750 HRS	HAZE
277	6.75	-9.0	85	0.278	29 " " 1930 HRS	SAME
187	14.9	-21.0	83	0.100	20 " " 1300 HRS	SAME
271	7.8	-7.0	85	0.330	29 " " 1020 HRS	SAME
228	2.7	-30.0	82	0.047	24 " " 1210 HRS	DENSE HAZE
245	4.75	-17.5	84	0.144	25 " " 1550 HRS	HAZE AND WIDELY SPACED SNOW
206	2.5	-22.0	82	0.100	21 " " 1610 HRS	DENSE HAZE
200	4.5	-18.4	79	0.122	25 " " 1845 HRS	HAZE
265	5.55	-5.0	80	0.330	28 " " 1910 HRS	SAME
250	3.9	-23.0	84	0.090	21 JAN 1968, 1010 HRS	HAZE AND WIDELY SPACED SNOW
243	9.37	-17.5	80	0.132	25 " " 1400 HRS	HAZE
272	8.8	-7.0	85	0.330	29 " " 1400 HRS	SAME
198	7.6	-18.0	85	0.144	20 " " 1820 HRS	SAME
260	1.92	-30.0	90	0.058	28 " " 1515 HRS	HAZE AND WIDELY SPACED SNOW

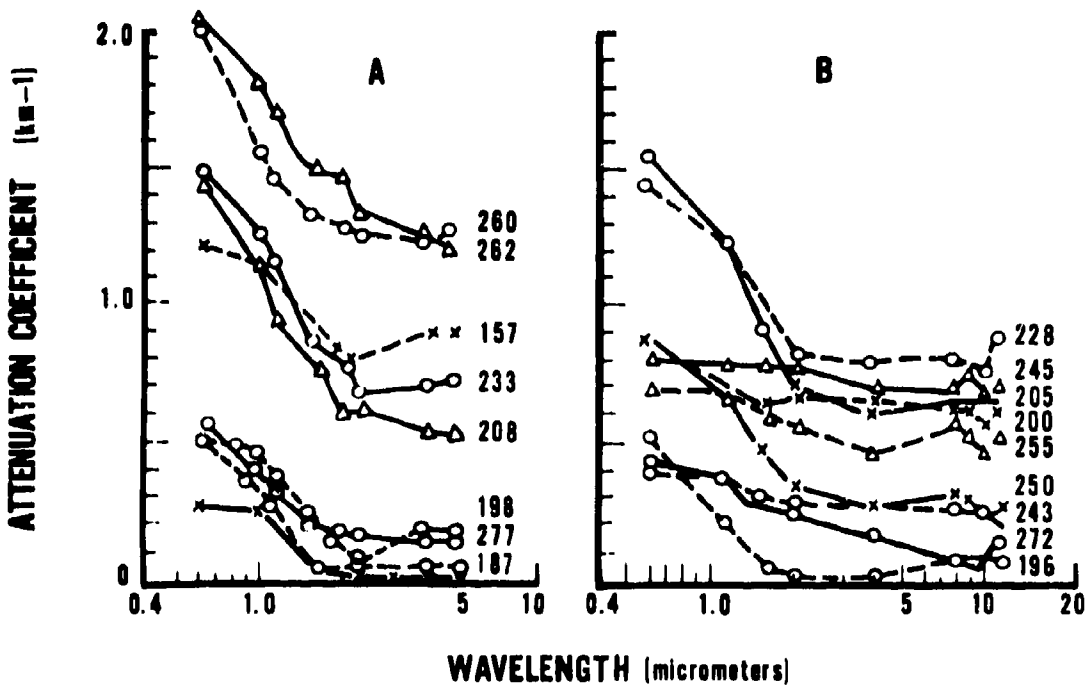

Fig. 23. Spectral attenuation coefficients for winter haze in the 0.59 to 5.0 μm and 0.59 to 12.0 μm regions reported by Filippov *et al.*

for winter haze measurements made by Filippov *et al.*[96] They have not published atmospheric transmittance for thick haze or light fog conditions.

Finally, the comparative studies of the effects of haze, rain, and snow on the propagation of laser radiation at 0.63, 3.5, and 10.6 μm as reported by Chu and Hogg are presented in Figs. 24, 25, and 26.[97] Figure 24 shows that in evolving haze and light fog, with changing number and size of aerosols, the transmittance of 10.6 μm radiation is much better than that of 3.5 μm and 0.63 μm radiation. In the earlier stage of haze development, the transmission, per kilometer, of 0.63 and 3.5 μm radiation was about 0.03 whereas that of 10.6 μm was 0.63. Later on, when the haze became thick and the transmittance of the 0.63 μm radiation fell down by two orders of magnitude, there was no appreciable change in the transmittance of the 10.6 μm and 3.5 μm radiation. Here, the conclusion is that small changes in the aerosol size can drastically affect wavelength dependence of transmission. Figure 25 shows the variation in transmittance with variable rainfall in the optical path. Here, the spectral transmittance is reversed with respect to that in haze or light fog. For rain, the transmission is the highest for 0.63 μm, is lower for 3.5 μm, and is the lowest for the 10.6 μm radiation. Figure 26 shows the variation of atmospheric transmittance with variable amounts of light snow in the optical path for the three laser wavelengths. The attenuation of 10.6 μm radiation appears to be larger than that of the other two wavelengths which appear to be equally attenuated.

Based upon outdoor, long-path, atmospheric spectral attenuation measurements, Knestrick, Cosden, and Curcio have computed atmospheric scattering coefficients in 10 narrow wavelength bands between 0.4 micrometer and 2.3 micrometers.[98] The wavelength bands were chosen so as to avoid atmospheric molecular absorption and were isolated by interference filters. Curcio, Drummeter, and Knestrick have made high-resolution ($\Delta\lambda = 0.2$A) spectral absorption measurements from 5400 A to 8520 A over a sea level, 16.25-km-long, horizontal, optical path over water.[99]

---

[96]V. L. Filippov, L. M. Artem'yeva, and S. O. Mirumyants, "Spectral Attenuation of Infrared Radiation in Winter Haze," Izvestiya, Academy of Science, U.S.S.R., *Atmospheric and Oceanic Physics. (English Translation)* 5, 521 (1969).

[97]T. S. Chu and D. C. Hogg, "Effects of Precipitation on Propagation at 0.63, 3.5, and 10.6 Microns," *The Bell System Tech. Jour.* 722 (1968).

[98]G. L. Knestrick, T. H. Cosden, and J. A. Curcio, "Atmospheric Scattering Coefficients in the Visible and Infrared Regions," *J. Opt. Soc. Am.* 52, 1010 (1962).

[99]J. A. Curcio, L. F. Drummeter, and G. L. Knestrick, "An Atlas of the Absorption Spectrum of the Lower Atmosphere from 5400 A to 8520 A," *App. Opt.* 3, 1401 (1964).

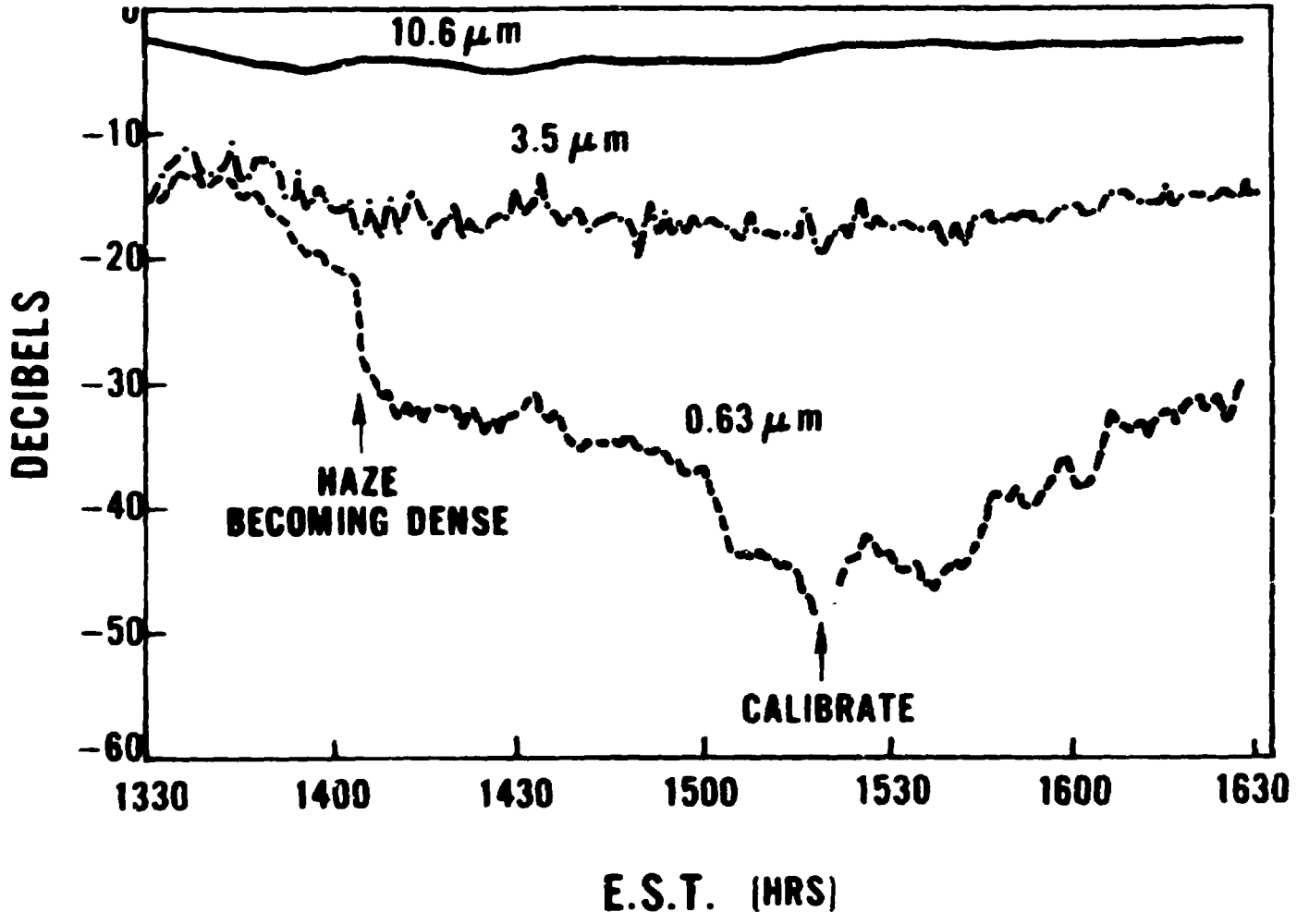

Fig. 24. Transmittance of 0.63 μm, 3.5 μm, and 10.6 μm laser radiation through variable haze over 2.6 km optical path as measured by Chu and Hogg.

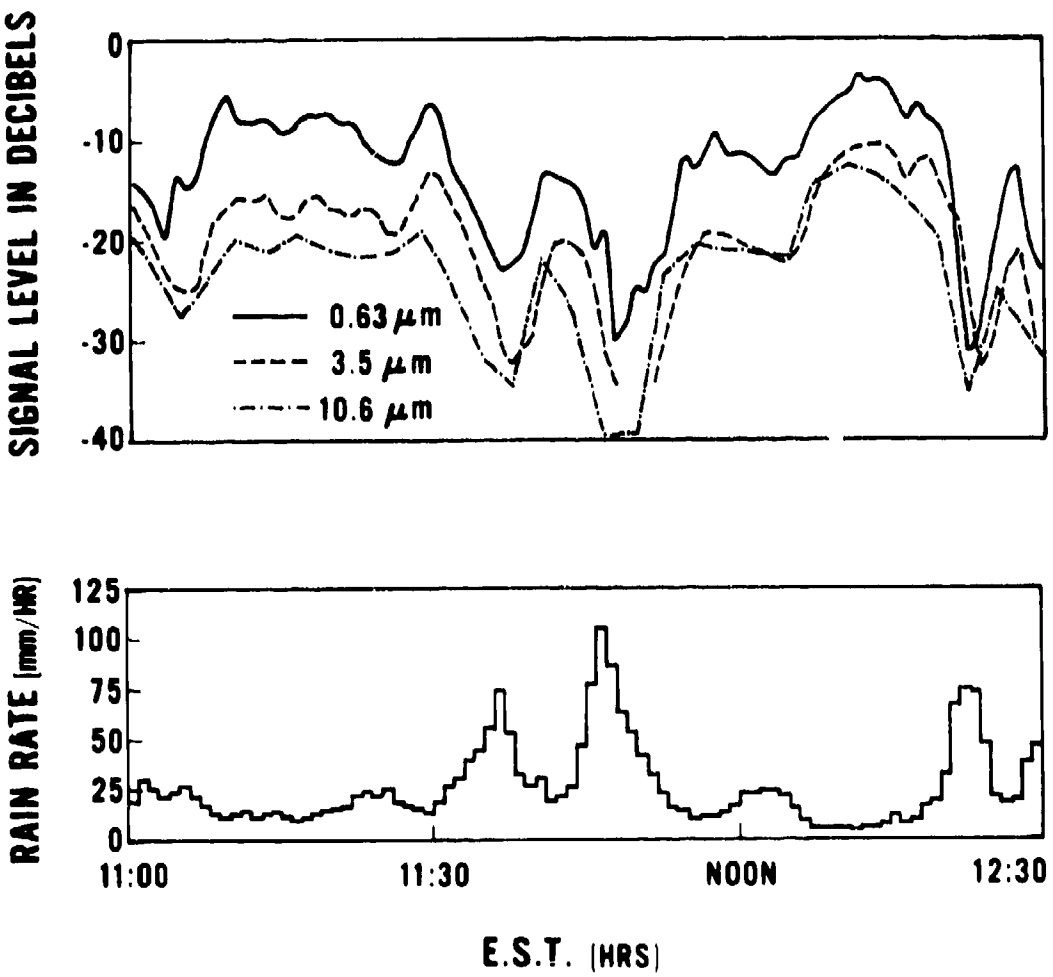

Fig. 25. Transmittance of 0.63 μm, 3.5 μm, and 10.6 μm laser radiation through variable rain in 2.6 km optical path as measured by Chu and Hogg.

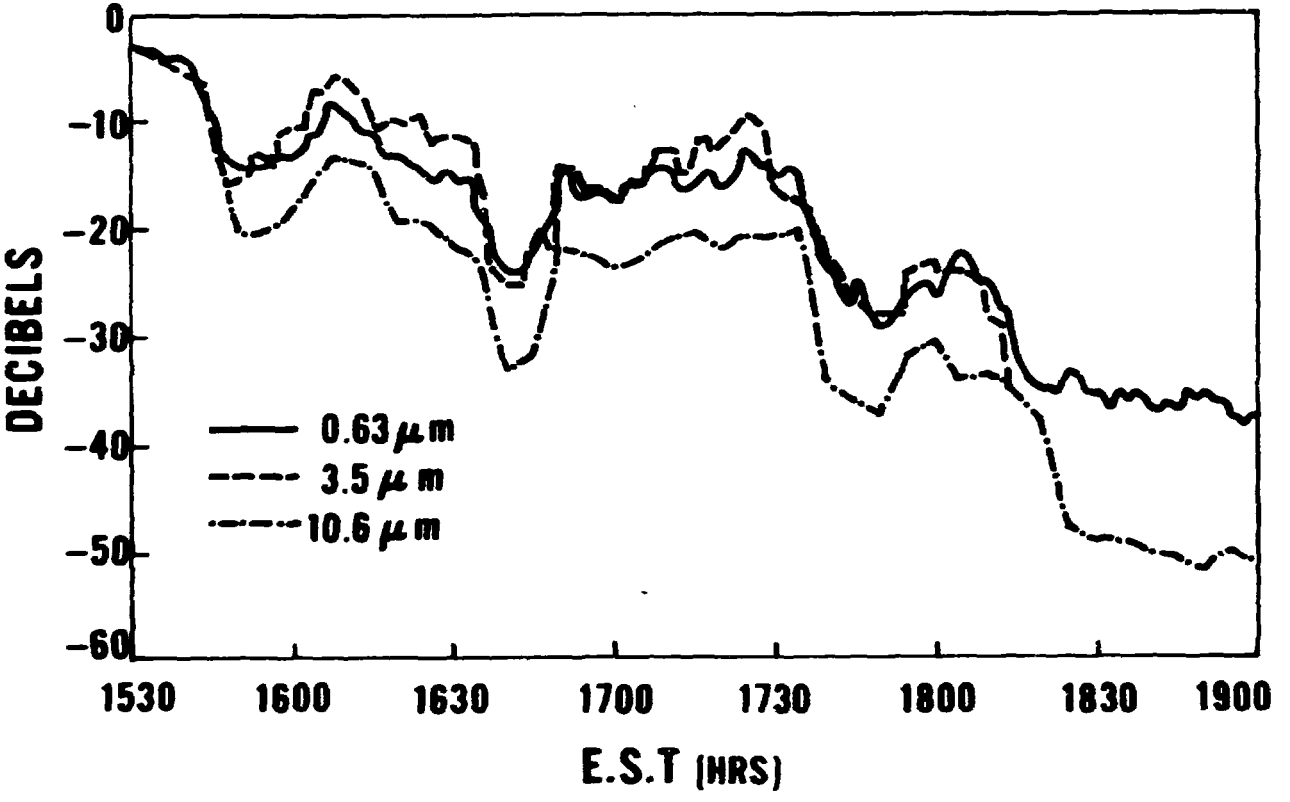

Fig. 25. Transmittance of 0.63 μm, 3.5 μm, and 10.6 μm laser radiation through light snow over 2.6 km optical path as measured by Chu and Hogg.

Attenuation of visible and infrared laser radiation by clouds was studied by Sanders and Selby using five continuous-wave lasers operating at wavelengths of 0.63, 1.15, 3.39 μm, (Helium-Neon), 10.6 μm (CO_2 - N_2 - Ne), and 337 μm (CN radical).[100] The meteorological optical ranges (visibilities) varied from 40 meters to 200 meters during the measurement period. They concluded that during these conditions there were no significant differences in cloud attenuation at 0.63, 1.15, and 3.39 μm; however, the attenuation at 10.6 μm averaged about half that at 0.63 μm when cloud density was not too high. The scattering loss at 337 μm in clouds is small in comparison with molecular absorption by water vapor.

Precipitable Water Vapor: The precipitable water vapor in the optical path is the amount of water that would be obtained if all the water vapor contained in a cylinder of unit area cross section extending along the entire optical path is precipitated. The height of this column of precipitable water vapor w, measured in centimeters, can be obtained by the following relations:

$$w\ (\text{pr cm } H_2O) = \left[\frac{2.88 \times 10^{-2}}{T}\right] p\ L, \tag{60}$$

or

$$w\ (\text{pr cm } H_2O) = \left[\frac{2.88 \times 10^{-2}}{T}\right] (RH)\ p_s\ L, \tag{61}$$

since

$$RH = p/p_s, \tag{62}$$

or

$$w\ (\text{pr cm } H_2O) = \rho(T)\ (RH)\ L \tag{62a}$$

where T is the air temperature in the optical path, expressed in degrees Kelvin, RH is the fractional relative humidity, p and p_s are respectively the partial and saturated pressures of water vapor at the temperature of measurement, in torr (mm Hg), $\rho(T)$ is the water vapor density at the ambient temperature T, and L is the optical path length expressed in meters. The saturated water vapor pressure and density are given in tables published in several handbooks (such as D-106 and E-11, *CRC Handbook*, 1966).[101] From equation (60), one should note that the amount of water vapor in the optical path is a function of the temperature and the partial pressure of the water vapor. It should be emphasized that the atmospheric transmittance is not a unique function of

---

[100] R. Sanders and J. E. A. Selby, *Comparative Measurements of the Attenuation of Visible and Infrared Laser Radiation in Cloud*, Report DMP 3151, EMI Electronics Limited, Hayes, Middlesex, England (1968).

[101] *Handbook of Chemistry and Physics*, The Chemical Rubber Co., Cleveland, Ohio (1966); also *Smithsonian Meteorological Tables*, By R. J. List, Smithsonian Institution, Washington, D. C. (1968).

precipitable water vapor in the optical path, but it is dependent upon the partial pressure of the water vapor, the total pressure, and the temperature of the medium.

7. Laboratory Studies of the Attenuation of Radiation by Atmospheric Gases. Since outdoor studies of atmospheric transmission cannot be conducted under controlled atmospheric environments, the alternate approach to study the properties of gaseous attenuation is to measure optical properties of individual atmospheric gases in the laboratory under controlled conditions. Multiple-path cells are used to study optical properties of gases. These cells are designed to study the spectral absorption of radiation by individual gases at various partial pressures, temperatures, and total pressures. A synthetic atmosphere is created by introducing a known amount of absorbing gas into the evacuated cell along with an infrared transparent gas such as nitrogen to create the desired total pressure in the cell. The variations in partial pressure of the absorber and the total pressure in the cell enable the simulation of atmospheric optical environments corresponding to those existing at various altitudes in planetary atmospheres.

The most notable laboratory studies of attenuation by atmospheric gases have been reported by Howard, Burch, and Williams;[102] and Burch *et al.*,[103] Gryvnak and Shaw,[104] Shaw,[105] and Rensch[106] of Ohio State University; Palmer of Johns Hopkins University;[107] Tidwell, Plyler, and Benedict of the National Bureau of Standards;[108] Burch and Gryvnak, of the Aeronutronic Division, Philco-Ford Corporation;[109] and Zuev of Tomask University.[110]

---

[102] J. N. Howard, D. E. Burch, and D. Williams, "Near-infrared Transmission Through Synthetic Atmospheres," *J. Opt. Soc. Am.* *46*, 186, 237, 243, 334, 452 (1956).

[103] D. E. Burch, E. B. Singleton, W. L. France, and D. Williams, "Infrared Absorption by Minor Atmospheric Constituents," Final Report, C-AF19(604)-2633 (1960); also Sci. Reports 1 (1960) and Sci. Report 2 (1961) Ohio State University, Columbus, Ohio; AFCRL Rept.-62-698 (1962); *Applied Optics*, *1*, 359, 473, 587, 759 (1962), *2*, 585 (1963) and *3*, 55 (1964).

[104] D. A. Gryvnak and J. H. Shaw, Sci. Rept. 2, AF19(604)6141, The Ohio State Univ. (1961).

[105] J. H. Shaw, Report No. AF19(122)-65, The Ohio State University (1954).

[106] D. B. Rensch, *Extinction and Backscatter of Visible and Infrared Laser Radiation by Atmospheric Aerosols*, Report 2467-3, The Ohio State University (1969).

[107] H. Palmer, *J. Opt. Soc. Am.* *47*, 367, 1024, 1028, 1054 (1957); *49*, 1139 (1959); *50*, 1232 (1960).

[108] E. D. Tidwell, E. K. Plyler, and W. S. Benedict, *J. Opt. Soc. Am.* *50*, 1243 (1960).

[109] D. E. Burch and D. A. Gryvnak, Aeronutronic, Philco-Ford Reports U-2955, U-2995, U-3127, U-3200, U-3201, U-3202, U-3204, U-3857, U-3930, U-3972, U-4076, U-4132 (1964-67).

[110] V. E. Zuev, *Atmospheric Transparency in the Visible and the Infrared English Translation*, Israel Program for Scientific Translations, Jerusalem (1970), also *Propagation of Visible and Infrared Radiation in the Atmosphere*, Sovietskoye Radio Press, Moscow (1970).

McClatchey of the Optical Physics Laboratory, AFCRL, is presently compiling the latest fundamental spectroscopic data on the spectral lines of all molecules responsible for atmospheric absorption. The spectral line data are to include frequency, line intensity, half width, and energies of the quantum mechanical energy states involved in the radiation transfer process. The gases involved in this study are CO_2, H_2O, O_3, N_2O, CO, CH_4, O_2, N_2, and HNO_3. A report on this work is expected to be completed by the end of 1972.[111]

Recently, Perry, Layman, and Ealy have conducted a study of the "atmospheric window" transmittance through artificial fog.[112] They have measured the relative transmittance in the "visible," 3-5 μm, and 8-12 μm spectral bands through a 45.72 m (150 ft) optical path. The fog chamber is reported to have the capability to produce homogeneous fog with variable density but with a constant relative size distribution of fog droplets. Figure 27 shows the relative size distribution of fog particles used in this study. Figure 28 presents the relative transmittance for their "visible," 3-5 μm, and 8-12 μm spectral band radiation-detection-systems through artificial fog of varying optical density or transmittance. From Fig. 28, it is clear that the relative spectral band transmittance through fog increases with wavelength in the three atmospheric windows under consideration. However, the transmittance for the 3-5 μm and 8-12 μm spectral band system falls to 0.02 and 0.2, respectively, when the optical density of fog reaches a value of 2 (visible transmission of 0.01). Further, the relative transmittance of the 8-12 μm spectral band detection system falls below a rather low value of 0.02 when the optical density of fog reaches 2.7 (visible transmittance of 0.002). The real outdoor fogs have optical densities varying from 1.7 to 30 which correspond to visible ranges of 1 km to 50 meters, respectively (see Fig. 17). The 8-12 μm spectral band system has a reasonable transmittance advantage over the visible and the 3-5 μm band systems especially in the optical density range of 1.7 to 2.7 (visible range 1000 - 630 m) where the transmittance of the 3-5 μm system falls below 0.02.

8. **Fundamental Principles of Gaseous Absorption.** The spectral transmission of radiation by the atmospheric constituents is rather complex owing to the multiplicity of physical processes involved in the interaction of radiation and matter. A complete treatment of the theory of atmospheric gaseous absorption is presented in a number of

---

[111] R. A. McClatchey, private communication.

[112] J. E. Perry, S. F. Layman, and W. R. Ealy, *Comparison of the Transmission Through Fog of the 3-5 and 8-14 μm Spectral Regions as a Function of the Visible Transmission*, Research and Development Technical Report ECOM-7013, U. S. Army Electronics Command, Fort Monmouth, New Jersey (1971).

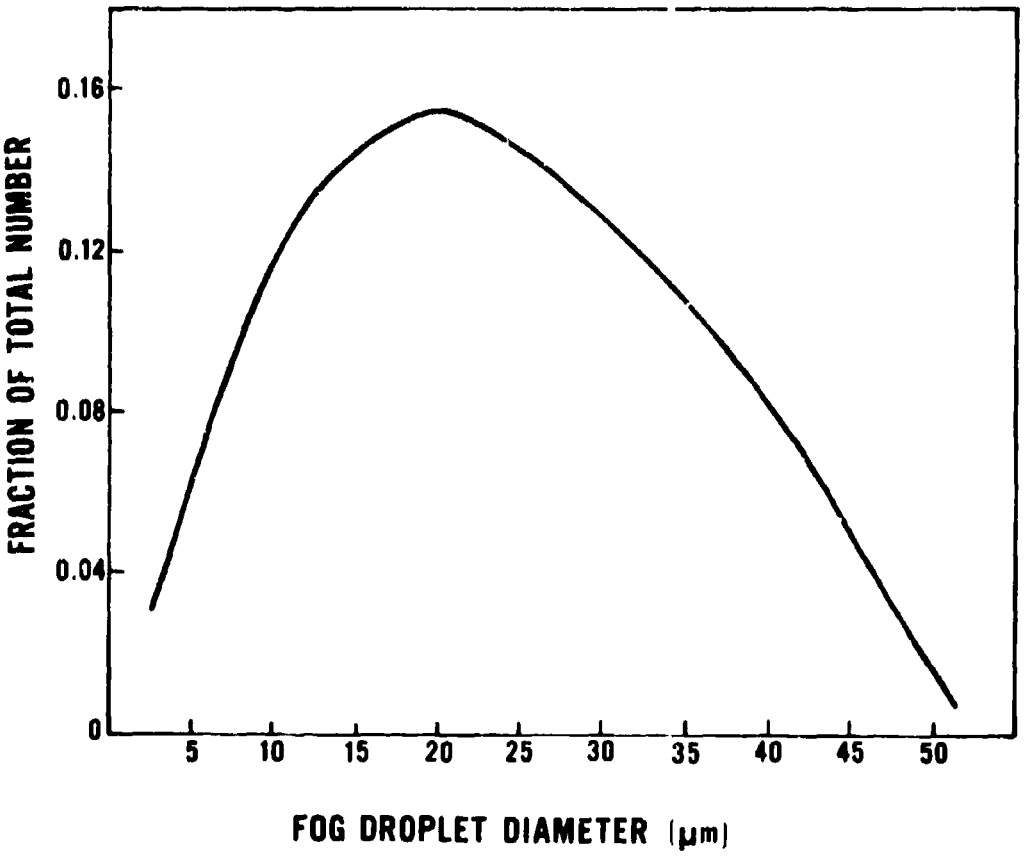

Fig. 27. Relative size distribution of fog particles in the fog chamber as reported by Perry and Layman.

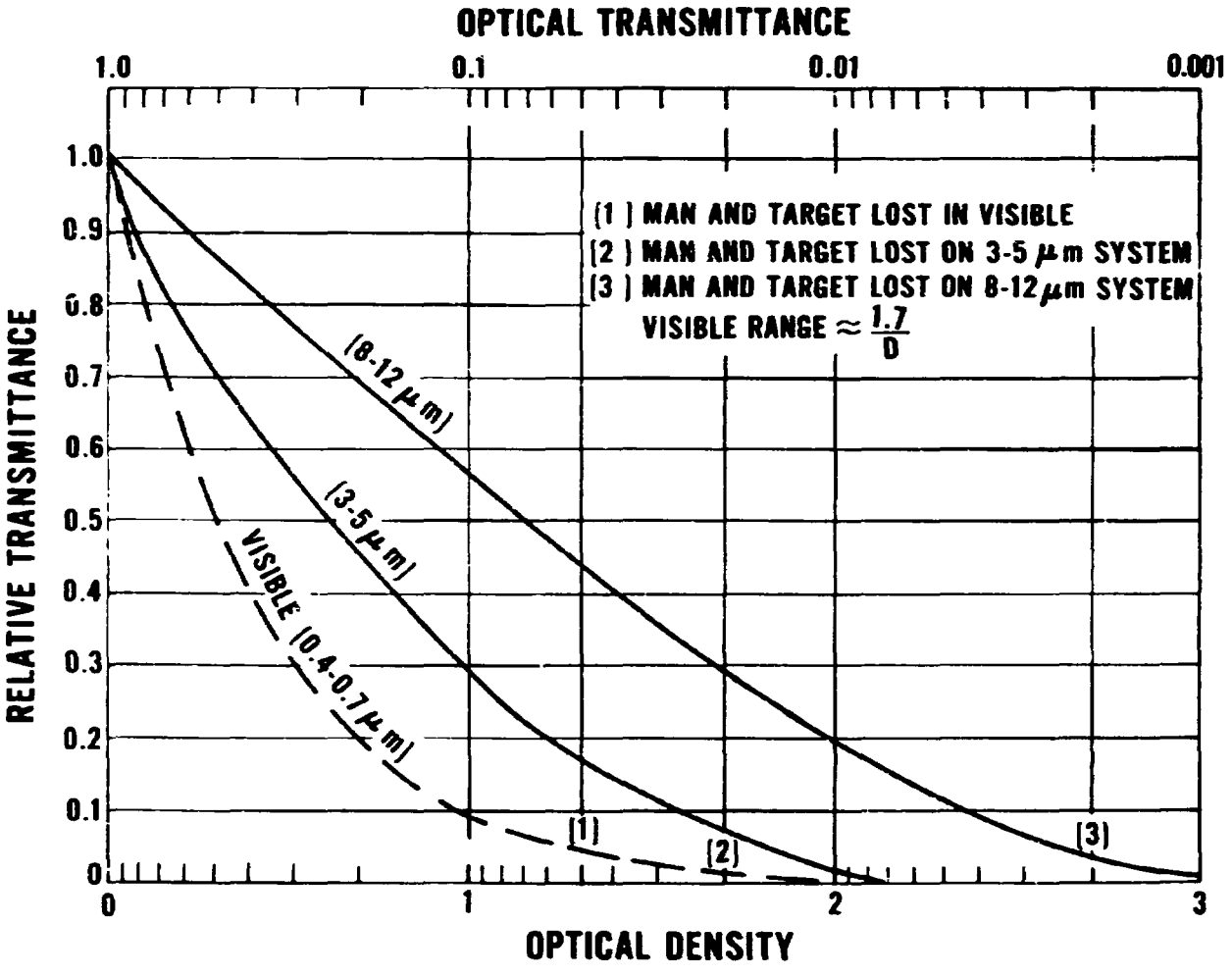

Fig. 28. Relative transmittance of visible, 3 to 5 μm, and 8 to 12 μm radiation through artificial fog with varying optical density as measured by Perry and Layman.

recent publications and references listed therein.[113] [114] Only the basic principles are presented here.

a. The Shape and Width of a Spectral Line. The molecular spectral lines have a number of analytical shapes or contours and half-widths which are determined by the following processes:

(1) Natural broadening.

(2) Pressure or collision broadening due to interaction among molecules.

(3) Doppler broadening due to relative motion of molecules.

The natural width of a spectral line is set by Heisenberg's Uncertainty Principle which states that if the lifetime of a molecule in an excited state is Δt, then the uncertainty in its energy ΔE will be given by

$$\Delta E \approx h/2\pi(\Delta t) \tag{62}$$

where h is Planck's constant. This excitation energy is released as a photon of frequency interval $\Delta\nu'$ (Hz) given by

$$\Delta E = h\,\Delta\nu'. \tag{63}$$

In terms of wave-numbers, ν in cm^{-1}

$$\Delta E = h\,c\,\Delta\nu\,, \tag{64}$$

where

$$\nu = \nu'/c\,. \tag{65}$$

A comparison of equations (62) and (64) gives

$$\Delta\nu_N \approx \frac{1}{2\pi\,c\,(\Delta t)}\ cm^{-1}\,. \tag{66}$$

In the infrared, the vibrational energy region states have a lifetime of the order of 0.1 second. Substitution of this value for (Δt) and 3×10^{10} cm/sec for c gives the natural width of a spectral line $\Delta\nu_N$

---

[113] K. Ya. Kondratyev, *Radiation in the Atmosphere*, Academic Press, New York (1969).

[114] R. M. Goody, *Atmospheric Radiation*, Oxford University Press, London (1964).

$$\Delta\nu_N \approx 5 \times 10^{-11}\ \text{cm}^{-1} \tag{67}$$

which is trivial as compared to wave numbers associated with infrared radiation in atmospheric phenomena (25000 – 666 in 0.4 - 15 μm region), and the broadening caused by the Doppler effect and collision broadening.

The theory of collision or pressure broadening was given by Lorentz; according to this theory, the shape of a gaseous absorption line is given by the relation:[115]

$$k_\nu = \frac{S}{\pi} \frac{\alpha_L}{(\nu - \nu_o)^2 + (\alpha_L)^2} \tag{68}$$

where

$$\alpha_L = \alpha_{L_o} \left[\frac{P}{P_o}\right] \left[\frac{T_o}{T}\right]^{0.5} , \tag{69}$$

and

$$S = S_o \left[\frac{T_o}{T}\right]^n \exp\left[-\frac{E''}{k}\frac{T_o - T}{T\,T_o}\right] . \tag{70}$$

where k_ν is the frequency-dependent absorption coefficient, S is the strength of the spectral line (intensity), E'' is the vibration-rotational energy of the ground state. P and T are the effective pressure and temperature of the absorbing gas, ν_o is the frequency at the center of the spectral line, α_L is the half-width of the spectral line, and n is a constant, different for each gaseous specimen (n = 1 for linear molecules and n = 1.5 for assymetric and linear top molecules). The subscript o in equations (69) and (70) refers to the quantities at standard conditions of temperature and pressure.

The Doppler effect profile caused by the component of velocity of molecules along the direction of emission of radiation is given by

$$k_\nu = k_o \exp(-y^2) , \tag{71}$$

where

$$k_o = \frac{S}{\alpha_D}\left[\frac{\ln 2}{\pi}\right]^{1/2} . \tag{72}$$

and

$$y = \frac{(\nu - \nu_o)}{\alpha_D} |\ln 2|^{1/2} \tag{73}$$

---

[115] D. Anding, *Band-Model Methods for Computing Atmospheric Molecular Absorption*, Report No. 7142-21-T, Willow Run Laboratories, The University of Michigan, Ann Arbor, Michigan (1967).

and $$\alpha_D = 3.58 \times 10^{-7} \left[\frac{T}{M} \right]^{1/2} \nu_o \, . \qquad (74)$$

Here α_D is the Doppler half-width and M is the molecular weight of the absorber.

The Doppler width of the 5577 A line of atomic oxygen at 300° K is 3.3×10^{-2} cm^{-1}, while the typical Lorentz (or collision) widths at the standard temperature and pressure (S.T.P.) are of the order of 8×10^{-2} cm^{-1}. Doppler and Lorentz line widths are comparable at higher altitudes. For the lower atmosphere where the pressure is high, the Lorentz profile is the most predominant. In the upper atmosphere, the effect of collision broadening decreases and Doppler broadening is more important. Figure 29 shows the relative shapes of the Doppler and Lorentz spectral lines of the same strength.

In the real atmosphere, the absorption lines obtained with a spectrometer are caused by the simultaneous absorption of all absorbers. Thus, the resulting spectra have blended shapes modified by the slit function of the spectrometer. The Beer-Lambert-Bouger law may not hold for such spectral regions.

A number of modified forms of Lorentz and some totally new spectral-line profiles have been proposed by a number of investigators.[116] One should note that the half-width of a pressure-broadened or Lorentz line varies linearly with the total pressure and approximately inversely as the square root of the absolute temperature and that the intensity or strength of a spectral line is a function of temperature.

b. The Rigorous Method for Computing Gaseous Spectral Absorptance. The spectral absorptance A_ν rather than spectral transmittance T_ν is generally computed since the absorption curves "grow" in depth and width as the amount of the absorber is increased. The average absorptance $\bar{A}_\nu$ over a bandwidth $\Delta\nu$ is given by Lambert's law:

$$\bar{A}_\nu = \frac{1}{\Delta\nu} \int_{\nu_1}^{\nu_2} \left\{ 1 - \exp \left[- \sum_{i=1}^{N} \int_0^X k(x, \nu) \, \rho(x) \, dx \right] \right\} d\nu \qquad (75)$$

where N corresponds to the number of different absorption lines contributing to absorption in the interval ν_1 to ν_2 (assuming that there is no appreciable variation in absorption coefficient with wavelength in this interval). The rigorous method for the computation of absorption is direct integration using equation (75). For this method, one has

[116] R. M. Goody, *Atmospheric Radiation*, Oxford University Press, London (1964).

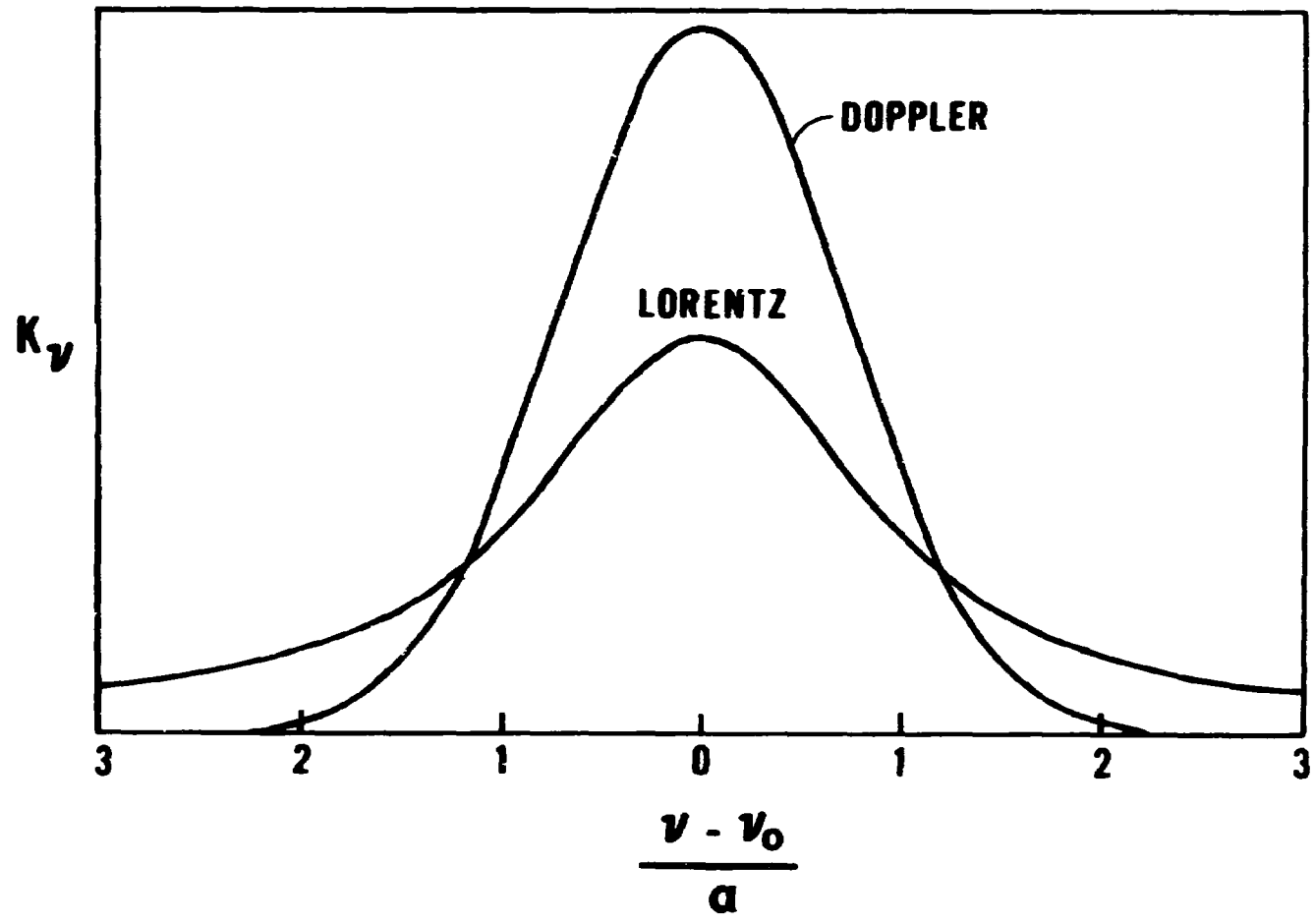

Fig. 29. Doppler and Lorentz spectral line shapes for similar strengths (intensities) and line widths.

to know the absorption coefficient $k(x, \nu)$ at each frequency and at each point along the optical path. This method requires exact knowledge of the characteristics of each spectral line, namely its position (center), line shape, half-width, and intensity, as well as the concentration of each absorber. The rigorous method should produce very accurate absorption spectra if all the parameters are well known and all the corrections due to the variations of temperature, pressure, and concentrations are completely taken into account. This does require a great deal of computation effort and patience. A complete data bank on spectral lines is still in preparation in 1972.[117]

For the transmission of laser radiation, one does require high-resolution, spectral-transmission data to make accurate computations.

c. **Band Models for Computing Spectral Absorptance.** Lambert's law of absorption is obeyed for monochromatic radiation within one-fifth of its line width which varies from 2×10^{-2} cm^{-1} for a gas at S.T.P. to about 2×10^{-4} cm^{-1} for Doppler broadening. This presents a formidable challenge for experimental and computational task. The present conventional spectrometers do not have the required resolution. One may have to use Fourier Spectrometers to obtain high-resolution spectra to study the real spectral line shapes, width, and intensity variations with absorber concentrations. For the sake of practical compromise, the spectral lines are averaged into spectral bands. A spectral band is assumed to contain an array of spectral lines of a certain shape, intensity, and half-width and spacing distributed according to some statistical pattern. In the real spectra, this is not so. This is a major source of discrepancy between real and computed spectra. A number of statistical models have been proposed for calculating absorption due to molecules of various gases as the patterns of the arrangement or repetition of molecular spectral lines are different for various types of molecules. The main features of the band models are discussed in detail in the literature.[118] [119] [120]

The Elsasser, or regular, model assumes that a band is made up of an infinite array of spectral lines of equal intensity, half-width, and spacing. This model is applicable to bands of linear molecules. Lorentzian line shape is used. Absorption for various values of optical thickness (a function of absorber amount, line intensity, and spacing) can be computed for various values of the line-discreteness parameter.

---

[117] R. A. McClatchey, private communication.

[118] K. Ya. Kondratyev, *Radiation in the Atmosphere*, Academic Press, New York (1969).

[119] R. M. Goody, *Atmospheric Radiation*, Oxford University Press, London (1964).

[120] D. Anding, *Band-Model Methods for Computing Atmospheric Molecular Absorption*, Report No. 7142-21-T, Willow Run Laboratories, The University of Michigan, Ann Arbor, Michigan (1967).

The statistical, random, or Mayer-Goody, model assumes that the positions and line intensities are random and are given by a probability function. This model has been used for water vapor using the Lorentz profile. Telles, Mayer, and Goody developed this model.

The random Elsasser, Plass, or Kaplan model assumes a random superposition of Elsasser bands of different intensities, half-widths, and spacing intervals. This model predicts absorption intermediate between the regular Elsasser and random Goody models.

The quasi-random model of Wyatt, Stull, and Plass assumes that the spectral lines are randomly distributed into small-frequency intervals.[121] [122] The transmission over larger frequency intervals is calculated by averaging the results from the smaller intervals. The spectral lines are grouped into intensity subgroups which simulate actual intensity distribution. The contribution from the wings of the spectral lines whose centers are outside a given spectral interval is included. This method has been applied to water vapor and carbon dioxide molecules. Transmittance tables for various amounts of absorber are available in the literature.[123]

Recently Zachor and Gibson and Pierluissi have proposed generalizations of the Mayer-Goody statistical model. Zachor has used his model to calculate absorption by carbon dioxide.[124] Gibson and Pierluissi have proposed a "five-parameter" model and have applied it to the infrared transmittance of water vapor and carbon dioxide.[125]

Various workers have prepared computer programs for the computation of molecular absorption by H_2O, CO_2, N_2O, O_3, and CH_4 using various band models in different spectral regions.[126] [127]

---

[121] P. J. Wyatt, V. R. Stull, and G. N. Plass, "The Infrared Transmittance of Water Vapor," *Appl. Opt.* 3, 229 (1964).

[122] V. R. Stull, P. J. Wyatt, and G. N. Plass, "The Infrared Transmittance of Carbon Dioxide," *Appl. Opt.* 3, 243 (1964).

[123] S. L. Valley, *Handbook of Geophysics and Space Environments*, McGraw-Hill, New York (1965).

[124] A. S. Zachor, *J. Quant. Spectros. Radiat. Transfer* 8, 771, 1341 (1968).

[125] G. A. Gibson and J. H. Pierluissi, "Accurate Formula for Gaseous Transmittance in the Infrared," *Appl. Opt.* 10, 1509 (1971).

[126] D. Anding, *Band-Model Methods for Computing Atmospheric Molecular Absorption*, Report No. 7142-21-T, Willow Run Laboratories, The University of Michigan, Ann Arbor, Michigan (1967).

[127] B. M. Golubitskiy and N. L. Moskalenko, "Spectral Transmission Functions in the H_2O and CO_2 Bands," *Bull. (Izv.) Aca. Sc. USSR Atmos. and Ocean. Phys.* 4, 194 (1968).

d. Empirical Methods for Calculating Spectral Transmittance. McClatchey *et al.* have prepared a set of empirical transmittance functions and a computer program to calculate horizontal or slant-path transmittance from ground level to an altitude of 100 km for a set of ten model atmospheres.[128] The spectral region covered is from 0.25 micrometer to 25 micrometers with a resolution of 20 cm^{-1}. There are two haze models corresponding to visible ranges of 23 and 5 kilometers. Figures 30 and 31 present atmospheric transmittance functions per kilometer horizontal optical path length for five atmospheric models containing haze with 23 and 5 km horizontal visibility ranges.

Golubitskiy, Moskalenko, and Mirumyants have developed an empirical method for computing atmospheric spectral transmittance using the general form of Lambert's law:[129-134]

$$T_\nu = \exp\left[-\beta_\nu w^{m_\nu} p_e^{n_\nu} \right] \tag{76}$$

where w is the absorbing mass, P_e is the effective pressure (for water vapor, $P_e = P_{N_2} + B P_{H_2O}$, where B is self-broadening coefficient), m_ν, n_ν, and β_ν are wavelength-dependent parameters determined from experimental data. They have described the method for computing the constants and have prepared extensive tables of constants for the computation of spectral transmittance in the infrared region. This method is

---

[128] R. A. McClatchey, R. W. Fenn, J. E. A. Selby, F. W. Volz, and J. S. Garing, *Optical Properties of the Atmosphere (Revised)*, AFCRL-71-0279, Environ. Res. Paper No. 354, Air Force Cambridge Research Laboratories, Bedford, Massachusetts (1971).

[129] B. M. Golubitskiy, and N. L. Moskalenko, "Spectral Transmission Functions in the H_2O and CO_2 Bands," *Bull. (Izv.) Acs. Sc. USSR Atmos. and Ocean. Phys.* 4, 194 (1968).

[130] B. M. Golubitskiy and N. L. Moskalenko, "Measurement and Calculation of Spectral Transmission in the N_2O Bands in the Near Infrared Region," *Bull. (Izv.) Acs. Sc. USSR Atmos. and Ocean. Phys.* 4, 204 (1968).

[131] N. L. Moskalenko, "Spectral Transmission Functions in Some H_2O-Vapor, CO, and CH_4 Bands," *Bull. (Izv.) Acs. Sc. USSR Atmos. and Ocean. Phys.* 4, 445 (1968).

[132] N. L. Moskalenko, "The Spectral Transmission in the Bands of Water Vapor O_3, N_2O, and N_2 Atmospheric Components," *Bull. (Izv.) Acs. Sc. USSR Atmos. and Ocean. Phys.* 5, 678 (1969).

[133] N. L. Moskalenko and S. O. Mirumyants, "Calculation Methods of Spectral Absorption of Infrared Radiation by Atmospheric Gases," *Bull. (Izv.) Acs. Sc. USSR Atmos. & Ocean. Phys.* 6, 665 (1970).

[134] V. L. Filippov and S. O. Mirumyants, "Comparative Study of Experimental and Calculated Infrared Transparency Spectra of Ground Level Horizontal Atmospheric Paths," *Bull. (Izv.) Acs. Sc. USSR, Atmos. and Ocean. Phys.* 6, 676 (1970).

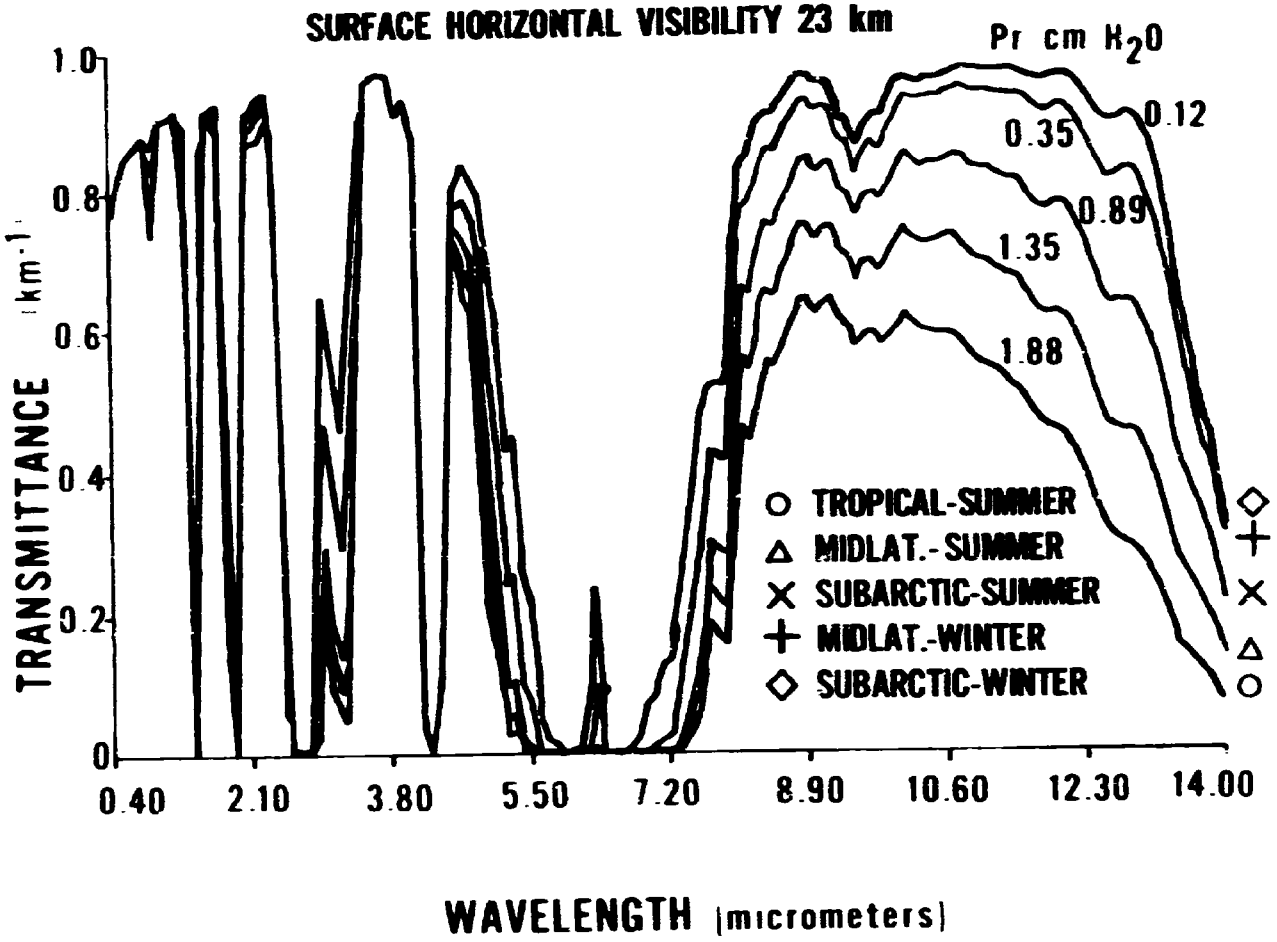

Fig. 30. Computed spectra of atmospheric transmittance for five model atmospheres with 23 km horizontal visibility.

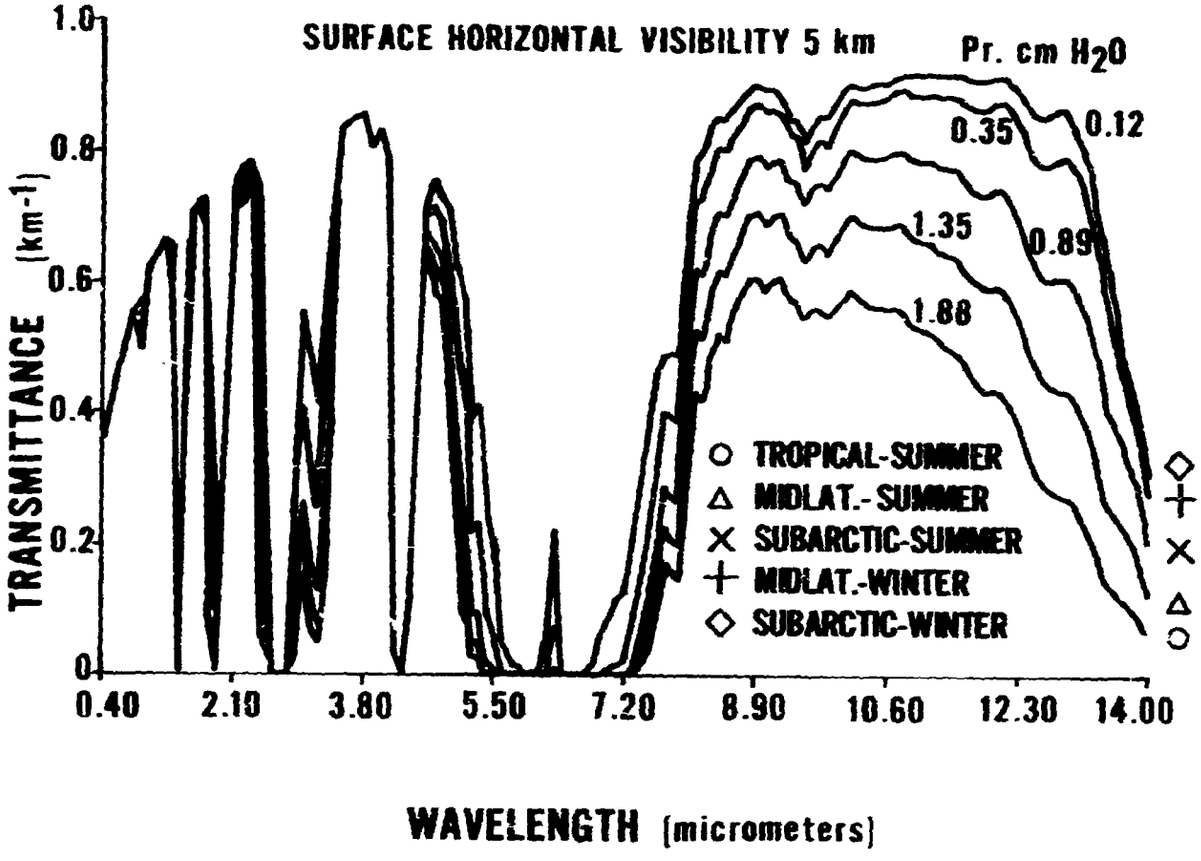

Fig. 31. Computed spectra of atmospheric transmittance for five model atmospheres with 5 km horizontal visibility.

reported to provide, in some cases, better accuracy than the quasi-random, Wyatt-Stull-Plass band model if the spectral resolution $\geq$ 5-20 cm^{-1}. An accuracy of 5 to 7% in computed values of spectral transmittance is obtained. Furthermore, a correction for the temperature effect is included.

At present, to our knowledge, there are no satisfactory atmospheric models to compute spectral transmittance covering the spectral range from 0.5 micrometer to 15.0 micrometers for low-visibility, atmospheric environments characterized by thick haze, fog, dust, and smoke where the horizontal, visible range is reduced from 4 kilometers to 20 meters or so.

9. Scattering of Radiation by the Atmosphere. The attenuation of radiation by scattering is caused by the spatial inhomogeneities in the refractive index of the medium of propagation. In the terrestrial atmosphere, the main scatterers are the aerosols (water droplets, dust, or smoke particles) and air-density fluctuations. The scattering due to the fluctuations in air density is caused by molecules of the atmospheric gases (molecular scattering). If the wavelength of incident radiation is considerably smaller than the size of the scattering particles, the interaction is called Rayleigh scattering. The scattering of ultraviolet and visible radiation by molecules and ultrahigh frequency radio waves by cloud particles is Rayleigh scattering. When the wavelength of radiation is comparable to the dimensions of the scattering particles, the interaction is called Mie scattering. There are a number of excellent treatises on the theory of electromagnetic scattering.[135-138] The main features and terminology of the Rayleigh and Mie scattering phenomena are outlined, and the procedures to compute scattering and attenuation coefficients in each case are described in the following paragraphs.

a. Rayleigh Scattering. The Rayleigh scattering coefficient $\sigma_R(\theta)$ in a direction θ with respect to the direction of incidence is given by:[139 140]

---

[135] H. C. Van de Hulst, *Light Scattering by Small Particles*, John Wiley, New York (1957).

[136] M. Kerker, editor, *Electromagnetic Scattering*, The Macmillan Co., New York (1963), and *The Scattering of Light and Other Electromagnetic Radiation*, Academic Press, New York (1969).

[137] D. Deirmendjian, *Electromagnetic Scattering on Spherical Polydispersions*, Elsevier, New York (1969).

[138] R. Penndorf, "Angular Mie Scattering," *J. Opt. Soc. Am.*, *52*, 402 (1962).

[139] K. Ya. Kondratyev, *Radiation in the Atmosphere*, Academic Press, New York (1969).

[140] R. Penndorf, *Tables of the Refractive Index for Standard Air and the Rayleigh Scattering Coefficient for the Spectral Region between 0.2 and 20.0 μm and Their Application to Atmospheric Optics*, AFCRC-TN-55-206, p. 26, Air Force Cambridge Research Laboratories, Bedford, Massachusetts (1955).

$$\sigma_R(\theta) = \frac{\pi^2 (m^2 - 1)^2}{2 N \lambda^4} (1 + \cos^2 \theta) \qquad (77)$$

where m is the refractive index, N is the number of scatterers per unit volume, and λ is the wavelength of the incident radiation. The factor $(1 + \cos^2 \theta)$ is called the "Rayleigh scattering function." It has maximum values for $\theta = 0$ and $\theta = 180°$ (forward and back scattering) and minimum values for $\theta = 90°$ and $\theta = 270°$. Equation (77) also shows that the volume scattering coefficient is inversely proportional to the fourth power of the wavelength of the incident radiation. The integral of equation (77) over the scattering angle θ gives the Rayleigh volume scattering coefficient σ_R:

$$\sigma_R = \frac{8\pi^3 (m^2 - 1)^2}{3 N \lambda^4} . \qquad (78)$$

This relation is strictly accurate only for transparent nonconductors. If there are any absorbing conductors in the scattering medium, the complex refractive index is given by $m = n_1 - i n_2$ where n_1 is the real refractive index (same as m for a non-absorbing medium) and n_2 is the absorbing index. In the case of small absorbing particles, the absorption coefficient is not given by the Rayleigh formula. Following Shifrin,[141] the attenuation coefficient due to the absorption and scattering by a single particle is given by

$$\alpha_\lambda = \frac{36\pi n_1 n_2}{(m^2 + 2)^2} \frac{V}{\lambda} , \qquad (79)$$

where α_λ is the attenuation coefficient and V is the volume of the particle. Equation (79) shows that the attenuation coefficient for an absorbing particle is inversely proportional to the wavelength of the incident radiation.

b. **Mie Scattering.** Several treatises mentioned earlier give a detailed account of the mathematical treatment of the Mie theory which describes the attenuation of radiant flux by aerosols whose size is comparable to the wavelength of the incident radiation. Particles of a size greater than 0.03 micrometer radius must be treated according to the exact-diffraction theory given by Mie.

Mie solved the case of a monochromatic plane wave incident on a homogeneous, isotropic sphere of radius r surrounded by a transparent homogeneous and isotropic medium. The incident wave induces forced oscillations of free and bound charges

[141] K. S. Shifrin, *Scattering of Light in a Turbid Medium*, Gostekhizdat, Moscow (1951), or NASA Technical Translation, NASA TTF-477, National Aeronautics and Space Administration, Washington, D. C. (1968).

in synchronism with the applied field resulting in a secondary electric and magnetic field—one outside and the other inside the sphere. The intensity of the scattered radiation at a large distance from the scattering aerosol particle at a scattering angle θ is given by

$$I = I_o \frac{\lambda^2}{8\pi^2} \left\{ \iota_1(m,x,\theta) + \iota_2 (m,x,\theta) \right\} , \qquad (80)$$

where m = the refractive index of the particle

x = $2\pi r/\lambda$, dimensionless size parameter

r = radius of the spherical particle

θ = angle between the incident and the scattered radiation direction ($\theta = 0$ for the forward direction)

I_o = the intensity of the incident radiation.

The intensity functions ι_1 and ι_2 are proportional to the components of the electric field perpendicular and parallel to the scattering plane. The intensity functions are given by the squares of amplitude functions $S_1(\theta)$ and $S_2(\theta)$ where

$$S_1(\theta) = \sum_{n=1}^{\infty} \frac{2n+1}{n(n+1)} (a_n \pi_n + b_n \tau_n) ,$$

$$S_2(\theta) = \sum_{n=1}^{\infty} \frac{2n+1}{n(n+1)} (b_n \pi_n + a_n \tau_n) , \qquad (81)$$

where $$\pi_n = \frac{1}{\sin\theta} P_n^{\ell}(\cos\theta) ,$$

$$\tau_n = \frac{d}{d\theta} P_n^{\ell}(\cos\theta) .$$

The terms P_n^{ℓ} are associated Legendre Polynominals and π_n and τ_n are functions of the scattering angle θ. Figure 32 shows the variation of π and τ for $n = 1$ to $n = 6$. The coefficients a_n and b_n in equation (81) are Riccati-Bessel functions which can be written in terms of spherical Bessel functions, and a_n and b_n are functions of x and m but are independent of the scattering angle.

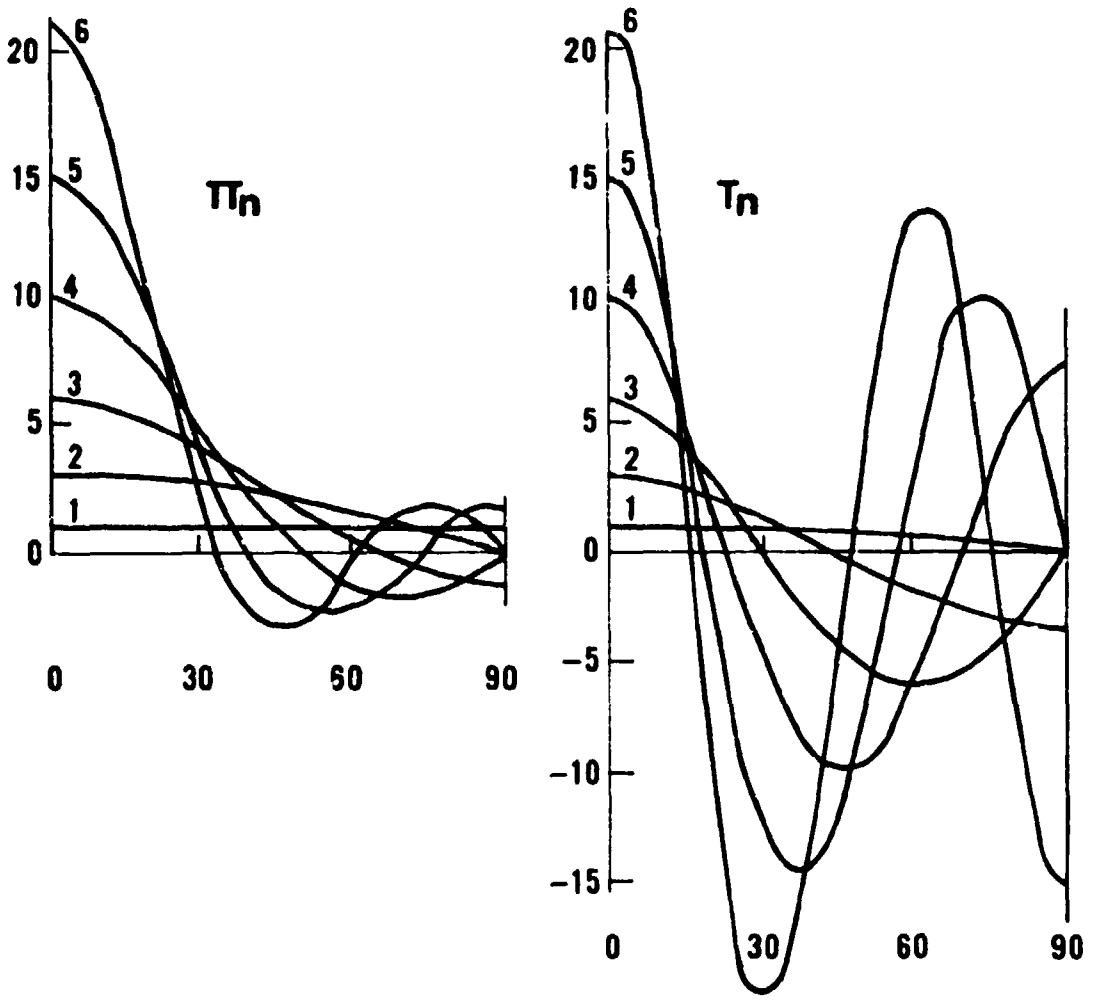

Fig. 32. π_n and τ_n functions of scattering angle for n = 1 to 6 used in MIE theory (after Van de Hulst).

The scattering efficiency K_s is defined as the ratio of the scattered flux to the incident flux per unit cross-sectional area of the scattering particle. The efficiency factors are given by the expressions:

$$K_s = \frac{2}{x^2} \sum_{n=1}^{\infty} (2n + 1)(|a_n|^2 + |b_n|^2) , \tag{82}$$

$$K = \frac{2}{x^2} \sum_{n=1}^{\infty} (2n + 1)\, \mathrm{Re}\,(a_n + b_n) , \tag{83}$$

$$K_a = K - K_s , \tag{84}$$

where the subscripts a and s refer to absorption and scattering, respectively. and K is the attenuation efficiency of the scattering particle.

If a unit volume of scatterers contains N particles of the same relative size parameter $x = 2\pi r/\lambda$, then the volume scattering coefficient is given by the relation

$$\sigma = N \pi r^2 K_s \quad , \tag{85}$$

For a polydisperse system of scatterers with a size distribution n(r), the scattering coefficient is given by the integral

$$\sigma = \pi \int_{r_1}^{r_2} K_s\, n(r)\, r^2\, dr \tag{86}$$

or, alternately, in terms of the size parameter x,

$$\sigma = \frac{\lambda^3}{8\pi^2} \int_0^{\infty} x^2\, n(x)\, K_s\,(x)\, dx. \tag{86a}$$

Similarly, the attenuation coefficient α can be computed by using the appropriate value of attenuation efficiency K in equation (86),

$$\alpha = \pi \int_{r_1}^{r_2} K\, n(r)\, r^2\, dr. \tag{86b}$$

Atmospheric aerosols have been studied by a number of workers. Junge has found that the size distribution of natural "continental" aerosols is given by the relation

$$N(r) = (c/2.3)\, r^{-(\nu+1)} \tag{86c}$$

where c is a constant and ν varies between 2.5 and 4.0.[142]

Figure 33 shows the wavelength dependence of the attenuation and scattering coefficients for various aerosol models based upon Diermendjian's haze and cloud models.[143] Figure 34 shows a similar set of attenuation coefficients computed by Rensch.[144] In Figure 33, the M, L, and H curves represent three haze models, and C_1, C_2, and C_3 are cloud models. Figure 34 contains attenuation coefficients for four atmospheric models characterized by clear and light haze to light fog. For atmospheric models with low visibility, the attenuation coefficient is comparatively a very slowly varying (almost constant) function of wavelength in the visible and near infrared region, and it has a minimum value between 10 and 12 μm in the far infrared region. On the other hand, for atmospheric models which correspond to comparatively better visibility, there is a rapid decrease in attenuation with increase in wavelength; and there are sharp maxima of attenuation coefficients near 2.7 μm and 6.3 μm which correspond to the centers of the strong water vapor absorption bands. If one compares these calculated spectra with the measured haze and fog spectra given in Figs. 17a to c and Fig. 23, based upon the work of Arnulf *et al.* and Filippov *et al.*, one notices that in the measured spectra there are no such peaks shown at 2.7 μm and 6.3 μm. This is due to the deliberate exclusion of the water vapor absorption bands by the experimenters.

The normalized intensity or phase function $P(\lambda,m,\theta)$, introduced by Chandrasekhar,[145] is defined as

$$P(\lambda,m,\theta) \equiv \tfrac{1}{2}\,[\,P_1(\theta) + P_2(\theta)\,] \equiv \frac{2[i_1(\theta) + i_2(\theta)]}{x^2\, K_s(x)} \tag{87}$$

The phase function represents the ratio of the radiant energy scattered per unit solid angle in a given direction to the average radiant energy scattered per unit solid angle in all directions.

---

[142] C. E. Junge, *Air Chemistry and Radioactivity*, p. 118, Academic Press, New York and London (1963).

[143] D. Deirmendjian, *Electromagnetic Scattering on Spherical Polydispersions*, Elsevier, New York (1969).

[144] D. B. Rensch, *Extinction and Backscatter of Visible and Infrared Laser Radiation by Atmospheric Aerosols*, Report 2467-3, The Ohio State University (1969).

[145] S. Chandrasekhar, *Radiative Transfer*, Clarendon Press, Oxford (1950), also Dover Publications, New York (1960).

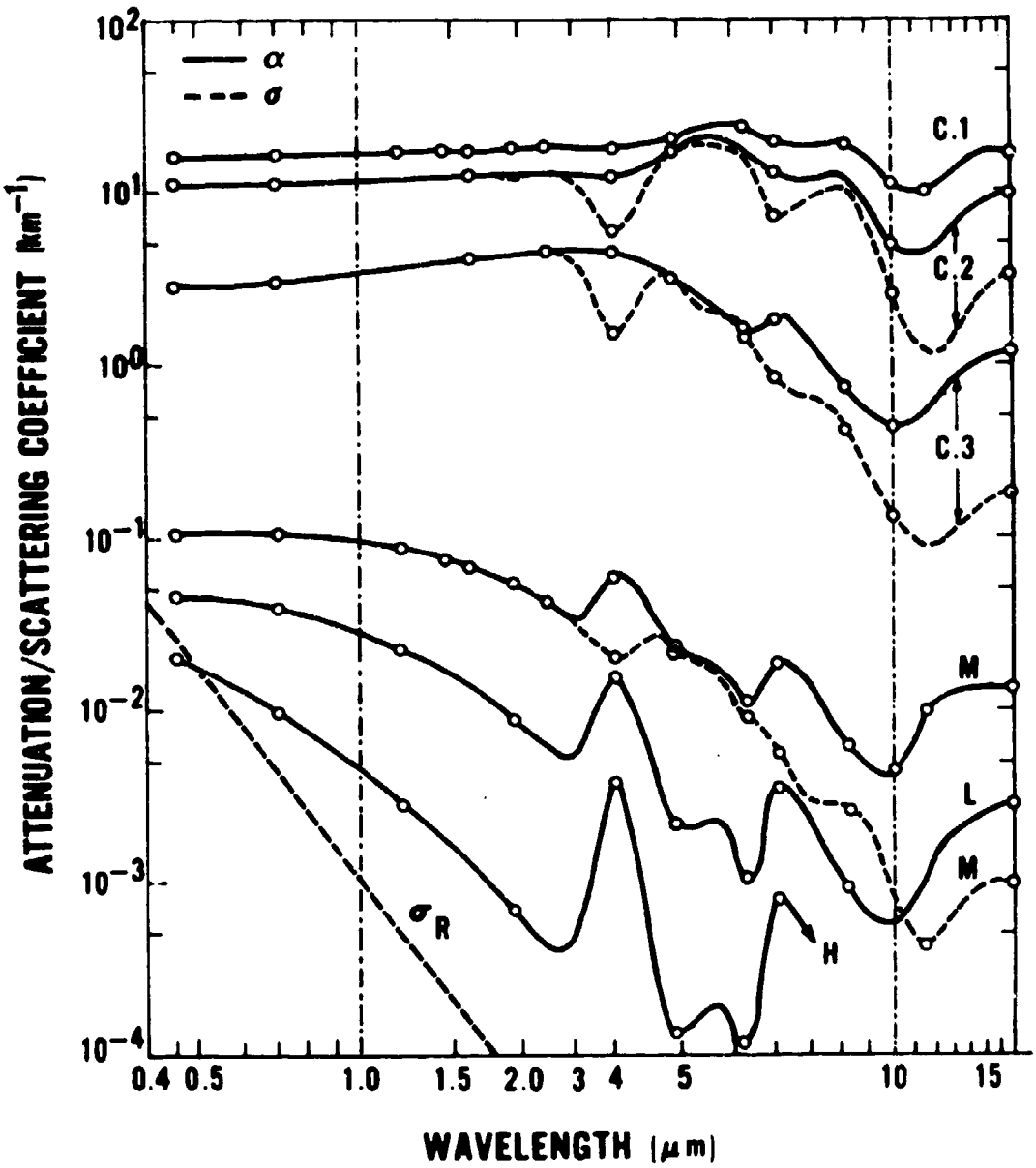

Fig. 33. Spectral attenuation and scattering coefficients for various haze (L, M, H) and cloud (C_1, C_2, C_3) models (adapted from Deirmendjian).

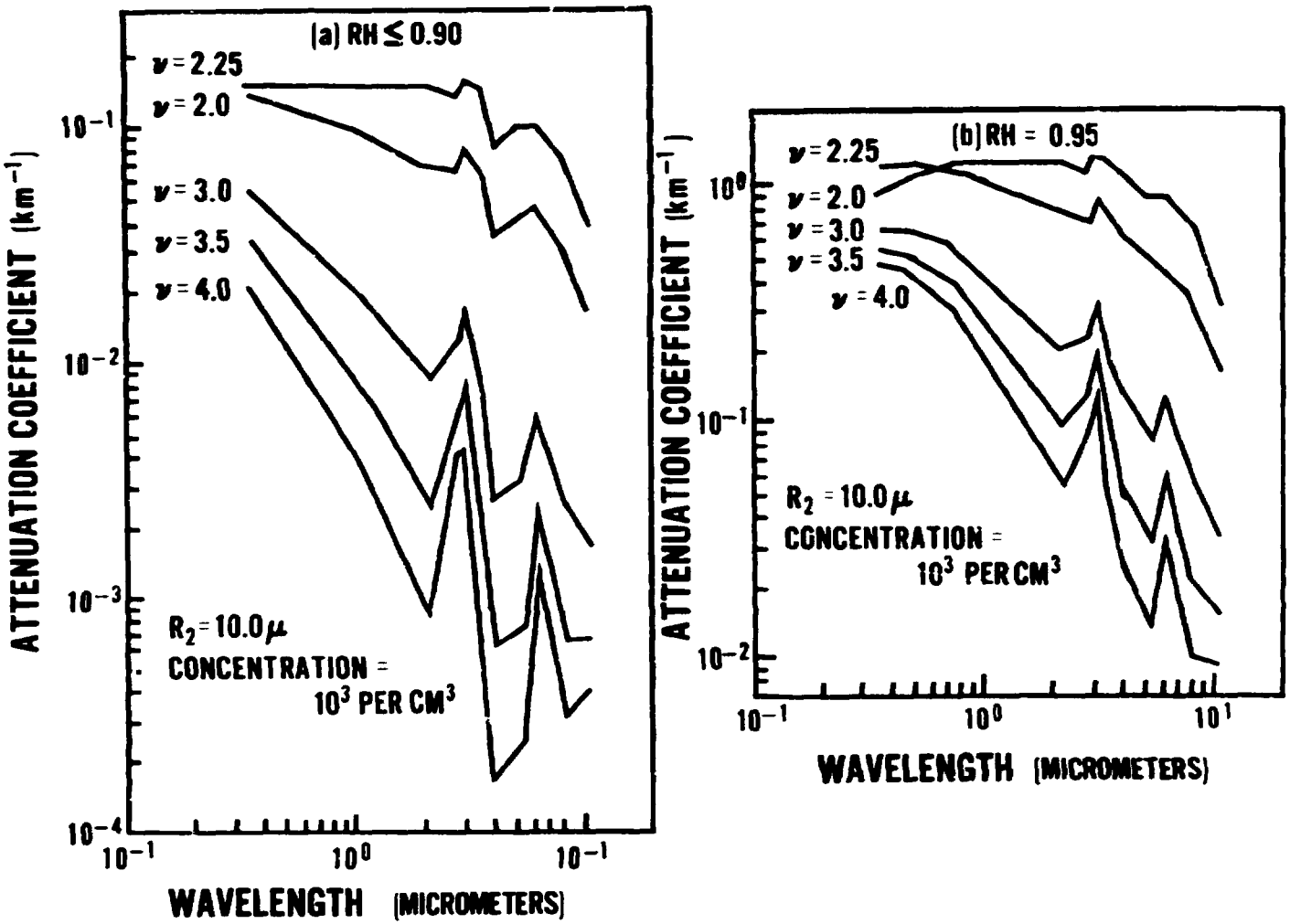

Fig. 34. Spectral attenuation coefficients for various models of continental haze: (a) relative humidity ≤ 0.90, and (b) relative humidity ≅ 0.95 as reported by Rensch.

For a polydisperse system of scatterers with size distribution n(x), the phase function is given by

$$P_j(\theta) = \frac{4\pi}{k^3 \sigma} \int_0^\infty n(x)\, i_j(\theta)\, dx \qquad (88)$$

where σ is the scattering coefficient and $k = 2\pi/\lambda$ is the propagation constant.[146]

The normalized phase function for backscattering ($\theta = 180°$) is given by

$$P(\lambda,m,180°) = \frac{4\pi}{k^2 \sigma} \int_{r_1}^{r_2} | S(\lambda,m,180°) |^2 n(r)\, dr \qquad (88a)$$

where $S(\lambda,m,180°)$ is the backscatter amplitude function for a single particle. An exact calculation of $S(180°)$ is made by the Mie method; but, for particles for which the size parameter is large, the computations become rather lengthy. Some approximate methods have been used to determine this function. Rensch and Long have calculated values of attenuation and backscattering coefficients for various theoretical models of haze, fog, and rain aerosols for the wavelength range from 0.34 μm to 10.6 μm.[147]

The backscattered radiant energy in watts Q_R $(\lambda,180°)$ is given by the equation

$$Q_R(\lambda,180°) = E_\lambda A L \omega T_1 T_2 [P(\lambda,180°)/4\pi] \sigma \qquad (89$$

where E_λ is the radiant incidance (irradiance) ($W \cdot cm^{-2}$) on the scattering volume having an area A (cm^2) perpendicular to the optical path of length L (cm) of the scattering volume, T_1 is the atmospheric transmittance between the radiator and the scattering volume, T_2 is the transmittance between the scattering volume and the detector, ω is the solid angle subtended by the optical system of the receiver (sr), σ is the atmospheric volume scattering coefficient (cm^{-1}), and $P(180°)$ is the backscattering phase function. Diermendjian has tabulated values of the normalized phase function for various models of haze and cloud aerosols of various compositions.[148]

---

[146] D. Deirmendjian, *Electromagnetic Scattering on Spherical Polydispersions*, Elsevier, New York (1969).

[147] D. B. Rensch, *Extinction and Backscatter of Visible and Infrared Laser Radiation by Atmospheric Aerosols*, Report 2467-3, The Ohio State University (1969).

[148] D. Deirmendjian, *Loc. cit.*

The atmospheric aerosols have a real refractive index if they are completely transparent. However, the natural aerosols have a complex refractive index (they have some absorption). The behavior of the variation of attenuation efficiency is a very sensitive function of the size parameter and the absorption index of aerosols. Figure 35 shows the variation of the attenuation efficiency K as a function of the size parameter x for various values of refractive indices. For a large value of the size parameter x, the attenuation efficiency factor K approaches the value 2. Small changes in the absorption index have quite large effects on the attenuation efficiency of the particle. Deirmendjian has tabulated values of complex refractive indices for the common constituents of atmospheric aerosols such as water droplets (at various temperatures), ice, silicate, limonite, and iron.[149] The Mie theory has been extended to nonspherical particles also.[150]

The natural dust aerosols contain mostly clay minerals of aluminum silicates, silica, metallic oxides, and calcium carbonate. The dust particles range in diameter from 0.1 to 100 μm, but the most probable sizes are between 0.1 μm to 1.0 μm. The dust particles have quite significant absorption in the infrared region particularly around 9.6 micrometers.[151] There are, of course, innumerable other types of aerosols in the atmosphere. These aerosols can be organic, inorganic, or biological; and their sources of origin include the sea, forest fires, volcanic eruptions, industrial emissions, meteoric dust, and debris from thermonuclear explosions in the atmospheric or space environment. Mie scattering by atmospheric aerosols must account for their complex refractive index and nonspherical shape.

c. **Atmospheric Turbulence.** Atmospheric turbulence causes further scattering of electromagnetic radiation in addition to that caused by the atmospheric gaseous molecules and aerosols. This scattering is caused by the large-scale (compared to molecular dimensions) inhomogeneities in the refractive index of the medium of propagation in the optical path. The effect of turbulence on the degradation of imagery has been studied by Smith, Saunders, and Vatsia during the daytime for horizontal, ground-level, outdoor conditions.[152] Figure 36 shows the degradation of photographic resolution as a function of horizontal range for various values of exposure time. There is a

---

[149] D. Deirmendjian, *Electromagnetic Scattering on Spherical Polydispersions*, Elsevier, New York (1969).

[150] M. Kerker, editor, *Electromagnetic Scattering*, The Macmillan Co., New York (1963), and *The Scattering of Light and Other Electromagnetic Radiation*, Academic Press, New York (1969).

[151] D. F. Flanigan and H. P. DeLong, "Spectral Absorption Characteristics of the Major Components of Dust Clouds," *Appl. Opt. 10*, 51 (1971).

[152] A. G. Smith, M. J. Saunders, and M. L. Vatsia, "Some Effects of Turbulence on Photographic Resolution," *J. Opt. Soc. Amer. 47*, 755 (1957).

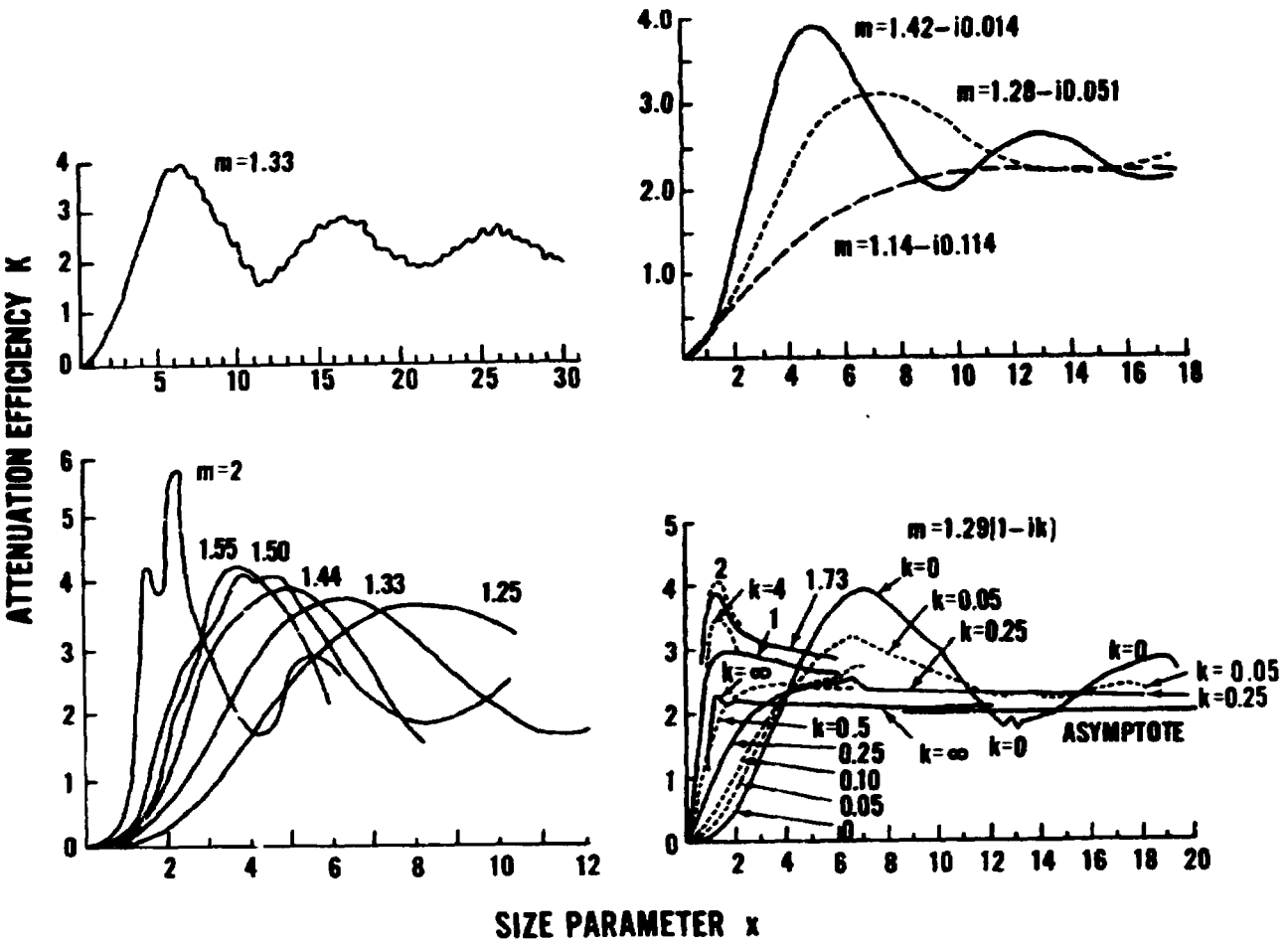

Fig. 35. Variation of attenuation efficiency K with size parameter x for various values of refractive indices (adapted from Van de Hulst).

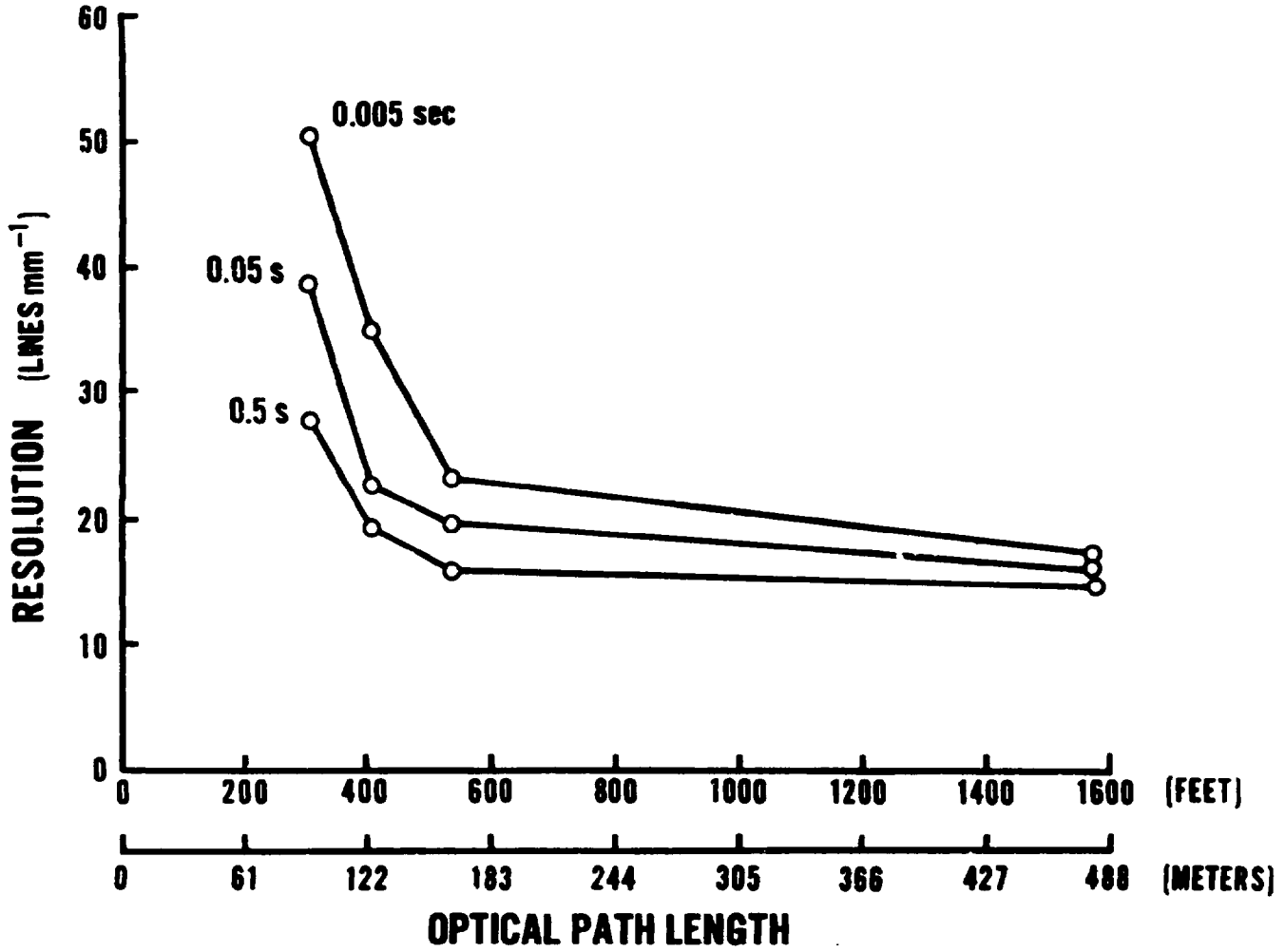

Fig. 36. Variation of photographic resolution as a function of optical path length for various values of exposure time as measured by Smith, Saunders, and Vatsia.

great deal of interest in the measurement of the intensity of turbulence and its temporal and spatial variations for various types of terrain and surfaces under various atmospheric optical environments.[153-158] The variation of image degradation as a function of the intensity of turbulence needs to be further investigated in order to determine the quantitative effects of atmospheric turbulence on the performance of electro-optical devices under various types of atmospheric optical environments.

d. Multiple Scattering. Numerous investigators have developed a number of computational methods which have been used with limited success for multiple-scattering calculations. Some of these methods compute both intensity and polarization of scattered radiation.

The Monte Carlo method, first used by Collins and Wells for the study of atmospheric scattering,[159] has been used most prolifically by Plass and Kattawar.[160] This method is versatile and provides a tractable approach to a number of problems including anisotropy and inhomogeneities in the density and refractive index in the horizontal or vertical directions in the atmosphere. Blättner, Collins, and Wells have extended the applications of the Monte Carlo method to calculations in spherical-shell

---

[153] R. S. Lawrence and J. W. Strohbehn, "A Survey of Clear-Air Propagation Effects Relevant to Optical Communications," *Proc. IEEE, 58*, 1523 (1970).

[154] R. G. Buser, "Interferometric Determination of the Distance Dependence of the Phase Structure Function for Near-Ground Horizontal Propagation at 6328 A," *Jour. Opt. Soc. Am. 61*, 488 (1971).

[155] R. G. Buser and G. K. Born, "Determination of Atmospherically Induced Phase Fluctuations by Long-Distance Interferometry at 6328 A," *Jour. Opt. Soc. Am. 60*, 1079 (1970).

[156] P. M. Livingston, P. H. Deitz, and E. C. Alcaraz, *Light Propagation through a Turbulent Atmosphere: Measurement of the Optical Filter Function*, BRL Memo, Report 2018, Ballistic Research Laboratory, Aberdeen Proving Ground, Md. 21005 (1969), and *J.O.S.A. 60*, 925 (1970).

[157] E. C. Alcaraz and P. M. Livingston, *Measurement of the Beam Wander Phenomenon in a Turbulent-Medium*, BRL Technical Report, Ballistic Research Laboratory, Aberdeen Proving Ground, Md. 21005 (1970).

[158] M. L. Wesely and E. C. Alcaraz, *Diurnal Cycles of the Refractive Index Structure Function Coefficient*, Ballistic Research Laboratory, Aberdeen Proving Ground, Md. 21005 (1972).

[159] D. G. Collins and M. B. Wells, *Monte Carlo Codes for the Study of Light Transport in the Atmosphere*, Vol. I and II, Radiation Research Associates, Inc., Fort Worth, Texas (1965).

[160] G. N. Plass and G. W. Kattawar, "Monte Carlo Calculations of Light Scattering from Clouds," *Appl. Opt. 7*, 415 (1968).

atmospheric problems.[161] The main disadvantage of this method is that to achieve a high accuracy the computational time becomes very large.

Dave has recently used the Gauss-Seidel iteration scheme for the solution of the equation of radiative transfer to calculate multiple scattering for Rayleigh and Mie atmospheres with good accuracy.[162] [163] This method involves the expansion of the phase function into a series of Legendre polynomials. It has been applied successfully to study plane-parallel, horizontally homogeneous atmospheres. The latest form of this method reported by Dave and Gazdag is the "modified Fourier transform" method for multiple-scattering calculations.[164]

Hansen has used the "doubling method" to compute multiple scattering of polarized light reflected by terrestrial water clouds at 1.2, 2.25, 3.1, and 3.4 micrometers.[165] [166] His study shows that polarization characteristics are more sensitive than the intensity characteristics to aerosol size, shape, and number distributions. Other investigators who have contributed substantially to the study of atmospheric scattering include Chandrasekhar,[167] Sekera, Coulson *et al.*,[168] Mullikan, Querfeld,[169] Twomey,

---

[161] W. G. Blättner, D. G. Collins, and M. B. Wells, *Monte Carlo Calculations in Spherical Shell Atmospheres*, RRA-T7104, Radiation Research Associates, Fort Worth, Texas (1971).

[162] J. V. Dave, "Coefficients of the Legendre and Fourier Series for the Scattering Functions of Spherical Particles," *Appl. Opt.* 9, 1888 (1970).

[163] J. V. Dave, "Intensity and Polarization of the Radiation Emerging from a Plane-Parallel Atmosphere Containing Monodisperse Aerosols," *Appl. Opt.* 9, 2673 (1970).

[164] J. V. Dave and J. Gazdag, "A Modified Fourier Transform Method for Multiple Scattering Calculations in a Plane Parallel Mie Atmosphere," *Appl. Opt.* 9, 1457 (1970).

[165] J. E. Hansen, "Multiple Scattering of Polarized Light in Planetary Atmospheres. Part I. The Doubling Method," *J. Atmos. Sci.* 28, 120 (1971), and "Part II. Sunlight Reflected by Terrestrial Water Clouds," *J. Atmos. Sci.* 28, 1400 (1971).

[166] W. G. Blättner, D. G. Collins, and M. B. Wells, *Loc. cit.*

[167] S. Chandrasekhar, *Radiative Transfer*, Clarendon Press, Oxford (1950), also Dover Publications, New York (1960).

[168] K. L. Coulson, J. V. Dave, and Z. Sekera, *Tables Related to Radiation Emerging from a Planetary Atmosphere with Rayleigh Scattering*, University of California Press, Berkeley and Los Angeles, California (1960).

[169] C. W. Querfeld, *Multiple Scattering in a Synthetic Foggy Atmosphere*, Ph.D. Dissertation, Clarkson College of Technology (1969) University Microfilms 70-20,0004, Ann Arbor, Michigan (1970).

Jacobowitz, and Howell, Bullrich and de Bary. Herman, Browning, and Curran[170] who list all the relevant references, present a good introduction to the problems associated with this important and most complicated experimental and theoretical problem in atmospheric physics.

There is a need for more observational data on the variation of aerosols with height and the variations in their size distribution and index of refraction. Volz has recently published infrared absorption properties of atmospheric aerosol substances.[171] Solution of the problem of multiple scattering is far from satisfactory at the present time.

10. Tables of Attenuation Coefficients. Some investigators have calculated attenuation parameters, based upon various models of atmospheric optical environments, over a wide range of wavelengths from ultraviolet to far infrared. McClatchey *et al.* have computed values of attenuation coefficients at 12 laser wavelengths, namely 0.3371, 0.4880, 0.5145, 0.6328, 0.6943, 0.86, 1.06, 1.536, 3.392, 10.591, 27.9, and 337 micrometers, for 10 model atmospheres for altitudes ranging from 0 to 100 kilometers above sea level.[172] Elterman has computed attenuation parameters at 20 wavelengths from 0.27 micrometer to 2.17 micrometers for 8 surface meteorological ranges for altitudes from 0 to 50 kilometers.[173] Deirmendjian has calculated attenuation coefficients for two haze models and three cloud models.[174] One should remember that all the calculations mentioned above are based upon well-chosen, representative, atmospheric optical environmental parameters. In real, outdoor, atmospheric environments, there can be wide variations in atmospheric optical conditions. Tables X through XIII contain attenuation coefficients in the spectral range of 0.4 to 14 μm for calculating horizontal, ground-level atmospheric transmittance for various types of haze and fog conditions as specified by the visual range (at 0.55 μm). Similar data for other visible

---

[170] B. M. Herman, S. R. Browning, and R. J. Curran, "The Effect of Atmospheric Aerosols on Scattered Sunlight," *J. Atmos. Sci.* *28*, 419 (1971).

[171] F. E. Volz, "Infrared Absorption by Atmospheric Aerosol Substances," *J. Geophys. Res.* 77, 1017 (1972), and "Infrared Refractive Index of Atmospheric Aerosol Substances," *Appl. Opt.* *11*, 755 (1972).

[172] R. A. McClatchey, R. W. Fenn, J. E. A. Selby, F. W. Volz, and J. S. Garing, *Optical Properties of the Atmosphere (Revised)*, AFCRL-71-0279, Environ. Res. Paper No. 354, Air Force Cambridge Research Laboratories, Bedford, Massachusetts (1971).

[173] L. Elterman, *Vertical Attenuation Model with Eight Surface Meteorological Ranges 2 to 13 Kilometers*, AFCRL-70-0200, Environ. Res. Paper No. 318, U. S. Air Force Cambridge Research Laboratories, Bedford, Massachusetts (1970).

[174] D. Deirmendjian, *Electromagnetic Scattering on Spherical Polydispersions*, Elsevier, New York (1969).

Table X. Attenuation Coefficients for Haze for Various Values of Horizontal Visible Ranges (Adapted from Elterman)

VISIBILITY (AT .55 μm)	2 km		6 km		10 km		23 km	
ATTEN. COEFF. /TRANSM. (km^{-1}) / λ (μm)	α	T	α	T	α	T	α	T
0.40	2.66	0.07	0.904	0.405	0.553	0.575	0.243	0.78
0.45	2.34	0.10	0.788	0.455	0.478	0.620	0.206	0.82
0.50	2.13	0.12	0.713	0.490	0.429	0.651	0.184	0.83
0.55	1.95	0.14	0.652	0.521	0.391	0.676	0.170	0.84
0.60	1.74	0.17	0.578	0.561	0.346	0.707	0.159	0.85
0.65	1.57	0.21	0.523	0.593	0.312	0.732	0.148	0.86
0.70	1.47	0.23	0.488	0.614	0.291	0.747	0.139	0.86
0.80	1.29	0.27	0.427	0.652	0.254	0.776	0.130	0.88
0.90	1.17	0.31	0.386	0.680	0.229	0.795	0.122	0.88
1.06	1.05	0.35	0.345	0.708	0.205	0.815	0.114	0.89
1.26	0.946	0.39	0.312	0.732	0.185	0.831	0.108	0.90

Table XI. Spectral Attenuation Coefficients for Fog for Visibilities of 0.100 and 0.755 km (Adapted from Arnulf *et al.*)

VISIBILITY	0.1 km		0.755 km	
WAVELENGTH (μm)	α (km^{-1})	T(km^{-1})	α (km^{-1})	T(km^{-1})
0.35	42.568	< 10^{-10}	4.89	0.0075
0.45	40.608	"	5.04	0.0065
0.55	39.690	"	5.18	0.0056
0.75	39.386	"	7.20	0.00075
1.24	39.386	"	8.06	0.00032
1.70	39.386	"	7.20	0.00075
3.70	39.386	"	8.35	0.000236
10.00	20.607	10^{-9}	3.45	0.0317

Table XII. Spectral Attenuation by Haze and Light Fog Visibility ≈ 1 km (Adapted from Chu and Hogg)

WAVELENGTH (μm)	ATTENUATION COEFFICIENT (km^{-1})	TRANSMITTANCE T (km^{-1})
0.63	3.09998	0.04505
3.5	1.5046	0.2221
10.59	0.3544	0.7016

Table XIII. Spectral Attenuation Coefficients for Coastal or Marine Haze with Horizontal Surface Visibility of 2 Kilometers (Adapted from Deirmendjian)

WAVELENGTH (μm)	ATTENUATION COEFF. σ (km^{-1})	TRANSMITTANCE T (km^{-1})
0.45	1.956	0.141
0.70	1.954	0.142
1.19	1.634	0.195
2.25	0.785	0.456
3.00	1.099	0.333
3.50	0.963	0.382
3.90	0.436	0.647
5.30	0.208	0.812
6.05	0.351	0.704
8.15	0.116	0.890
10.00	0.083	0.920
11.50	0.180	0.835
13.00	0.222	0.801
14.00	0.232	0.793

ranges may be generated from the spectral transmittance or attenuation curves of Figs. 16 through 26 for the conditions under which the measurements presented in these figures were made. Interpolation between measured wavelength points should be made with care. The absorption bands of water vapor and carbon dioxide should be kept in mind (see Fig. 15).

Computer programs to calculate atmospheric transmittance in the 0.3 μm to 15 μm spectral region for various model atmospheres for horizontal and slant optical paths have been developed by various workers.[175]

III. CONTRAST TRANSFER BY THE ATMOSPHERE

The apparent difference between the radiant sterance (radiance) of an object and its surroundings enables an observer to detect the object in his field of view. The characteristic variations in the radiant sterance of the object provide cues for the recognition or identification of the object. The apparent difference in sterance is a measure of the contrast between the object and its surroundings. Although the concept of contrast is easy to grasp, it is rather difficult to agree upon a standard, internationally recognized definition of this term. Furthermore, the measurement of contrast is one of the most complex and difficult problems in the multidisciplinary field of visionics involving vision, psychology, atmospheric optics, and electro-optical technology. Some important contributions on this subject are reported in the literature.[176-180]

11. Definitions of Contrast. Let us consider an isolated object or target surrounded by a uniform and fairly extensive background. The contrast between the target and

---

[175] R. A. McClatchey, R. W. Fenn, J. E. A. Selby, F. W. Volz, and J. S. Garing, *Optical Properties of the Atmosphere(Revised)*, AFCRL-71-0279, Environ. Res. Paper No. 354, Air Force Cambridge Research Laboratories, Bedford, Massachusetts (1971).

[176] W. E. K. Middleton, *Vision Through the Atmosphere*, University of Toronto Press (1952).

[177] S. Q. Duntley, R. W. Johnson, J. I. Gordon, and A. R. Boileau, *Airborne Measurements of Optical Atmospheric Properties ta Night*, AFCRL-70-0137, SIO Ref. 70-7, Scripps Institute of Oceanography, Visibility Laboratory, University of California, San Diego, Calif. (1970).

[178] L. M. Biberman and S. Nudelman, Editors, *Photoelectronic Imaging Devices*, Vol. 1, Plenum Press, New York (1971).

[179] F. E. Nicodemus, *Radiometric Nomenclature*, Michelson Laboratory, Naval Weapons Center, China Lake, California (1971).

[180] F. E. Nicodemus, *Applied Optics and Optical Engineering*, Volume IV, Editor R. Kingslake, Academic Press, New York (1967).

the background may be expressed in a number of ways, for example,

$$C_1 = \frac{L^T - L^B}{L^B} , \tag{90}$$

$$C_2 = \frac{L^T - L^B}{L^T} , \tag{91}$$

$$C_3 = \frac{L^T - L^B}{L^T + L^B} , \tag{92}$$

and

$$C_4 = \frac{L^T}{L^B} , \tag{92a}$$

where C is contrast, L represents the radiant sterance (variously called radiance, luminance, or brightness), and superscripts T and B indicate target (object) and background, respectively. C_1 is sometimes called "Weber's fraction" by psychologists. C_3 is now called "modulation," though earlier it was named "visibility" by Michelson in connection with interferometric fringes. As the relative sterance of the object (target) becomes larger or smaller with respect to that of the background, C_1 varies from -1 to $+\infty$, C_2 varies from +1 to $-\infty$, and C_3 varies from 0 to 1; C_1 and C_2 change sign, but C_3 and C_4 do not change sign.

For an electro-optical system such as a TV-type monitor display where there are gain (contrast) and reference radiation level (brightness) controls, the significant quantity in the electro-optical image is the minimum-detectable, luminous-sterance (brightness) difference,

$$\Delta L = | L^T - L^B | . \tag{93}$$

For infrared imaging systems, the minimum-detectable radiant sterance (radiance) is generally given as the minimum-detectable, sterance temperature difference,

$$\Delta T = | T_L^T - T_L^B | , \tag{94}$$

where T_L is sterance temperature.

12. The Alteration of Contrast by the Atmosphere. The apparent contrast of a distant object is modified by two factors: (1) the atmospheric attenuation causes a

reduction in the amount of radiation propagating from the distant target object to the observer; and (2) the molecules and aerosols contained in the optical path contribute to the observed radiation by scattering and emission. The net radiation due to the second factor produces the so-called "optical path sterance (radiance)."

The apparent contrast of a target object, located at a distance R from the observer, according to equation (90), is given by

$$C_R = \frac{L_R^T - L_R^B}{L_R^B} \quad , \tag{95}$$

and the inherent contrast (at distance approaching zero) is given by

$$C_o = \frac{L_o^T - L_o^B}{L_o^B} \quad . \tag{96}$$

The ratio of the apparent contrast to the inherent contrast, called the "atmospheric contrast transferance," T_c (variously called atmospheric contrast transmittance or atmoaspheric contrast transfer function) is given by

$$T_c \equiv \frac{C_R}{C_o} \quad . \tag{97}$$

Let T_R and L_R^P denote, respectively, the atmospheric transmittance and radiant sterance (radiance) of the optical path of length R between the observer and the target. Thus, the apparent sterance of the target L_R^T and that of the background L_R^B will be given by

$$L_R^T = L_o^T T_R + L_R^P \quad , \tag{98}$$

$$L_R^B = L_o^B T_R + L_R^P \quad . \tag{99}$$

Combining equations (95), (96), and (97), we get

$$T_{c_1} = \frac{(L_R^T - L_R^B) L_o^B}{(L_o^T - L_o^B) L_R^B} \quad . \tag{100}$$

Substituting the values of L_R^T and L_R^B from equations (98) and (99) into equation (100) gives

$$T_{c_1} = \frac{(L_o^T T_R - L_o^B T_R) L_o^B}{(L_o^T - L_o^B)(L_o^B T_R + L_R^P)} ,$$

or

$$T_{c_1} = \frac{T_R L_o^B}{T_R L_o^B + L_R^P} = \frac{T_R L_o^B}{L_R^B} , \tag{101}$$

i.e.,

$$T_{c_1} = \frac{\text{Transmitted Background Sterance}}{\text{Apparent Background Sterance}} . \tag{101a}$$

Division of the middle terms in equation (101) by $T_R L_o^B$ gives

$$T_{c_1} = \left[1 + \frac{L_R^P}{T_R L_o^B} \right]^{-1} , \tag{102}$$

i.e.,

$$T_{c_1} = \left[1 + \frac{\text{Optical Path Sterance}}{\text{Transmitted Background Sterance}} \right]^{-1} \tag{102a}$$

If the contrast definitions expressed by equations (91) and (92) are used in equation (97) and the values from equations (98) and (99) are again substituted, the expressions for T_{c_2} and T_{c_3} are given by

$$T_{c_2} = \left[1 + \frac{L_R^P}{T_R L_o^T} \right]^{-1} , \tag{103}$$

or

$$T_{c_2} = \left[1 + \frac{\text{Optical Path Sterance}}{\text{Transmitted Target Sterance}} \right]^{-1} \tag{103a}$$

and

$$T_{c_3} = \left[1 + \frac{2 L_R^P}{T_R (L_o^T + L_o^B)} \right]^{-1} , \tag{104}$$

or

$$T_{c_3} = \left[1 + \frac{2\,(\text{Optical Path Sterance})}{\text{Transmitted Sterance of Target and Background}} \right]^{-1} \tag{104a}$$

A comparison of the three defining equations of contrast and the corresponding equations for contrast transferance reveals that the divisor in the defining

equation of contrast and that in the second term in the corresponding expression for contrast transferance is the same.

The important conclusion here is that the atmospheric contrast transferance is a function of: (a) the radiant sterance (radiance) of the optical path, (b) the atmospheric transmittance, and (c) the inherent radiant sterance of the background and/or the target. The atmospheric contrast transferance is thus dependent upon the complex nature of the optical state of the optical path. The atmospheric phenomena of scattering, absorption, emission, and turbulence all play important roles in the transfer of contrast by the atmosphere. Thus, a knowledge of the composition of atmospheric gases, the physical characteristics of atmospheric aerosols, and the ambient radiant incidance is essential for a complete description of an atmospheric optical environment.

Equations (101) and (102) are the most general expressions for the law of contrast transfer by the atmosphere. The value of atmospheric contrast transferance decreases with increasing values of optical path sterance as expected. The use of gated viewing techniques at nighttime minimizes the optical path sterance and thus enhances the apparent contrast.

The contrast transferance of the atmosphere is a wavelength-dependent parameter; it increases with increase in wavelength as does atmospheric transmittance, except in atmospheric absorption bands.

13. Optical Measurements for Derivation of Atmospheric Contrast Transferance. Using the Monte Carlo method, Wells *et al.* have made theoretical computations of atmospheric contrast transferance (transmittance) for two model atmospheres having ground-level, horizontal, visible ranges of 23 km (clear) and 3 km (hazy).[181] Figure 37 based upon Wells' study indicates that for various values of the nadir angle (180° minus the zenith angle) the contrast transferance can decrease by a large factor if a target is viewed through a long optical path, especially under reduced visibility conditions. This study indicated the necessity for field measurements. Under an Air Force Cambridge Research Laboratories' program directed by R. W. Fenn and supported by Visibility Laboratory, Duntley, Johnson, Gordon, and Boileau have conducted extensive airborne and ground-level measurements of the properties of the atmosphere at night.[182] They

---

[181] M. B. Wells, D. G. Collins, and F. A. Hooper, *Contrast Transmission Data for Clear and Hazy Model Atmospheres*," Report AFCRL-68-0660, I, II, III, Radiation Research Associates, Fort Worth, Texas (1968).

[182] S. Q. Duntley, R. W. Johnson, J. I. Gordon, and A. R. Boileau, *Airborne Measurements of Optical Atmospheric Properties at Night*, AFCRL-70-0137, SIO Ref. 70-7, Scripps Institute of Oceanography, Visibility Laboratory, University of California, San Diego, Calif. (1970).

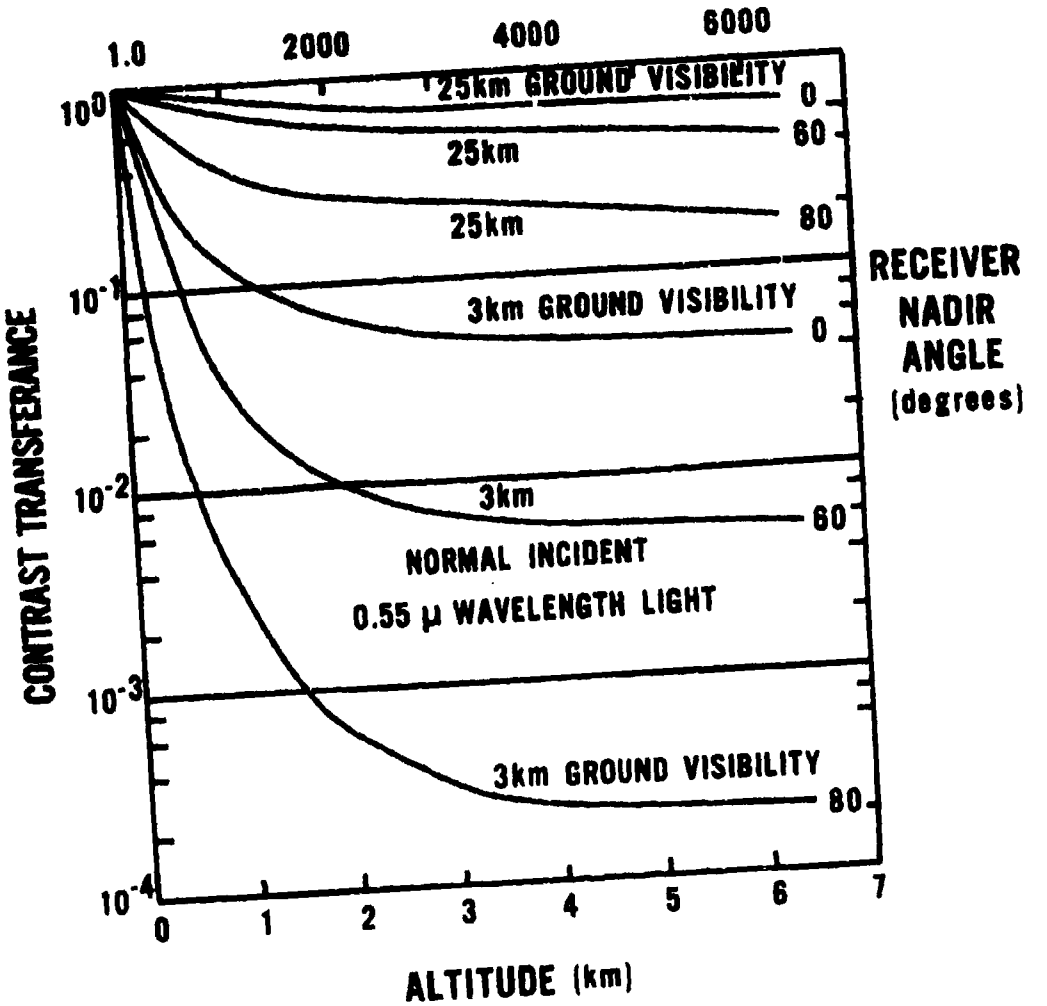

Fig. 37. Variation of atmospheric contrast transferance (transmittance) with observer altitude for various look (nadir) angles for two model atmospheres (adapted from Wells *et al.*)

have made measurements of optical parameters necessary to compute optical path radiant sterance (radiance). The airborne measurements of atmospheric optical parameters included: (1) upwelling and downwelling (terrain and sky) radiant sterance (radiance) each over a 2π steradian field of view, (2) directional and total scattering coefficients, (3) upwelling and downwelling radiant incidance (irradiance), (4) number and size distribution of aerosols, and (5) usual meteorological parameters such as dew point and ambient air temperature, pressure, relative humidity, altitude, and air speed. The ground-based measurement systems were similar to those used for airborne observations. Special care was taken to make terrain directional reflectance and ground-level radiant incidance and sky radiant sterance measurements. The aerosol counters were operated on a 24-hour duty cycle at a few times.

The atmospheric contrast transferance (transmittance) was computed using the alternate relation

$$T_c = [\, 1 + (\rho_R^P / \rho_o^B) \,]^{-1} \tag{105}$$

where ρ_o^B is the directional inherent background reflectance and ρ_R^P is the "directional path reflectance" defined as

$$\rho_R^P = \pi L_R^P / E\, T_R \quad , \tag{106}$$

where L_R^P is the optical path sterance, E is the downwelling incidance, and T_R is the atmospheric transmittance. All the quantities in this work have wavelength, altitude, and directional dependence.

The beam transmittance was computed from scattering measurements of the nephelometer.

The optical path sterance L_R^P was computed using the relation

$$L_R^P = \sum_{t=1}^{n} L_{D_t}^P\, T_{R_t}\, \Delta R \tag{107}$$

where L_D^P is the Duntley "optical path sterance function" defined by the relation

$$L_{D_t}^P = L_{q_t}\, \sigma_{t_t} \tag{108}$$

where L_{q_t} is the "equilibrium sterance" and σ_{t_t} is the total scattering coefficient at an altitude level t.

The equilibrium sterance L_q is computed using the relation

$$L_q = \int_{4\pi} L \left[\frac{\sigma_\beta}{\sigma_t}\right] d\Omega \qquad (109)$$

where L is the apparent sterance of the sky or ground in a particular direction, σ_β is the directional scattering coefficient, and $[\sigma_\beta/\sigma_t]$ is called the "proportional directional scattering coefficient" along the scattering direction β.

Thus the calculations are made in the following order: (1) equilibrium sterance, (2) Duntley's optical path sterance function, (3) optical path sterance, (4) directional path reflectance, and (5) atmospheric contrast transferance (transmittance). Figure 38 shows the variation of contrast transferance with altitude for two types of backgrounds observed in a vertical, downward direction using the detector with an S-20 spectral response. The contrast transferance is higher for the background with higher reflectance.

Direct nighttime field measurements of ground-level, horizontal-optical-path sterance require the use of a sensitive, large-aperture teleradiometer aimed at a large radiation trap.

Schie has made nighttime measurements of the distance at which the atmospheric contrast transferance is 0.5 using a teleradiometer with S-20 response.[183] A two-dimensional histogram, expressing the level of luminous incidance and the percentage of occurrence when a certain distance for which 0.5 of the inherent contrast is obtained, has been presented. This study indicates that the most probable range of about 300 meters for $T_c = 0.5$ occurs for luminous incidance of 10^{-4} lux.

14. The Effect of Contrast on the Performance of Viewing Systems. The performance of a viewing device is proportional to the square of the apparent contrast of an object according to the well-known Rose equation

$$L\,C^2\,\alpha^2 = \text{Constant} \qquad (110)$$

where L is the luminous sterance (luminance) of the scene, C is the apparent contrast of the object, and α is the angular size of the object.[184]

---

[183] J. van Schie, *Nocturnal Illumination and Decrease of Contrast in the Atmosphere*, Report Ph. L. 1969-4, Physics Laboratory TNO, National Defence Research Organization, The Hague, Netherlands (1969).

[184] A. Rose, "The Sensitivity Performance of the Human Eye on an Absolute Scale," *J. Opt. Soc. Am. 38*, 196 (1948).

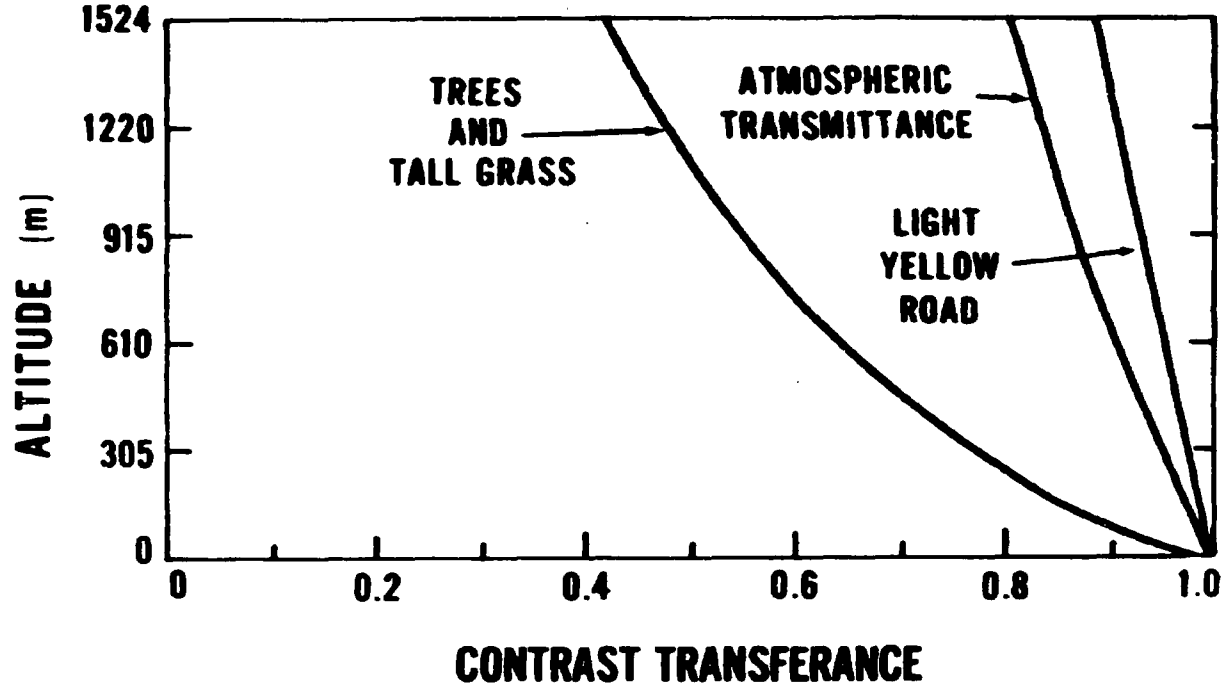

Fig. 38. Atmospheric contrast transferance as a function of altitude for two types of background (adapted from Duntley *et al.*)

From equation (110), it is clear that an accurate determination of the apparent contrast or the atmospheric contrast transferance (see equation (97)) is essential for the determination of the performance of visual or imaging systems which have to be used in the natural outdoor atmospheric optical environments.

A nighttime-contrast-measuring system using a 3-stage image intensifier and a teleradiometric system has been designed by Vatsia and used for nighttime, outdoor, contrast studies.[185] These studies confirm that there can be quite a considerable degradation of apparent contrast by thick haze and fog.

15. Meteorological Visibility of Objects Seen Against the Sky Background. The meteorological visibility is defined as the farthest distance at which a black object, subtending an angle between 0.5° and 7.0° at the observer's eye, can be recognized with unaided eye against the horizon sky (or, in the case of night observation, could be recognized if the general illumination were raised to the daylight level).

The meteorological visibility, when objectively measured, equals the optical path which will have a transmittance of 0.05 for a collimated beam from an incandescent lamp operating at a color temperature of 2700° K when measured with a photopic (luminous) flux meter.

If one uses the criterion of detection of the object (rather than recognition), the transmittance of 0.02 is used for the corresponding meteorological, optical range.

The atmospheric-contrast transferance is given by the general expression

$$T_{C_1} = \frac{C_R}{C_o} = \frac{L_o^B T_R}{L_R^B} . \qquad (101)$$

In the special case, when the background is the horizon sky, the ratio $|L_o^B/L_R^B|$ is unity for all values of the optical range. Equation (101), therefore, reduces to the simple form:

$$T_R = T_C . \qquad (111)$$

That is, when objects are seen against the horizon sky, the atmospheric-contrast transferance equals the atmospheric transmittance. Writing the value of T_R in terms of the

---

[185] J. R. Moulton, G. P. Intano, W. E. Stump, D. B. Newman, R. P. Bliss, and D. Dunlap, *A Search Performance Test on Ground Based Thermal Imaging and Pulse Gated Intensifier Night Vision Systems*, Preliminary Report, Visionics Technical Area, Night Vision Laboratory, Fort Belvoir, Virginia (1972).

attenuation coefficient α, we get

$$e^{-\alpha R} = T_C \tag{112}$$

where α is the attenuation coefficient and R is the optical path length. On taking the natural logarithm, equation (112) takes the form:

$$-\alpha R = \ell n\,[T_C]\,,$$

or

$$R = \frac{1}{\alpha}\,\ell n\,[1/T_C]\,. \tag{113}$$

This equation implies that for objects seen against the sky background the optical range, or visibility, equals the natural logarithm of the reciprocal of the atmospheric-contrast transferance or "threshold contrast" divided by the attenuation coefficient of the medium in the optical path. If $T_C = 0.02$, the optical range is variously called the meteorological optical, visual range, or visibility $V_{.02}$, and we obtain

$$V_{.02} = \frac{1}{\alpha}\,\ell n\,[1/0.02]\,,$$

$$V_{.02} = 3.912/\alpha\,. \tag{113a}$$

Similarly, if one uses the value 0.05 for the threshold contrast, or T_C, the meteorological optical range is given by the expression

$$V_{.05} = \frac{1}{\alpha}\,\ell n\,[1/0.05]\,,$$

or

$$V_{.05} = 2.9957/\alpha \approx 3/\alpha\,. \tag{113b}$$

When the optical medium has no absorbing gases or aerosols, the absorption coefficient is zero, and the attenuation coefficient of the medium is equal to the scattering coefficient σ. Therefore, one can replace α in equation (113) by σ. Thus, for a transparent medium the meteorological optical range, or visibility, is given by the expressions

$$V_{.02} = 3.912/\sigma\,, \tag{114a}$$

or

$$V_{.05} \approx 3/\sigma . \qquad (114b)$$

depending upon whether one chooses the value 0.02 or 0.05 for the threshold contrast.